

# Research **Report** 2012



**METEO FRANCE**  
Toujours un temps d'avance



# Research Report 2012



# Table of contents

---

## **Numerical weather prediction** ● page 6

- Modelling
- Assimilation
- Ensemble prediction forecast

## **Study of process** ● page 18

- Understanding
- Campaigns

## **Climate** ● page 20

- Climate and climate change studies
- Seasonal and climate forecasts

## **Chemistry, aerosols and air quality** ● page 36

## **Snow** ● page 40

## **Oceanography** ● page 44

## **Observation engineering** ● page 48

## **Research for aeronautics** ● page 54

## **Annexes** ● page 57



The mission statement of Météo-France is to “monitor the atmosphere, the upper ocean, and the snow mantel, anticipate their evolution, and distribute the corresponding information”. The organization is therefore in charge of carrying out the governmental duties in terms of security of people and goods with respect to the meteorological risks. The objective of the research activity is to help the organization improving continuously its operational services in meteorology and climate information. This has resulted in a high international reputation based on the quality of our weather forecasts and of our climate change analyses. Beside the applied research to improve models and climate data processing, we also carry out upstream research on atmospheric and climate processes, reaching the highest academic standard.

The research activity is mainly carried out in Joint Research or Service Units, shared with CNRS (the main French research agency) or the universities. These units participate aggressively into the general science competition, submitting proposals to the calls of the National Research Agency and the European Commission, with a notable success. They also contribute actively to teaching in engineering schools and universities. They are regularly evaluated by the Research Evaluation Agency and ranked at the highest level of research units. This policy will be pursued in the coming years. The collaboration with large university sites at Toulouse, Grenoble, Brest/Lannion and La Réunion will still be intensified.



© Camille Luxen

Regarding science themes, we have realized the importance of the interactions between the atmosphere, the ocean, the cryosphere, the land surfaces and the biosphere. This leads to recognize the need for a systemic research covering the whole of the climate system to address the various challenges of climate change. We therefore develop research programs on the physical and chemical aspects of the atmosphere and the ocean, on the energy and mass exchanges between these media, on the global carbon budget, on the snow mantel and the sea ice. However, Météo-France does not try to develop internally all tools necessary for its research. We actively look for collaborations with the best international teams to share developments and enlarge our scientific scope.

Météo-France has the privilege to be positioned at the intersection between applied and upstream research, with wide missions ranging from observation to operational weather prediction, from keeping the climate memory to predicting the climate of the future, with unique opportunities to transfer research results in operational practice without delay, and boost its academic partners into innovation at the international scale.

We strive to be recognized as an important partner in the upcoming National Research Strategy and in the “Horizon 2020” vision of the European Commission.



Philippe Bougeault  
Director, Centre National de Recherches Météorologiques.

# Numerical weather prediction

The research and development sections designing the numerical weather prediction (NWP) suites have successfully installed two experimental applications meant to help managing two field experiments.

One such experiment is the first special observing period of the HyMeX project. The suite is designed around a version of the non-hydrostatic AROME model with a horizontal resolution of 2.5km and 60 vertical levels, together with a 3-hourly data assimilation cycle. The NWP group has furthermore provided substantial support to the boundary layer constant pressure drifting balloon operations; several of its members have taken part to the activities of the HyMeX Operations Centre or those of the balloon base.

The other suite has been set up as part of a SESAR project (Single European Sky Air traffic management Research). On Météo-France side, this suite features hourly analyses followed by forecasts up to a few hours at 2.5 km resolution, developed in close cooperation with the Immediate Forecast section as well as a dynamical downscaling of the forecast to a 500m resolution over the Paris area including its airports. Short articles illustrate and describe further those suites. Beyond their primary use, those suites often have components meant to explore the future evolution of numerical weather prediction.

Other highlights of the year 2012: two large international scientific conferences have been organized, also very successfully, by members of the NWP group, as well as the meeting of the WMO working group on numerical experimentation (WGNE). The first conference has gathered remote sensing scientists at the end of March, especially focusing on the use of satellite observations in data assimilation. The second one, held in November, enabled to tour the various use of ensembles in geophysical data assimilation, from particle filters to ensembles of 4D variational minimizations. The success of these conferences highlights the level of international recognition reached by CNRM-GAME on these research topics, namely remote sensing and data assimilation, as has been well noted by the research evaluation agency AERES early this year.

A full operational suites update has been completed in September. It is not possible to list here all the changes included in this update. Some examples are a quasi doubling of the number of IASI channels assimilated, the implementation of a simple form of model error in the global assimilation ensemble or the use of new orographic and surface property data sources in the convective scale AROME model. Several new satellites have been launched since the end of 2011 and they will become important sources of data in the upcoming assimilation suites. The figures thus illustrate the setting up of important new data flows related to two of the new instruments from the Suomi-NPP US satellite platform. Many scientific and technical developments of the shared source code have been successfully integrated, together with scientists from the ALADIN and HIRLAM European consortia early in the year and later with ECMWF. Some of these changes result from the code reorganization part of the OOPS (object oriented prediction system) project. Several scientists from the group have been involved in the scientific review of the project, namely the evaluation of the match between the object oriented C++ code written so far and the initial objective of the project, that was to enable a more generic and extendable approach to data assimilation.

Other members of the group have played a key role in determining the most suitable proposal for renewing Météo-France high performance computer in 2014, while the detailed preparation of the future versions of the NWP suites for this computer has begun, with, for example, the design of the vertical level distribution of the next version of the AROME system. The Vortex project meant to share a common set of suite managing tools between research and operations has also delivered its first results and tests. The following short articles mostly illustrate some of the research results in the fields of numerical modeling, data assimilation and ensemble forecasting, research studies meant to be reasonably rapidly integrated into the operational versions on the next computer.

1

## Modelling

### Which vertical levels for next AROME model version?

Characterizing vertical resolution is an important step in the preparation of future AROME version on next computer. The number and thickness of vertical levels throughout the atmosphere should be optimized to simulate mesoscale meteorological phenomena while remaining compatible with the increase in computing resources.

Several distributions of 90 vertical levels were compared, and also a reference distribution with 120 levels, at 1.3km horizontal resolution over a domain covering an important part of France. The highest model level is lowered at

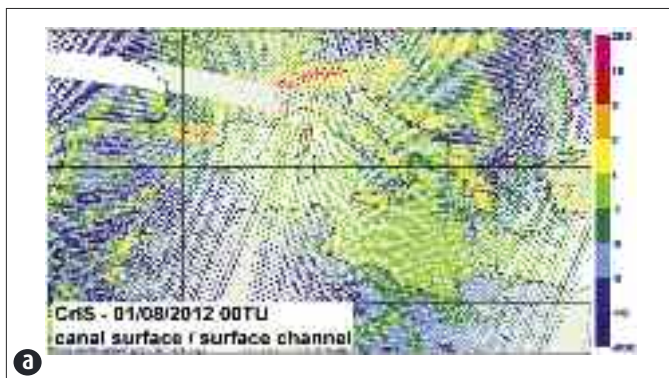
30km height to enhance the number of levels in the troposphere. Vertical resolution near the surface has been studied carefully, considering its importance for low clouds modelling and numerical stability. The best compromise can locate the future lowest level at 5m instead of 10m in the operational version. The left part of the figure shows the remarkable progress in the resolution below the first 500m when changing from 60 to 90 levels. The right part of the figure illustrates a fog event, with forecasted cloud water content as a function of time and height above Charles De Gaulle airport. The fog rises

an hour earlier in the simulation with 90 levels. This is a step in the right direction as indicated by observations, even a modest one.

The preparation of future AROME version will continue with the adaptation of others elements (coupling, numerical diffusion, physical parameterizations) to new resolutions.

2





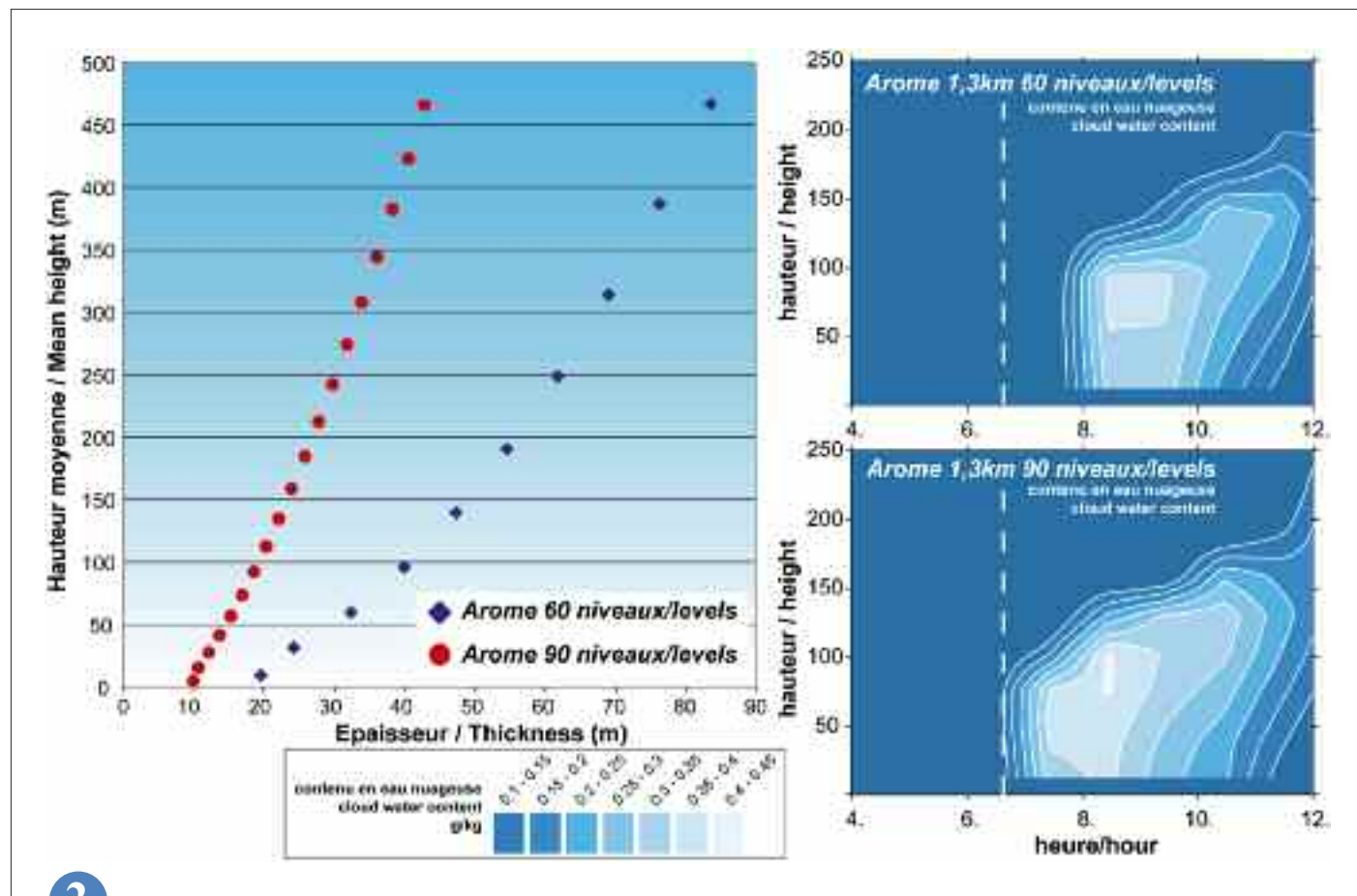
Maps of the first comparisons between observations from two new instruments of the US Suomi-NPP satellite and the simulated signal from those same instruments computed from a first guess ARPEGE global model state. (a): observation - first guess raw difference in one channel of the CrIS instrument. CrIS is an infrared interferometer with 1305 channels.

(b): same field for one channel of the ATMS instrument, a 22 channels microwave sounder. No bias correction has been introduced in these figures, nonetheless showing (with green spots) differences readily acceptable for assimilation. These maps correspond to a step in a rather long process. This step corresponds to both the data actually reaching the assimilation code core from the satellite and the correct behaviour of the code changes allowing the computation of the simulated channels from a model state.



1

On the left, vertical levels in the first 500 meters for operational AROME version since 2010 (blue squares) and an example of distribution with 90 levels and the lowest level at 5m (red dots). On the right, two vertical cross sections of cloud water content simulated by AROME with 60 and 90 levels of a fog event observed on Charles de Gaulle airport.



2

---

## A new bi-periodization algorithm for the AROME and ALADIN models

One specific strength of the limited area models AROME and ALADIN lies in that meteorological fields are horizontally represented through a spectral Fourier series expansion, which allows a highly accurate evaluation of the horizontal gradients. The use of such a Fourier series to approximate a non-periodic flow requires the fields to be made periodic on the limited-area domain. Although it has proven to work in practice, the current procedure for periodization, based on Spline cubic extension, suffers from serious deficiencies which may jeopardize the high-order accuracy of the spectral expansion: high-order derivatives remain discontinuous. A new algorithm, built

on a more sound mathematical grounds, based on infinitely differentiable “windowing functions” generally employed in wavelet theory, was recently implemented. It improves the convergence of the Fourier series, by ensuring both periodicity and infinite differentiability of fields. Academic tests and operational-like experiments with AROME and ALADIN models have demonstrated the benefit from this new algorithm of periodization.

3

---

## Spectral analysis of two non-hydrostatic models

Kinetic Energy (KE) spectra are used to evaluate two non-hydrostatic models (AROME and Meso-NH) for a case of isolated convection over the southwest of France.

Both models share the same physics parameterization but have different dynamical cores: the AROME model has a semi-implicit (SI) temporal scheme and a semi-Lagrangian (SL) advection scheme whereas the Meso-NH model is based on Eulerian centred schemes. Spectra represent the distribution of KE according to the spatial scales and illustrate the different damping mechanisms:

- explicit diffusion added to the model to prevent spurious accumulation at the shortest scales,
- implicit diffusion from the numerical schemes,
- subgrid mixing from parameterization.

Both models reproduce the observed  $k^{-5/3}$  wavenumber dependence characteristic of the meso-scale and the transition to a steeper  $k^{-3}$  regime at larger scales (Fig. a). The effective resolution, defined as the scale from which the model starts to underestimate the

variance, is about 4-6 Dx for Meso-NH and about 9 Dx for AROME (with Dx the horizontal grid spacing). The slope of the spectral tail is steeper for AROME suggesting a more dissipative effect and corresponding to smoother fields. This effect is emphasized when increasing the diffusion. When removing the explicit dissipation, a significant damping remains due to the implicit diffusion of the SISL scheme.

Several Meso-NH simulations have been conducted with finer horizontal resolutions ranging from 2.5km to 250 m (Fig. b). The peak of variance is shifted to finer scales when increasing the resolution as the vertical motions are better resolved. It stabilizes around 5.5km, suggesting that the fully explicit representation of convection needs a resolution close to 250m.

4

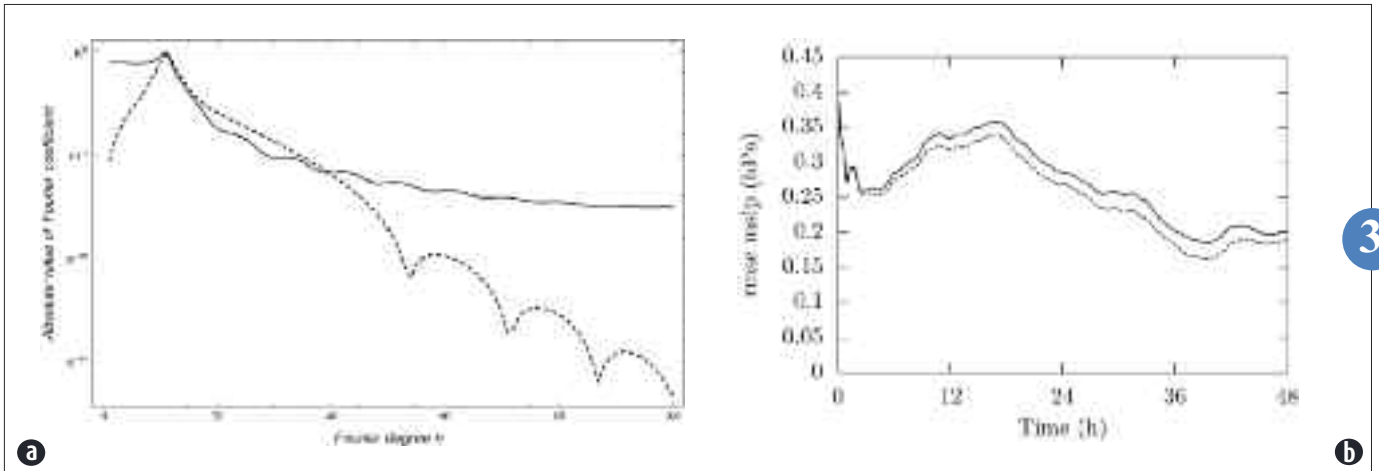
## Towards a parameterization of the convective turbulence at the sub-kilometric scales

The current resolution of NWP models at Météo-France is coarser than 2.5km. At such a scale, it is not possible to explicitly solve the boundary-layer atmospheric turbulence, whose size is of the order of one kilometer. At present, it is necessary to parameterize the entirely sub-grid turbulence. In a foreseeable future, super computers will allow downscaling to 1km or even to 500m. At such scales, part of the turbulence must be resolved. The aim of this study is to develop a parameterization that will provide an adequate turbulence to these new generation and high-resolution models.

High-resolution (grid mesh of 62.5m) simulations are computed using the Meso-NH research model. It is possible to get reference fields at resolutions of hundreds of meters or larger once computed fields are horizontally averaged.

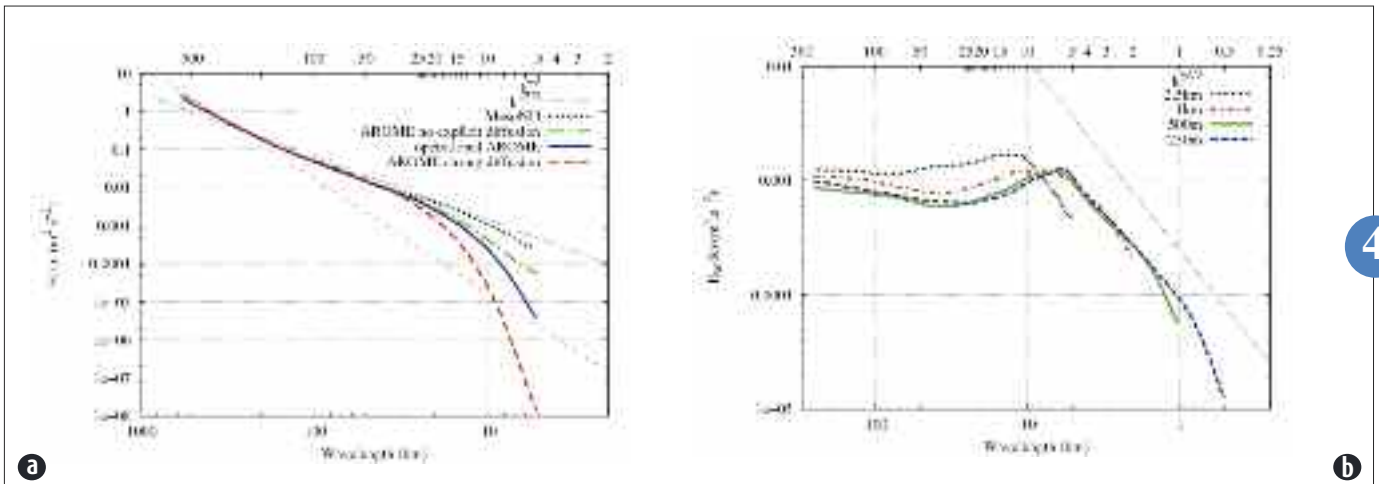
To assess the limits of current parameterizations, experiments were run using the Meso-NH model with 125m to 8km grids and with several options of the turbulence mixing. They were compared to the reference. Without a specific parameterization of the thermals, the resolved part is too large, whereas with it, it is too small. The hard fact is that some of the assumptions of the thermal parameterization are no longer valid at scales smaller than two kilometers. A micro-scale thermal parameterization was set by taken into account the neglected terms. Tests of the parameterization and its implementation into the AROME model will follow the study.

5



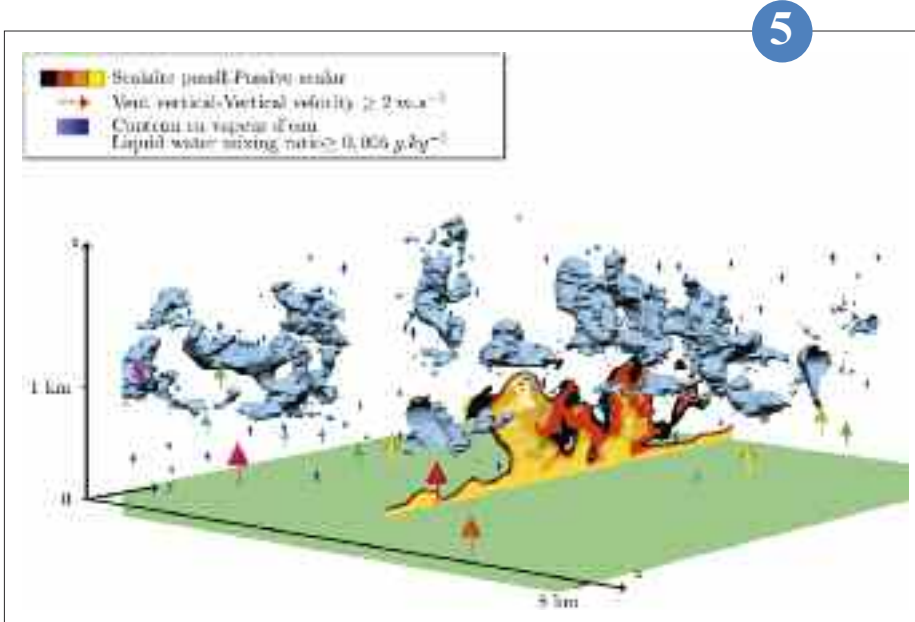
3

(a): Fourier expansion of an extended function  $f$  to  $x$  in  $[0,1]$ .  $f(x)$  is periodically extended via Spline cubic method (solid line) and using the new algorithm (dashed line, called Boyd method hereafter). It can be noticed that the spectral convergence speed of the Fourier series is faster when Boyd's method is used.  
 (b): Influence of bi-periodization methods on the error on mean-sea-level pressure: Spline bi-periodization (solid) and Boyd bi-periodization (dashed). The experiments are carried out for the famous and well-documented Lothar storm case of 26 December 1999.



4

(a): KE spectra on horizontal wind for 11 April 2007 averaged between 13 and 17 UTC over the free troposphere for Meso-NH and for AROME using different diffusions (simulation domain over the southwest of France).  
 (b): KE spectra on vertical velocity for 11 April 2007 averaged between 13 and 17 UTC over the free troposphere for Meso-NH using various horizontal grid spacings (simulation domain over the estuary of Gironde).



5

3D view (detail) of the high-resolution ARM simulation at 12h on a 62.5 m resolution grid. Liquid water mixing ratio ( $>5.10^{-3} \text{ kg.kg}^{-1}$ ) representing clouds are shown in blue. Arrows represent the vertical velocity ( $>2 \text{ m.s}^{-1}$ ). Warm colours represent the vertical cross-section of the concentration of a passive tracer emitted from the surface (thresholds  $0.5.10^{-3}$ ,  $0.75.10^{-3}$ ,  $0.875.10^{-3}$  and  $10^{-3} \text{ kg.kg}^{-1}$ ) shows boundary-layer thermals.

## A common thermal parameterisation in AROME and ARPEGE

In Météo-France operational models (AROME-ALADIN-ARPEGE) local turbulence, such as eddies, is expressed via a diffusivity equation, whereas non local turbulence or shallow convection is represented by a mass-flux scheme. The eddy-diffusivity part uses a prognostic turbulence kinetic energy formulation to compute turbulent exchange coefficients, both in ARPEGE and in AROME. By contrast, the shallow convection mass-flux parameterisations are presently distinct.

To ensure topmost scientific consistency among all these numerical prediction models, Météo-France try to use the same physical parameterisations at all scales. In this frame, a work was started to test the AROME shallow convection scheme in the global model ARPEGE.

To resolve numerical stability problems at large time steps, up to 1800s, an implicit common solver to the eddy diffusivity and mass flux scheme was built. Once this first algorithmic step was carried out, a scientific validation in the global model could start. Deficiencies of the scheme were identified, such as a too strong activity in the tropical area; they were not seen in the limited area configuration over France. New formulations of entrainment and detrainment were implemented and tested in 1D simulations of academic cases.

The impact of these modifications in the global model ARPEGE is positive, especially for wind, but there is always a slight degradation of temperature bias at the top of the tropical boundary layer.

6

## Improvements in tropical cyclone intensity forecasts using ALADIN-Réunion

Tropical cyclone forecasting is a major operational issue for the role of Météo-France as a RSMC in the southwest Indian Ocean. While track prediction has reached remarkably good performance, forecasting the strongest winds (intensity) remains very difficult. Yet, the cyclone intensity is important for predicting its consequences (wind, precipitation, waves and storm surge).

The operational model ALADIN-Reunion has been covering mostly the cyclone basin at 8-km horizontal resolution since 2010. Some recent works have significantly improved cyclone intensity forecasts using this model. The revision of the deep-convection scheme of ARPEGE and ALADIN models has severely limited some deficiencies of ALADIN-Réunion. False alarms of cyclogenesis no longer occur, and cyclone intensification rates are now more realistic. Some developments have also been done to

improve cyclone analysis at the initial forecast time. The equations of data assimilation have been corrected so that wind bogus (pseudo-observations deduced from satellite analyses) better constrains the cyclone intensity. Improving both the initial state and the model should provide more useful intensity forecasts. Further improvements are expected by refining the horizontal resolution of models. Some research work is under way using the model AROME at higher resolution than ALADIN-Réunion.

7

## Preparing a numerical weather prediction software for our new computer system: Implementing and using an IO server

The high performance computing trends over the last few years have brought the advent of “massively parallel” machines; some new problems ensue: some parts of the code turn out to be inefficient when run on these machines. These pieces of code are said to be not “scalable”; “scalability” is the term coined to measure the ability of software to accelerate when distributed over many more processors.

Météo-France shall renew its high performance computing system in 2013; this system will use several thousands of scalar processors. In order to prepare our code to this new machine, tests have been conducted on scalar architecture, and showed that the scheme used to produce the historic files of our models (AROME, ARPEGE and ALADIN) is not scalable.

The traditional output scheme involves the following steps:

- reconstitution of whole model fields on a limited set of processors,
- compression of these fields by processors mentioned in step 1,
- gathering and writing of compressed fields on processor number 1.

The two last aforementioned steps cannot use the full computing power allocated to the code, and therefore, are not scalable; hence, the traditional scheme used to produce model output cannot be accelerated causing a bottleneck for the whole model.

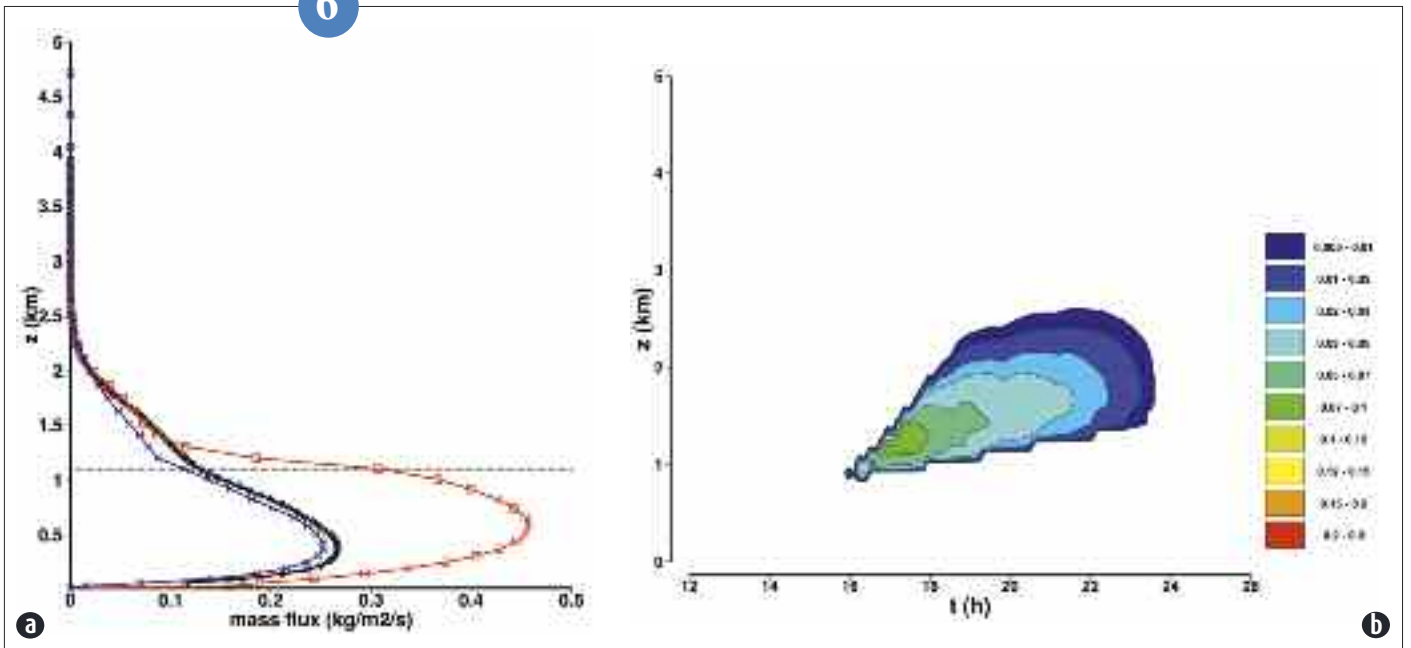
These considerations led us to isolate the code responsible for producing historical files and to distribute it on a much smaller set of processors which run what is commonly named an IO server. As shown on the diagram, compression and writing of fields is offloaded to the IO server.

This IO server was included in the final benchmark submitted to hardware vendors for the renewal of Météo-France high performance computing system, and was used by most bench markers to run forecast test cases (AROME and ARPEGE).

8

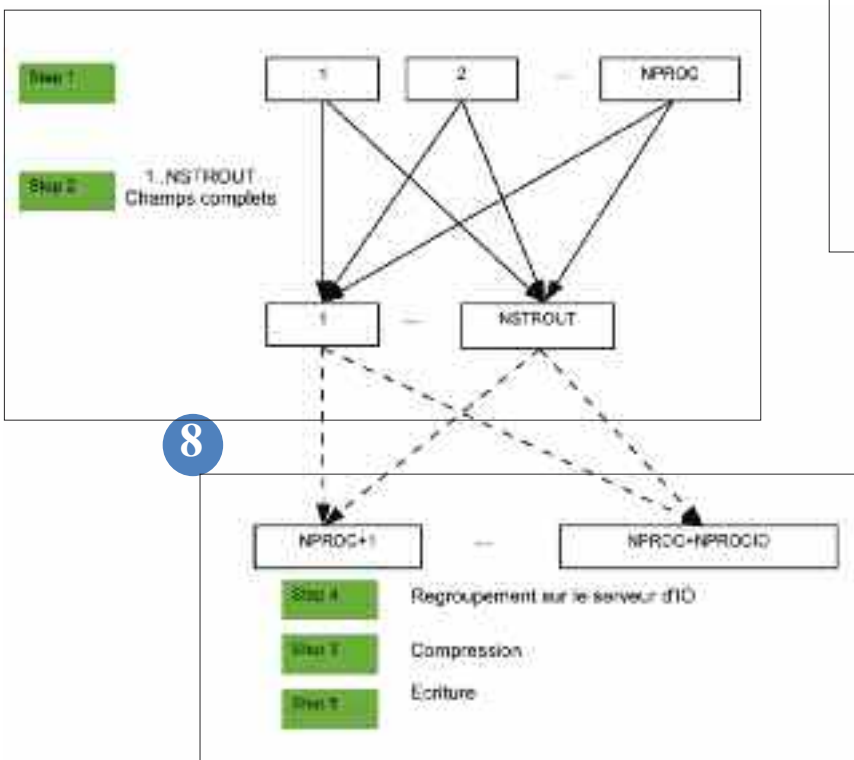


6

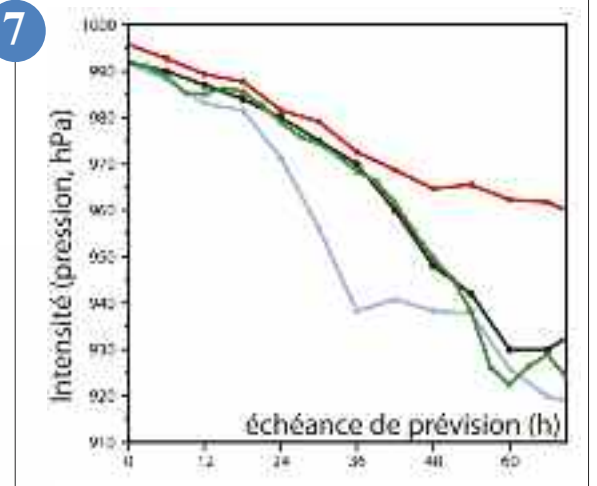


(a): Mass flux after 8 hours of simulation for the academic continental cumulus case. Red curve represents operational scheme solution. Black curve is the mass flux computed from Meso-Nh very high resolution simulations and represents the best approach of the exact solution. Blue curve is the solution of the scheme after modification of the entrainment and detrainment formulation. The dotted line shows the cloud base.  
 (b): Temporal evolution of cloud liquid water for the academic continental cumulus case, unit is g/kg.

Communication pattern of the IO server.



7



Intensity forecasts (pressure at the storm centre) of Gael (2009) by different configurations of ALADIN-Réunion: the operational configuration in 2009 (bleu curve, for which the cyclone intensifies too rapidly) and two experimental configurations with different parameters of the deep-convection scheme (green and red curves). The reference (intensity estimate by satellite) is in black. The configuration that has eventually been chosen for the operational model in 2011 corresponds to the green curve.

---

## Assimilation

### Observation impact on ARPEGE forecast computed with the adjoint method

The 4DVAR assimilation system of the global model ARPEGE processes a large amount of satellite and ground based observations. In order to improve weather forecasts and assimilations, the capability to compute the forecast sensitivity to observations (FSO) has been implemented.

This technique is used in many NWP centres as a complement to more classical sensibility to observations experiments. The FSO diagnostic requires both the adjoint of the forecast model and of the assimilation system to give a linear estimate of each observation contribution to the reduction of a short term forecast error measurement.

An experiment was made over the period going from December 2010 to January 2011. The figure on the left shows the impact results by observation group. The microwave sounder AMSU-A and the infrared sounder IASI have the largest impact on the forecast

error reduction partly because they give the largest amount of observations. The figure on the right shows the relative impact of a single source of observation. Ground observations from buoys and radiosondes are the most informative. Concerning individual satellite observation, the largest impact comes from Atmospheric Motion Vectors and GPS radio-occultation data.

The continual evolution of observations available for assimilation requires adaptation of models. This diagnostic is an additional tool to evaluate the impact of such changes on the quality of the forecast system.

9

---

### Observation impact on AROME analyses

The convective-scale Numerical Weather Prediction system AROME uses a 3D-Var assimilation scheme in order to determine its initial conditions. In addition to conventional and satellite observations used in global data assimilation systems, dedicated observations for meso-scale as, for instance, radar measurements (radial winds and reflectivities), are assimilated.

The impact of the various observation types on AROME analyses is assessed using an a posteriori diagnostic: the reduction of the error variance provided by the different observation subsets during the data assimilation process, estimated with a Monte-Carlo method. This diagnostic allows to investigate observation impact depending on the analyzed meteorological field, the height, the date, the analysis time or the spatial scale.

It reveals the important contributions of screen-level observations (2m temperature and relative humidity, 10m wind) for the lowest layers, of aircraft measurements for temperature and wind field analyses and of radar observations for wind and specific humidity in middle- and high-troposphere (see figure). These observations only appear to be informative for horizontal length scale less than 200km, while all the observations are mainly informative for longer length scales. This diagnostic, which increases the understanding of observation use, should allow to improve data assimilation system performances.

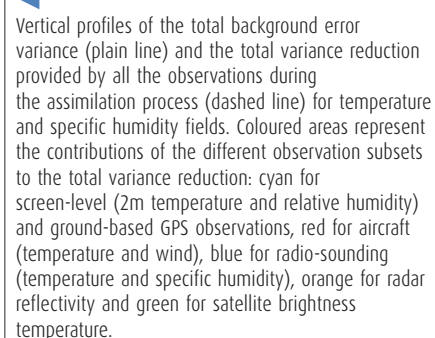
10

### Comparison of global and convective-scale forecast errors

In numerical weather prediction systems, it is required to estimate forecast error statistics in order to periodically adjust the model state toward the observations. This uncertainty, which is varying every day depending on the meteorological situation, can be estimated through the spread of an ensemble of perturbed forecasts. This method is already operational at Météo-France in the AEARP ensemble, based on the large scale model ARPEGE. In preparation for a similar ensemble a convective scale, uncertainty structures of the AROME model have been documented and compared to those of the ARPEGE model.

A study of the spread of large ensembles (for more accuracy) concludes to significant discrepancies for a case of heavy precipitations above Cévennes. Only the largest scales of the uncertainty of AROME are visible in the uncertainty of ARPEGE, whose forecasts give the boundary conditions of ARPME forecasts. This can be explained by important discrepancies in the representation and the scale of the resolved phenomenon by these models, but also by discrepancies in the type and spatial coverage of observations allowing the adjustment of the model state. Therefore, flow-dependency of the uncertainty at convective scale has to be taken in account specifically.

11



11



## Towards a more extensive use of IASI observations

With the launch of advanced infra-red sounders, AIRS in 2002 and IASI in 2006, observations of the Earth and of the atmosphere with satellite has been highly improved. These hyper-spectral sounders provide information on the atmosphere and terrestrial surface in many thousands of channels for each observation point.

Data of these sounders are mainly used in numerical weather prediction models over oceans for clear sky conditions, even though some cloudy observations are also assimilated. Sea surface properties (surface emissivity and temperature) are indeed relatively well known whereas large uncertainties still remain over land.

Studies have shown that these errors are larger for the surface temperature than for the emissivity in the infra-red spectrum. Hyper-spectral sounders are able to provide this temperature.

Figure (a) shows an example of differences between the model surface temperature and the one retrieved from IASI observations by EUMETSAT. These differences can exceed 10K during the day and they may lead to the observation being rejected during the data selection step.

If the surface temperature is previously retrieved from a IASI channel sensitive to the surface and if this temperature is used to simulate all the other IASI brightness temperatures, the simulation is closer to the observation than the one with the model surface temperature (figure b). The impact of the retrieved surface temperature on the cloud detection will be now studied prior to the assimilation of IASI channels sensitive to the surface over land.

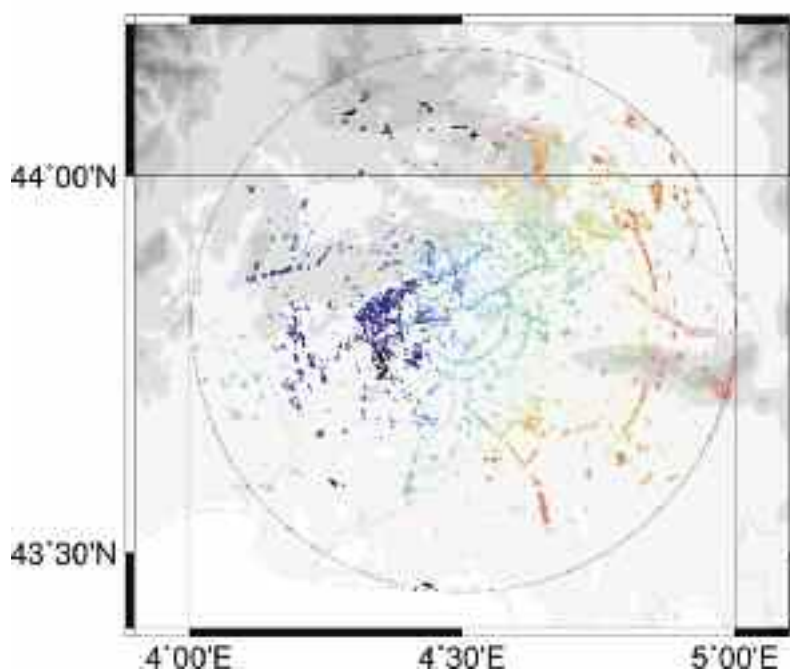
12

## Radar refractivity measurements and meso-scale modelling

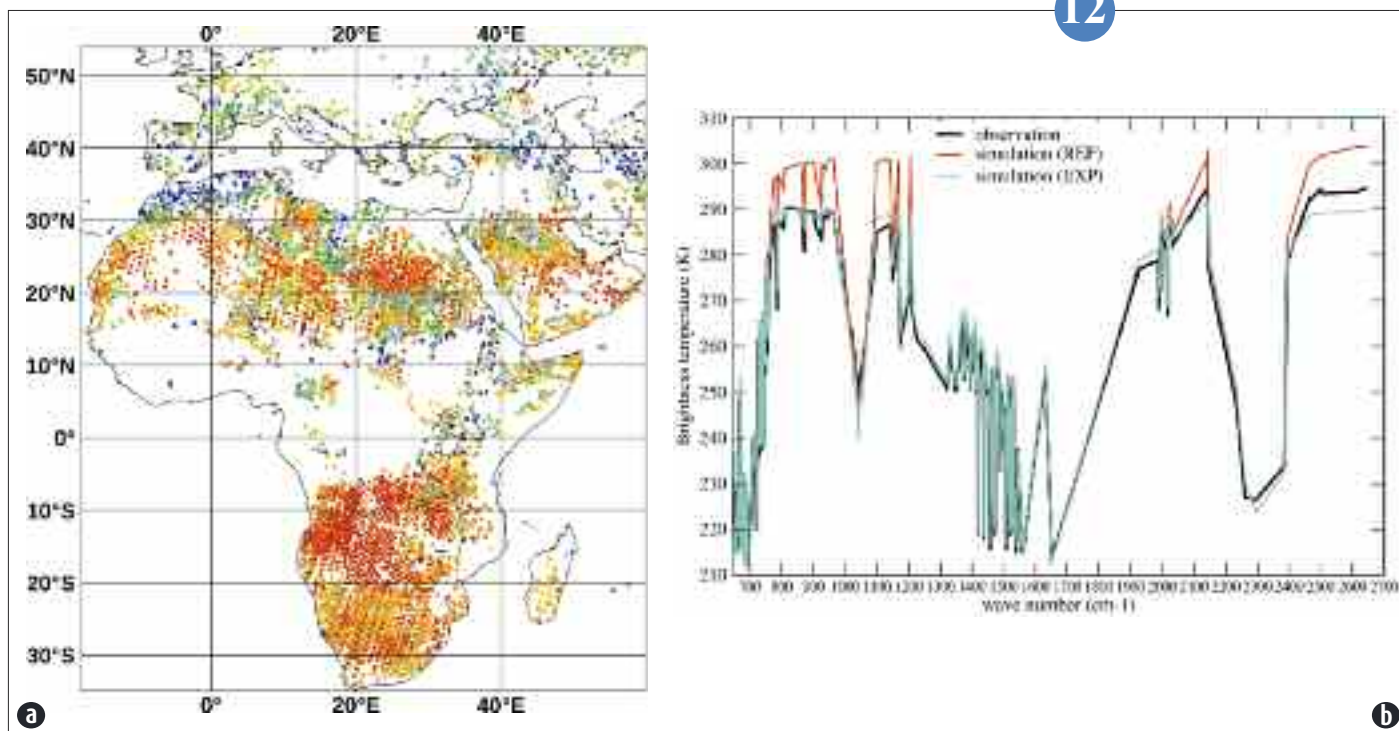
In order to estimate near-ground precipitation, weather radars scan the atmosphere at grazing incidences. Ground echoes hamper these precipitation measurements but may be used to measure the refractivity of the air through which radar waves go – be it in the presence of precipitation or not. This technique, which was worked out at the end of 1990s for North-American radars, consists of retrieving refractivity from the speed variations of radar waves between two consecutive sweeps. Refractivity depends on pressure, temperature, and humidity which are all prognostic variables in modern NWP models. Refractivity measurements therefore allow the provision of near-surface thermodynamic information at a spatial resolution that outperforms that of conventional automatic weather station networks within a 40km radar range.

The technique has been recently adapted for European radars and implemented in the French radar network. Refractivity maps have thus been produced in real time during the HyMeX field campaign. A refractivity simulator has been developed for AROME and comparisons with the corresponding observations (see example in figure) have shown that AROME was able to represent the observed structures, that assimilation of these data could potentially improve the model's initial state, and that a specific work had to be done on the quality of the data before any operational use. Work regarding the improvement of the data quality is in progress and currently focuses on the use of polarization diversity and several elevations to retrieve refractivity.

13

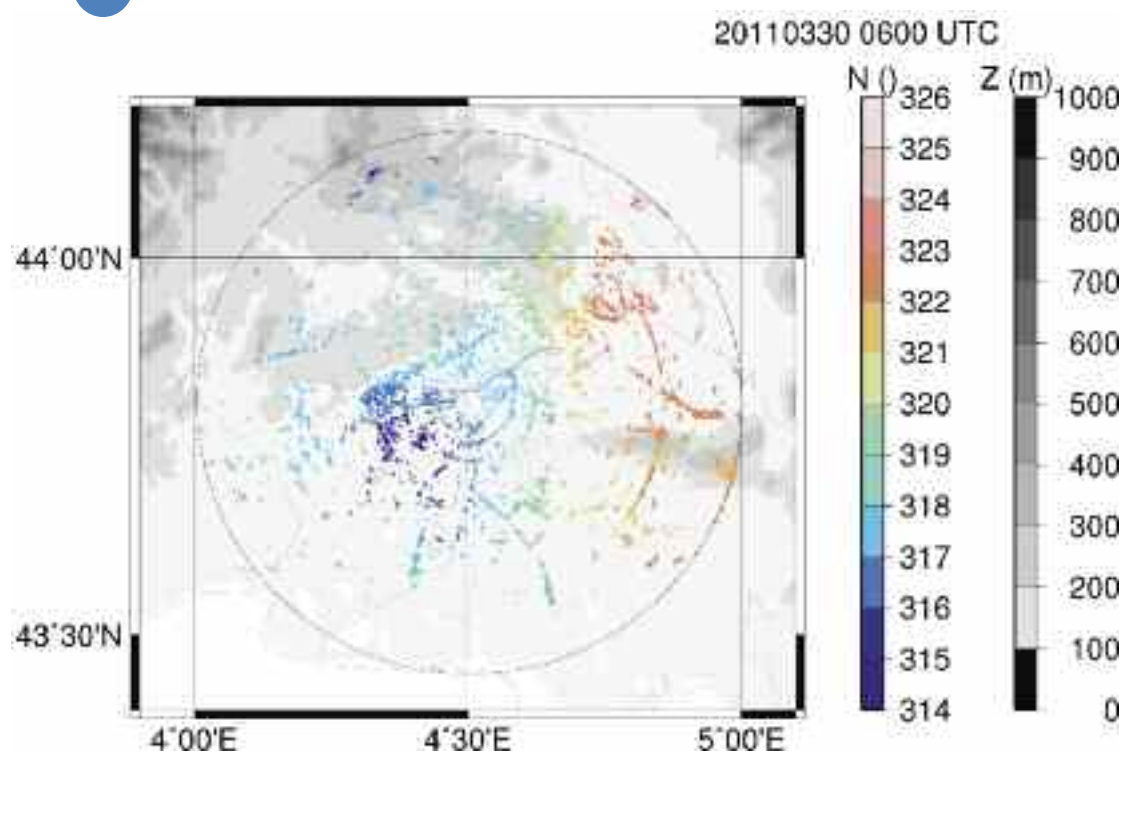






(a): Difference (K) between the surface temperature from the model and the surface temperature from EUMETSAT IASI observation retrieval.  
 (b): Impact of surface temperature from the model (in red) and from the IASI observation retrieval (in blue) on brightness temperature simulation of a IASI observation located over the Sahara desert.

Refractivity ( $N$ , in colour shades) as measured by the Nimes radar on 30 March 2011 at 0600 UTC, superimposed on the terrain altitude above the sea level ( $Z$ , in grey shades): observation (left panel) and corresponding AROME simulation (right panel). The circle represents the radar range of 40 km. The low values in refractivity to the west of the radar are mainly due to lower humidity values at this place.



# Ensemble prediction forecast

## Development of the AROME ensemble prediction system

The AROME ensemble prediction system under development aims to estimate short-range occurrence probabilities for fine scale events over France. This goal of Météo-France will involve resources from the next super-computer, since the equivalent of about ten instances of the current AROME prediction system will need to run in real time. The AROME ensemble will have multiple applications, among which the forecasting of severe precipitating or convective events. Recent experimentation of the system has focused on thunderstorm cases and high precipitation events over the Mediterranean, including the HyMeX field experiment where the system has been tested in real time. It has shown that the AROME ensemble will bring significant added value with respect to existing numerical weather prediction systems, by improving detection and false alarm rates on various kinds of weather events, including both common and high impact weather events.

The goal of current research on the AROME ensemble is to improve the forecast performance of the system by better modelling the various sources of forecast uncertainties: the use of observations to initialize the forecasts, model prediction equations, and the coupling of AROME with the ARPEGE large-scale ensemble prediction system. There are activities on product development, too, including precipitation post-processing, the identification of convective hazards to aviation, and the coupling with hydrological modelling systems for flood prediction.

14

## Bayesian weighting for lagged ensemble AROME forecasts

Ensemble prediction systems at convective scale are often under-dispersive because of the small ensembles used in particular (namely around 10 members). In order to alleviate this problem, a time-lagged ensemble can be created from ensemble forecasts initialized at different production times. This approach has been applied to a pre-operational version of the ensemble prediction system currently developed for the Arome France model, by combining the most recent ensemble forecasts with older ensemble forecasts started 6h and 12h earlier. A preliminary study showed that such a combination has a positive impact on probabilistic scores. While an equal-weight combination of lagged forecasts generally provides competitive results, the choice and the impact of a weighting scheme remain key questions. The proposed weighting method is based on the particle filter formalism, and the weights are determined online for each member according to the likelihood of the last available observations. The weights calculated in this manner tend to decrease with forecast range, while being close to the uniform weight (see figure). The impact of this Bayesian weighting on probabilistic scores is small on average, but reveals noticeable improvements for the verification of severe events, in particular heavy precipitations.

15

## Inter-comparison of different ensemble systems using the TIGGE database

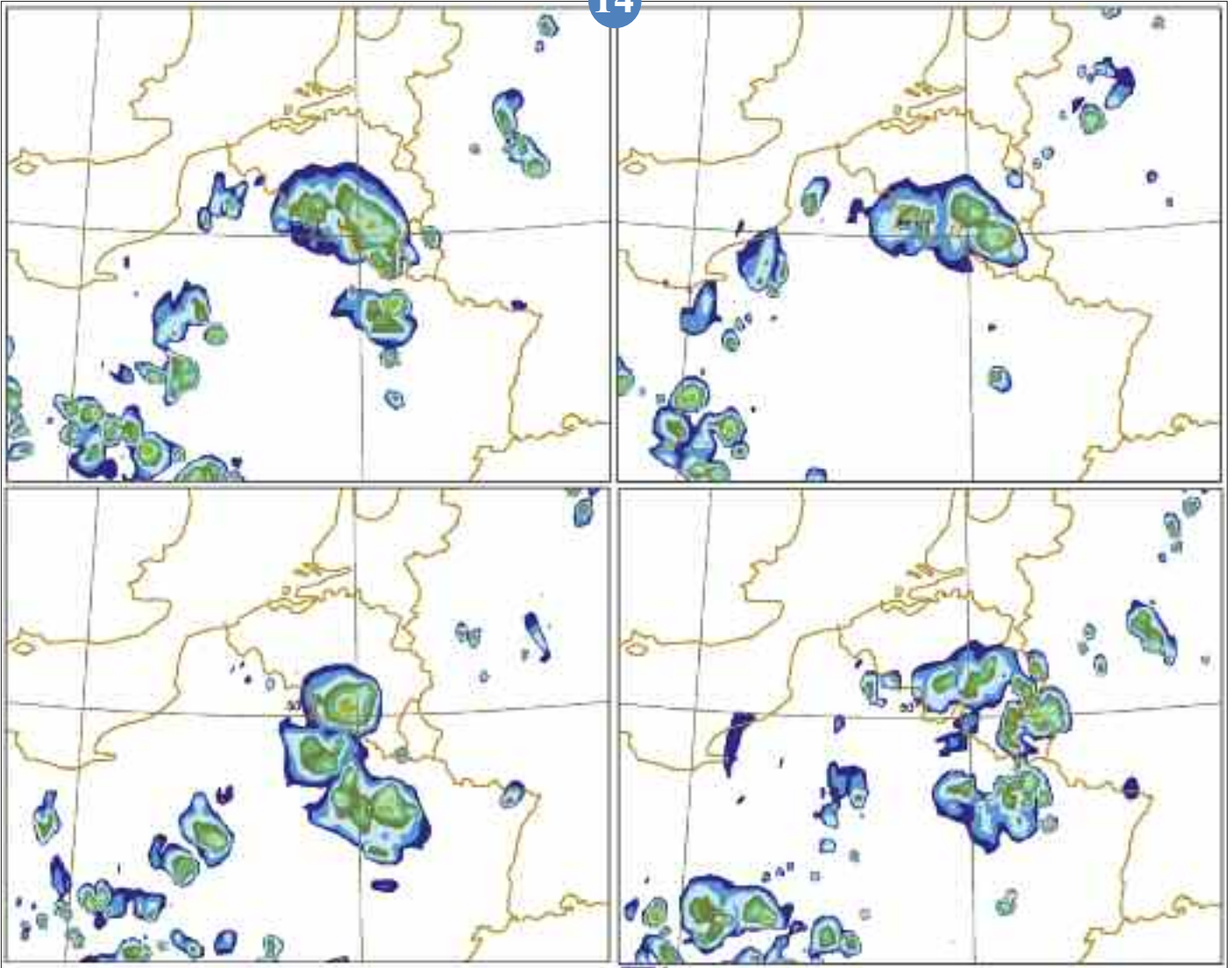
The development of a data base giving free access to ensemble prediction systems for researchers is one major deliverable of the World Meteorological Organization programme THORPEX. This data base named TIGGE (for Thorpex Interactive Grand Global Ensemble) is hosted at ECMWF and stores data from the ten global ensemble prediction systems in a near real time basis. PEARP, the French global ensemble system is one among them.

This data base has so far not been overused, especially in the short ranges. Nevertheless, it enables inter-comparison studies using data from different ensemble systems. The figure displays the short-range global skill of 5 different ensembles that may be found within TIGGE in terms of Continuous Rank Probability Score (referred to as CRPS by experts). This score measures the distance between the cumulative probability distributions of the ensembles and of observations. It considers the two main properties that an ensemble must fulfil, viz, the statistical reliability and the resolution which is the ability of the ensemble to discriminate events. For the case at hand, every system presents a degradation of the score with the forecast range. It appears that the best systems are those of ECMWF and PEARP.

16

Weights calculated for each member of the super-ensemble over a 2-week period in spring 2011. This super-ensemble is designed with the pre-operational version of the Arome ensemble prediction, made of six members. "Lag 0" members correspond to the most recent ensemble prediction, and "Lag 6" and "Lag 12" members correspond to ensembles started 6h and 12h earlier respectively. Each line represents the weights calculated for a particular date.

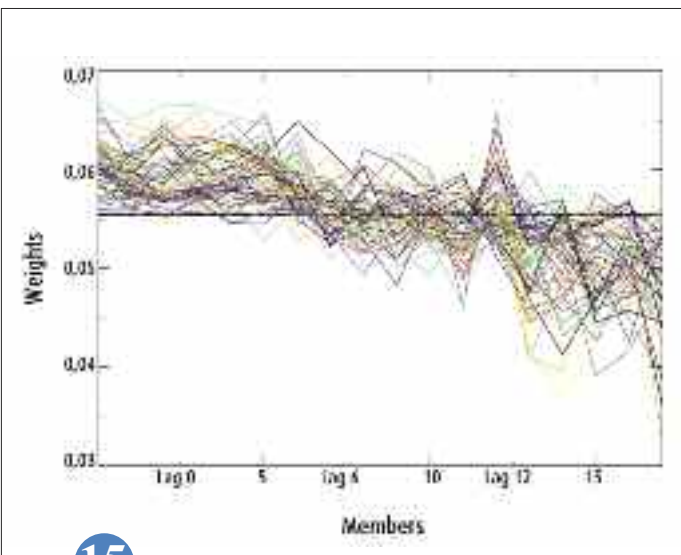
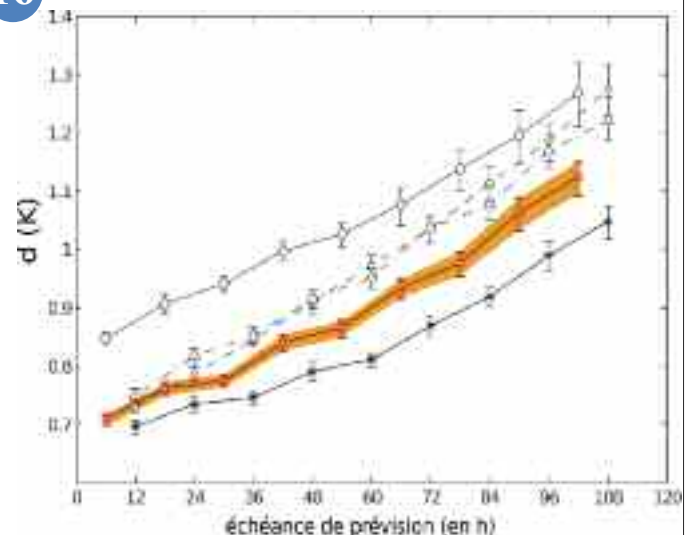
14



▲ Ensemble prediction of summertime thunderstorms along the Belgian border using AROME: The shading delineates rainy areas. The four maps show equally likely forecast scenarios, their mutual differences illustrate the uncertainties on thunderstorm location according to the experimental AROME ensemble prediction system. The future operational ensemble will produce about ten predictions, which will help quantifying precipitation risks in this kind of hard-to-predict weather.

Time evolution of  $d$ , the continuous rank probability score for 850 hPa temperature as a function of the forecast range. Canadian ensemble (circles and dashed lines), UKMO ensemble (triangles and dash dotted lines), ECMWF ensemble (stars and bold solid lines) and Météo-France PEARP (red squares and dashed lines). The bootstrap technique gives access to a measure of the score uncertainty (vertical bars, orange stands for PEARP ensemble).

16



15

# Study of process

---

The CNRM leads researches which the final objective is the permanent improvement of the various forecasts realized by Météo-France. For that, the CNRM leads numerous studies of processes in the domains of meteorology, climate, superficial oceanography, hydrometeorology and atmospheric chemistry. Both main components of this scientific approach are the numerical modelling and the experimental campaigns. By leaning on its important means for experimental measurements, the CNRM often plays a key role in the initiation of large international research programs, in the definition of their strategy, in their implementation and in their scientific exploitation.

This chapter illustrates this approach with articles on the realization in 2012 of campaigns like HyMeX on the intense Mediterranean precipitations, TRAQUA on the Mediterranean pollution and ALTIUS on the stratospheric ozone. The campaign Concordiasi realized in 2010 allows today to drive the adaptation of the world observation system to improve the forecasts in polar zone. Results of more conceptual works are also presented, in particular on the storm Xynthia, on the mechanisms of oscillation of the Oscillation the North-Atlantic Ocean (NAO), on storms and tropical cyclones of the Indian Ocean, as well as on the waves of the East African.

To observe, to model and to understand are the key words of this scientific approach which allows the improvement of the Météo-France operational models and so to supply information always more relevant on the future of our environment, from the very short-term (a few hours) up to the very long term (several decades).

1

---

## Understanding

### **Influence of the horizontal structure of the jet stream on a wind storm development (Xynthia, 28 February 2010)**

Mid-latitude cyclone dynamics is strongly linked with the westerly upper-level jet since it determines the course and intensity of cyclones. They draw their energy from the north-south temperature gradient (balanced with the vertical wind-shear, owing to the earth rotation). Recent work using idealized numerical models suggest that the horizontal gradient of the vertically averaged jet stream may influence the course of cyclones. This mechanism, known of old for planetary scale atmospheric patterns and in the ocean, is new in the context of mid-latitude cyclone

development. More recently, it has been demonstrated that the same mechanism may occurred during the development of the wind-storm Xynthia that hit France between 26 and 28 February 2010 and which is considered responsible for the storm surge that affected the Vendée shores. By means of a sensitivity study to the initial conditions, using the prediction model ARPEGE, it can be seen that the vertical average of the jet (see figure) interacts with the cyclone at its mature stage; the surface cyclone development is able to induce an anticyclonic wind circulation in the

upper-levels downstream (red pattern) and a cyclonic one upstream (the blue pattern). This wind circulation, above the surface cyclone, may, in turn, contribute to a northerly component of the cyclone trajectory.

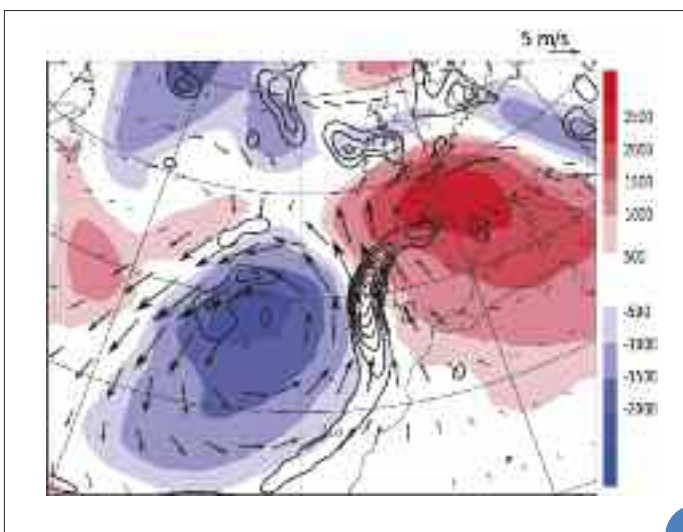
2





1

▲ HyMeX SOP1, 2012 autumn: the scientific directors and the SAFIRE pilots prepare a measurement flight to document the processes within thunderstorms. (photo credit MF).



2

▲ Surface cyclone at 12h UTC 27 February 2010 (850 hPa vorticity with black solid contours, interval:  $5 \cdot 10^{-5} \text{ s}^{-1}$ ). Geopotential anomalies (in  $\text{m}^2/\text{s}^2$ ) resulting from the interaction between the jet and the cyclone are shown at the level of the jet (blue shading stands for cyclonic patterns whereas red shading for anticyclonic pattern). The arrows display the component of the flow associated to this dipole that is able to modify the course of the surface cyclone.

## Interaction between the Pacific and Atlantic storm tracks and its implication on the North Atlantic Oscillation

The North Atlantic Oscillation (NAO) is the dominant mode of variability of the atmospheric circulation in the North Atlantic domain in winter. It is characterised by the latitudinal position of the eddy-driven jet (EDJ) in the North Atlantic domain: when the EDJ is shifted to the north, the phase of the NAO is said positive and when it is shifted to the south it is said negative.

The study of the intra-seasonal variations of the NAO highlights the presence of a low-frequency large-scale ridge in the Northeast Pacific during the onset of the positive phase (see figure). Its amplitude reaches a maximum four days before the maximum of the positive phase and then slowly decreases. A trough is observed in the North Pacific domain at the maximum of the negative phase, but it does not seem to precede the negative phase as the ridge does for the positive phase (see figure). We showed that this ridge, a potential precursor of the positive phase of the NAO, interacts in two ways with synoptic waves originating in the Pacific: it filters all the waves originating in the Pacific, but more small-scale waves than large-scale waves and it elongates the high-frequency perturbations entering the Atlantic domain preferentially in the NE-SW direction. These perturbations restore their energy to the flow in the North Atlantic domain leading to a northward shift of the EDJ, triggering the positive phase of the NAO.

3

## Numerical modelling of the interaction between a tropical cyclone and a trough using ALADIN-Réunion

Tropical Cyclone (TC) intensity prediction is a major operational issue that remains challenging. Forecast errors will be reduced by numerical modelling improvements and by a better knowledge of TC intensification and structure change mechanisms. In the southwest Indian Ocean in particular, TCs sometimes intensify in the vicinity of an upper-level trough (eddy) originating from the mid-latitudes. What are the physical processes at stakes during such TC-trough interactions and their impact on storm intensity?

Numerical simulations were carried out using ALADIN-Réunion. The initial inner-core structure of TC Dora (2007) is upgraded with pseudo-observations of wind constructed from satellite imagery. The model is skilful at predicting the two rapid intensification periods that Dora underwent. This allows diagnoses of intensification processes in relation with trough external forcing. The simulated TC-trough interaction is intricate. Potential vorticity from the trough enters into the TC core, which is responsible for a first period of rapid intensification inside the eye-wall. A secondary eye-wall formation resulting from spin-up at outer radii is then triggered by external forcing from the trough. Such a structure change leads to a second rapid intensification period as the outer eye-wall contracts and the inner eye-wall decays.

The study highlights the complexity of the interaction, the importance of initial conditions to obtain accurate forecasts, and the limitations of current numerical prediction systems in representing the processes at stake. Further work is needed to design a conceptual model for TC-trough interaction.

4

## Lightning activity in tropical cyclones of the south-west Indian Ocean

Over the past few decades tropical cyclone track forecast have improved faster than intensity forecasts. The detection of lightning activity as a possible precursor of cyclone intensification is thus studied.

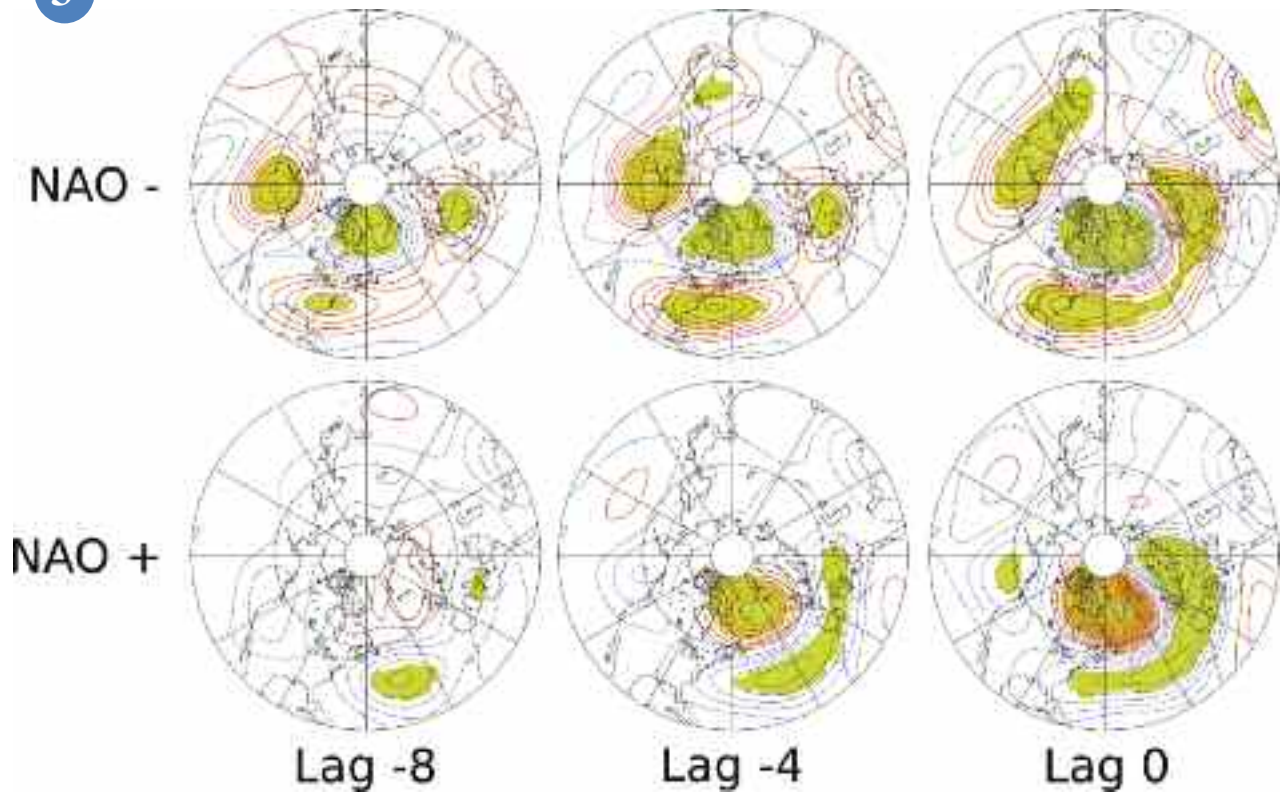
Lightning activity inside tropical cyclones in the south-west Indian Ocean is analyzed between 2005 and 2012. Lightning data from the global lightning detection network WWLLN and cyclone analyses from the RSMC of Météo-France at La Réunion are jointly analyzed. The study area is limited to the open ocean, more than 400km away from the eastern coast of Madagascar. The database is made up of 60 systems, decomposed in 1882 6-h periods. For the less intense systems (tropical depression or storm), lightning activity is distributed in as far as 100km from the storm center. When the system reaches the tropical cyclone stage, lightning flashes gather in the eye-wall (0 – 50km)

Since lightning activity is linked to the dynamics and to the ice particles distribution in convective cells, a lightning outbreak in the eye-wall is linked to rapid vertical winds, and to a possible intensification of the system. An intensification lower than 5 knots per 6 h is not preceded by a peak in the lightning activity. However, for systems rapidly intensifying ( $\geq 7.5$  knots/6h), the lightning density peaks 6h before the intensification, with a lightning density multiplied by 2 in 12h.

This study will be extended to systems approaching the coast. Numerical simulations of tropical cyclone lightning activity will be conducted to analyze the physical processes that lead to the observed behaviors.

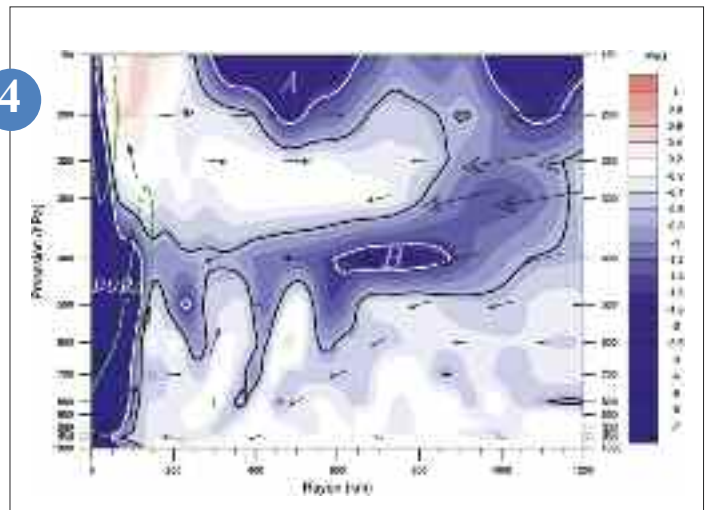
5

3

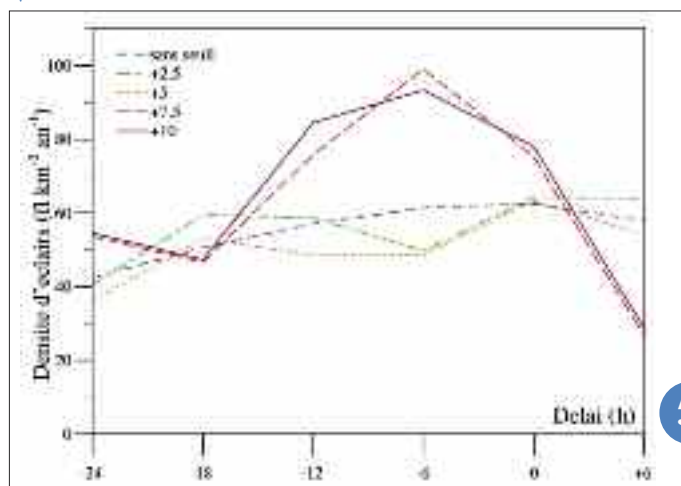


▲ Daily mean composites of the stream function anomaly at 200 hPa, eight days before the maximum of the NAO (lag -8), four days before the maximum of the NAO (lag -4) and at the maximum of the NAO (lag 0). The three upper figures are composites of the negative phase and the three lower figures are composites of the positive phase. The NAO is defined as the first Empirical Orthogonal Function of the 200hPa-streamfunction in the North Atlantic domain (20-80N, 90W-40E). Blue contours correspond to negative values of the composites and red contours to positive values. Interval is equal to  $2.10^6 \text{ m}^2 \text{ s}^{-1}$ . Green shading corresponds to areas where composites are significantly different from zero at 95%.

4



▲ Lightning density before (from -24h to -6h), during (0 h) and after (+6h) intensification over the open ocean in the eye-wall region (0 – 50km from the storm center). Five thresholds for intensification are used: no threshold (blue curve), +2.5 (green curve), +5 (yellow curve), +7.5 (red curve) and +10 (purple curve) knots per 6-hour period. It may be seen that strong intensification is preceded by a more intense lightning activity than medium intensification.



5

▲ Illustration of vorticity (structure B) feeding the inner core of tropical cyclone Dora (on the left), in relation with the upper-level trough (structure A). The figure is a vertical cross-section starting from the cyclone centre (on the left) towards the South-East (on the right), and from sea level (bottom) up to roughly altitude 15km (150 hPa, top). Cyclonic vorticity (blue) is transported by the wind (arrows). Regions of strong upward movement are in green dashed lines.

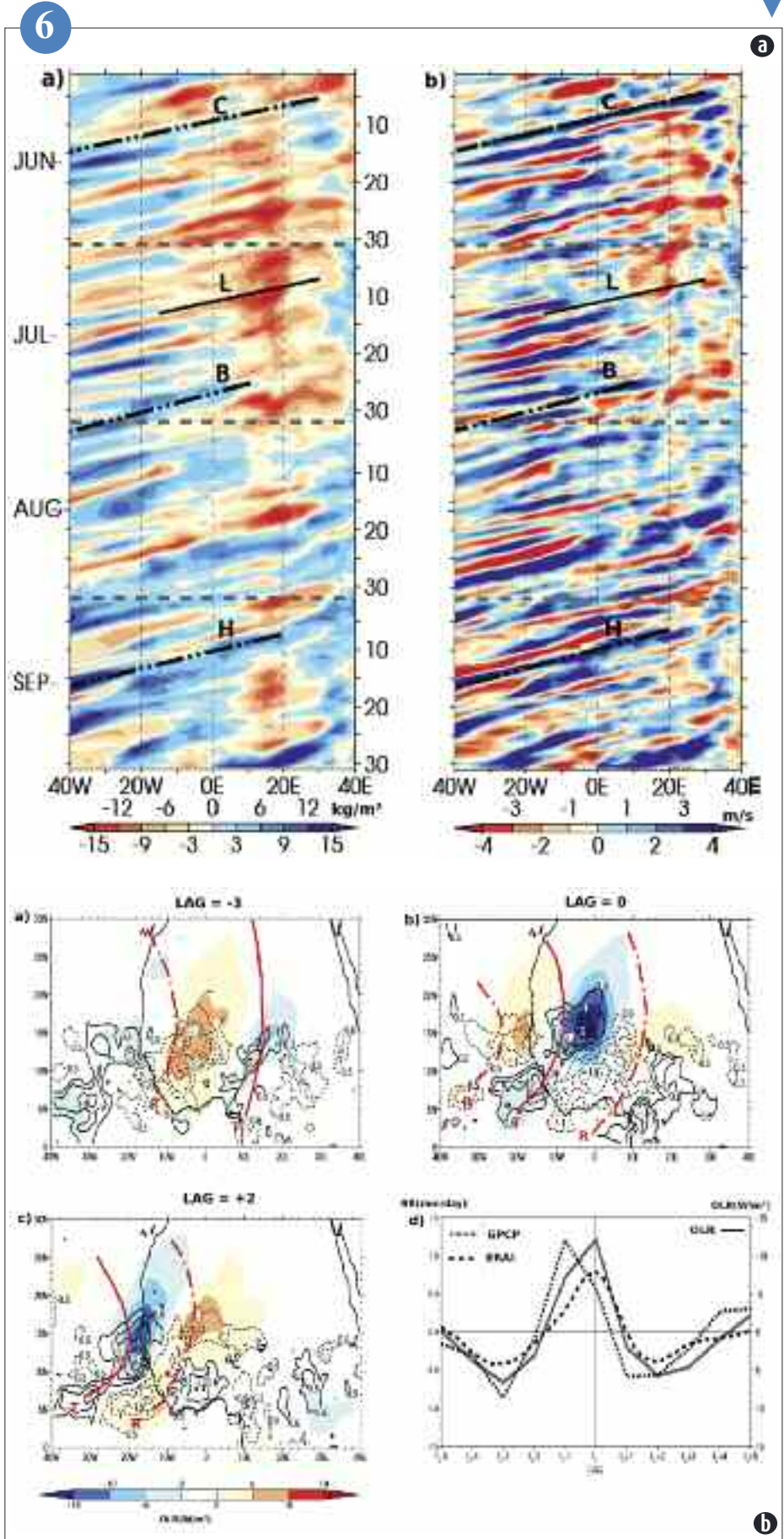


# Monitoring of African Easterly Waves with the precipitable water: A new contribution to the Sahel synoptic range predictability

The large variability of convection is a major issue in the tropic and is partly responsible for the low predictability of the African monsoon. Historically, the synoptic variability of the Sahel rainfall has been approached through the African Easterly waves (AEW) dynamics. Among other results, studies have shown that precipitation preferentially occurred in the region of the mid-tropospheric trough.

However, the dynamical view of AEW considered until now underestimates the important role played by humidity, especially over Sahel, where its values are much lower than in other regions and combined with large meridional gradients. Using the total Precipitable Water (PW), our study suggests that the seasonal anomalies of PW are well adapted to monitor the activity of AEW in the Sahel band. Figure 1a shows that these anomalies are frequent with significant amplitudes, westward propagating and can be detected as precursors of AEW over East Africa 5 days before. Ultimately, the link with the rainfall activity, presented in figure 1b, is shown to be strong. Over the continent and in the 10-20°N band, precipitations are maximum just on the western side of the PW maximum and are headed (one day) by the 600 hPa trough. In regions south of 10°N, the modulation of precipitations is opposite with its maximum in the vicinity of the trough consistently with previous studies.

(a): Seasonal anomalies of Precipitable Water (PW) averaged over 12-20°N during summer 2006.



(b): Composites of anomalies of GPCP rainfall in contours (mm/day) and NOAA-OLR in colours. The red lines represent the AEW 600 hPa trough (T) and ridge (R). The composites are computed with the index of 10 day-filtered PW averaged in the box 12-20°N, 2°W-2°E.



## Campaigns

### Concordiasi: results from the 2010 balloon campaign

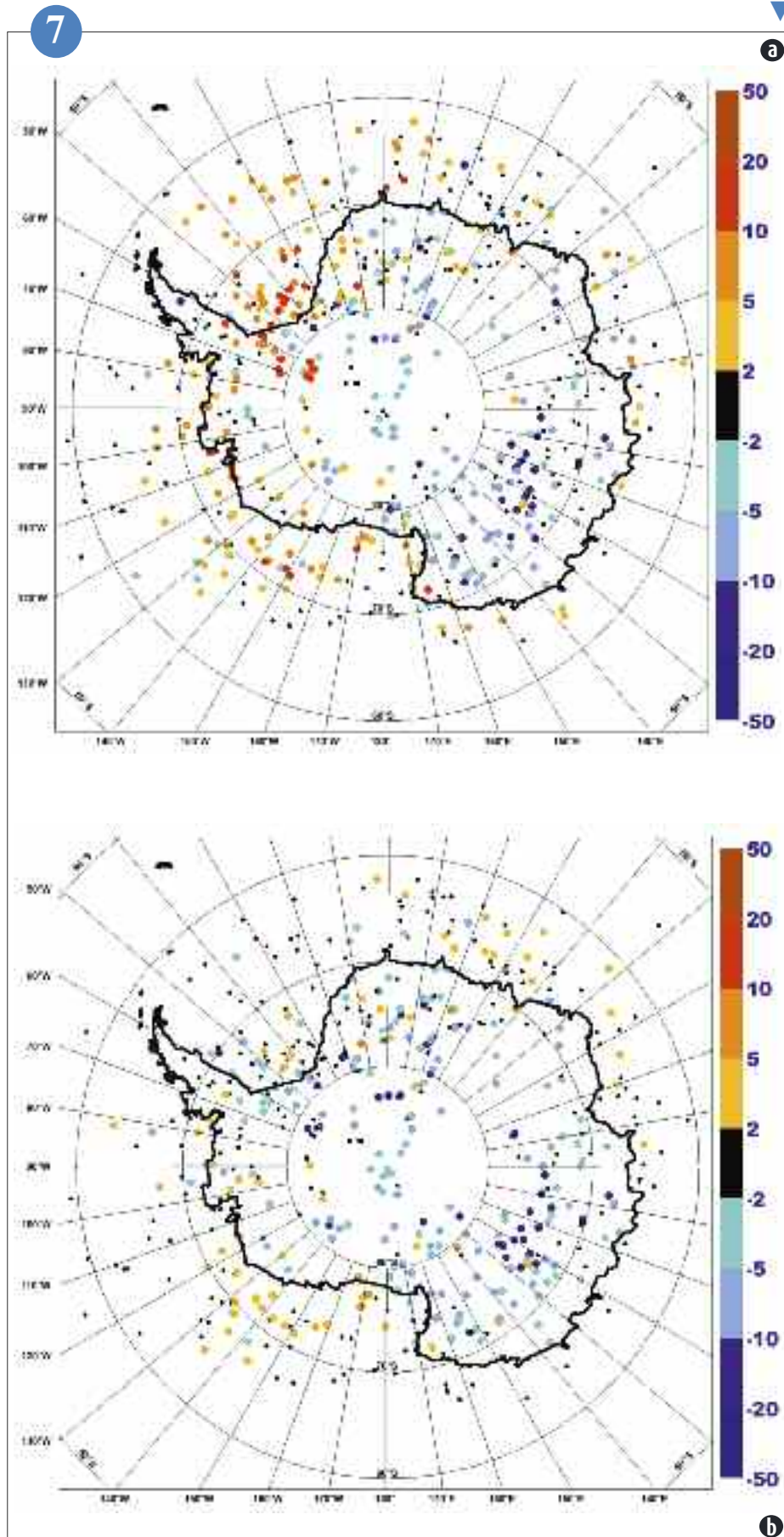
In the context of the Concordiasi project, an unprecedented field campaign took place over Antarctica in the autumn 2010. Nineteen super-pressure balloons from CNES were launched from the American McMurdo base. These balloons drifted at 17km height for a few weeks, releasing 640 NCAR drop-sondes measuring atmospheric profiles over a wide range of meteorological conditions over Antarctica and the surrounding seas.

Thanks to these data, obtained in areas usually unreachable by in situ observations, a thorough documentation of model performance and quality of satellite retrievals was performed. The IASI satellite data was found to reproduce observed temperature profiles reasonably well. The main limitation for an accurate retrieval was shown to be a lack of an accurate surface temperature description. A comparison between short-range forecasts and drop-sonde data was investigated for several NWP centres. Results show that models suffer from deficiencies in representing near-surface temperature over the Antarctic high terrain, where the very strong thermal inversion observed in the data is a challenge in numerical modelling. The difference between the drop-sonde and the model temperatures at the lowest model recorded by the data is presented in Figure “a” for the French global model and in Figure “b” for the ECMWF model. Both figures clearly show that the models are too warm over the Antarctic plateau. The impact of drop-sondes on the forecast quality was studied. It was found that temperature information is crucial at low levels whereas wind information is more beneficial at high levels of the atmosphere.

These results provide insight into how to enhance the global observing system to improve forecast performance over the polar areas.

7

(a): The difference between the drop-sonde and the model temperatures at the lowest model recorded by the data is presented for the French global model. Blue colours indicate that the drop-sonde is colder, which means that the model is too warm. Red colours indicate that the drop-sonde is warmer, which means that the model is too cold.



(b): The difference between the drop-sonde and the model temperatures at the lowest model recorded by the data is presented for the ECMWF global model.

Blue colours indicate that the drop-sonde is colder, which means that the model is too warm. Red colours indicate that the drop-sonde is warmer, which means that the model is too cold.

## Constant level drifting balloons in HyMeX and deployment strategies

During the first Special Observing Period (SOP1) of HyMeX, about fifteen Boundary Layer Pressurized Balloons (BLPB) from CNES have been launched from Mahon in Minorca. These balloons collected in-situ measurements of temperature, humidity and pressure and recorded their 3D position all along their isopical drift. The wind is derived from the balloon drift. The data are collected in real-time thanks to satellite communications. Filtered data are then disseminated to interested scientists who can use these data in their NWP models such as AROME West-Med. The primary objective of these balloons is to monitor the low level air parcels that bring Mediterranean Sea evaporated water into the convective cloud systems that trigger Heavy

Precipitation Events (FPE) and possible Flash Floods (FFE) on the elevated grounds that surround the basin (see HyMeX working package 3). The balloons are launched on alert, depending on the weather forecast, the IOP strategy chosen by the HyMeX Operation Center (located in La Grande Motte) and the predicted balloon trajectories that use various NWP systems (IFS, ARPEGE, AROME France and West-Med, PEARP). The final launch time is a trade-off between the predicted trajectories, local weather constraints (no rain, low or moderate wind) as well as air traffic control.

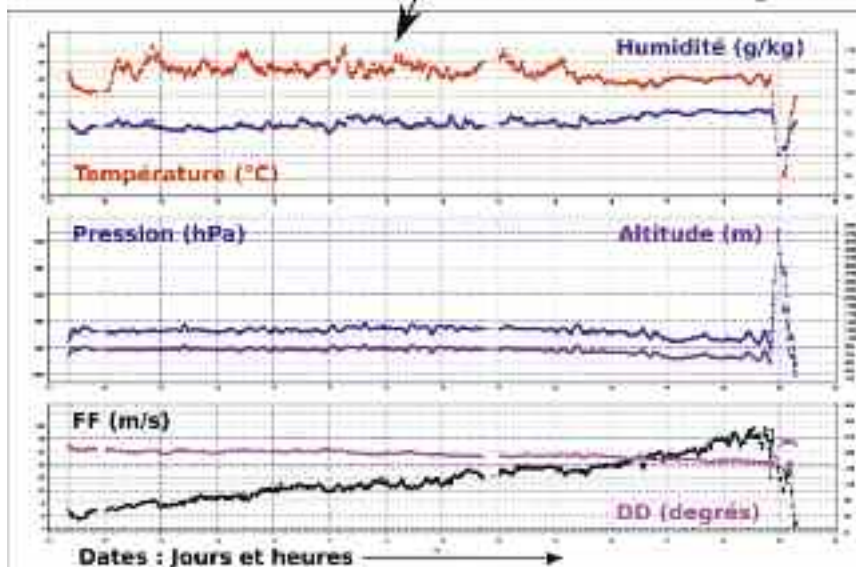
10

10



Trajectoire réalisée et simulation

Paramètres enregistrés



## Ground-based measurements during HyMeX SOP 1

As part of the first special observation period (SOP1) of the HyMeX international program, an unprecedented instrumental setup was deployed in Southern France to investigate the environmental conditions associated with the formation of heavy precipitation events. The Experimental and Instrumental Meteorology Division (GMEI) of CNRM has played a leading role in organizing HyMeX SOP1 through its participation in the definition of the observing strategy and through the deployment of many meteorological sensors along the Mediterranean coast. The GMEI teams have been involved in many activities including:

- the organization and management of the Candillargues “remote sensing” supersite, which concentrated in one place a unique set of meteorological sensors to describe the properties of heavy rain events (fig. a);
- the implementation of a mobile radio-sounding station allowing to perform radio-sounding at various location based on most relevant weather forecasts (fig. b);
- the collection of radiosonde and turbulent flux measurements onboard the vessel Provence;
- the Organization of weather radar deployment and operations (fig. c).

These observations, which are currently undergoing validation, will be made shortly available to the scientific community and will be exploited for several years.

11

Picture: Launch of BLPB B21, on the 14/10/2012 about 06 UTC on the tarmac of Mahon Aero club in Minorca. The sensors are located within the dedicated shelter at the top and outside the balloon envelope. The housekeeping systems are inside the balloon in the bottom gondola. The equatorial ribbon is a deflector/divertor for rain drops falling from the hydrophobic envelope.

Chart: Real trajectory (black) and predicted trajectories for BLPB B21 starting from a real 3D location (orange) and two others vertical positions (more or less 150 metres in blue and green): this is the trajectory “follow”, which give every 20 minutes a new prediction of the balloon's future route. Diagram: Overview of the B21 in-flight collected parameters.

This balloon fulfilled its objectives as it entered convective systems close to the French-Italian border at 19h15. The final ascent triggers the end of the flight.





**(a)**

Overview of the Candillargues experimental supersite. Observations at Candillargues are mainly based on active and passive remote sensing of the atmosphere via different types of lidars (aerosol, water vapor) and radars (wind profiler, polarimetric weather radar), sodar, microwave radiometer, and GPS station, among others. Observations were generally supplemented with high frequency radio-soundings during intensive observation periods.



**(b)**

The mobile radio-sounding station. 160 (out of a total of 192) mobile radio-soundings were made during the SOP1 of HyMeX at Vias, Marseilles, Frejus and Candillargues.



**(c)**

View of the National Severe Storm Laboratory (USA)'s polarimetric radar. This radar, deployed near Alès on top of Mount Bouquet, is one of the five research radars deployed during the HyMeX SOP1.

## AROME WMED, a model dedicated to the HyMeX campaign

The first special observations period of the HyMeX experiment occurred from 5 September to 5 November 2012. A dedicated AROME version, that covers the whole western Mediterranean basin, was developed at CNRM to provide real time forecasts to the HyMeX operational centre and for the decision making for the observation deployment. This model named AROME WMED has a larger domain (+ 11%) than the operational one and provides forecast up to 48 hour range available at 4h30 UTC from the analysis at 00UTC.

Despite real time constraints, more satellite micro-wave observations and additional Spanish surface data have been/were used in the analyses in order to improve the data coverage. A few experimental observations have been also assimilated.

The figure gives an example of the 24 hours rainfall rate predicted at 48 and 24 hour ranges with AROME WMED for the 26 October 2012 and the rainfall rate observed with rain

gauges. This case corresponds to a sevenol event and to high precipitations in Liguria-Tuscany and in Central Italy, followed by flash floods. These precipitating events are forecasted by the model at one day- and two day-ranges. In addition, a special effort was made to increase verification data density with additional Spanish and Italian surface data, provided by meteorological centres in near real-time.

AROME WMED will continue to provide analyses and forecasts in near real time for hydrological and oceanic purposes until 15th March 2013 when the HyMeX second SOP will end. These meso-scale meteorological fields are available in the HyMeX database.

12

## The TRAQA field experiment: characterization of the pollution over the Mediterranean

The TRAQA (Transport à longue distance et Qualité de l'Air dans le bassin méditerranéen) campaign took place on the Mediterranean basin from 26 June to 11 July 2012. The goal is focused on:

- the characterization of the dynamical processes which govern the export of polluted air masses from the remote regions of the basin;
- the quantification of the exchange between the boundary layer and the free troposphere;
- Lagrangian studies of ageing and mixing processes of polluted plumes in the lower troposphere.

A test of the representativeness of the case studies over a long period.

During this experiment, The ATR-42 aircraft of Météo-France operated by SAFIRE and atmospheric balloons (sounding and drifting) operated by CNES have been used to measure trace gases and aerosols. Five drifting balloons were launched (three of them have measured ozone). In total, seven intensive observations periods were made with a total of 60 hours of flight and as many as for balloons during a moderate Mistral cases. The MOCAGE model forced by ARPEGE analyses and the MACC outputs have been used

during the campaign in addition to the trajectory model (BAMED) based on AROME and ECMWF to forecast the favourable conditions to launch the balloons. Measurement will be treated and exploited for different episodes: a pollution event over the Gulf of Genoa, an event of desert dust transport from Africa, a pollution export from the region of Barcelona and an event of moderate Mistral. These events have been awarded "Golden Days" (Figure).

Acknowledgements:

TRAQA received financial support from the MISTRAL and PRIMEQUAL programs, the CNES, the OMP and LA as well as the participation of the following laboratories: CNRM, LA LATMOS, LISA, SAFIRE and the CNES balloon division.

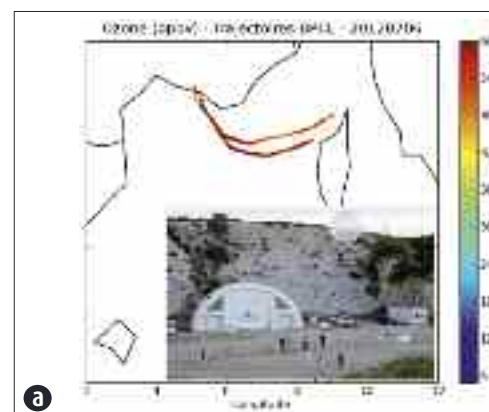
13

## ALTIUS campaign: measuring stratospheric ozone

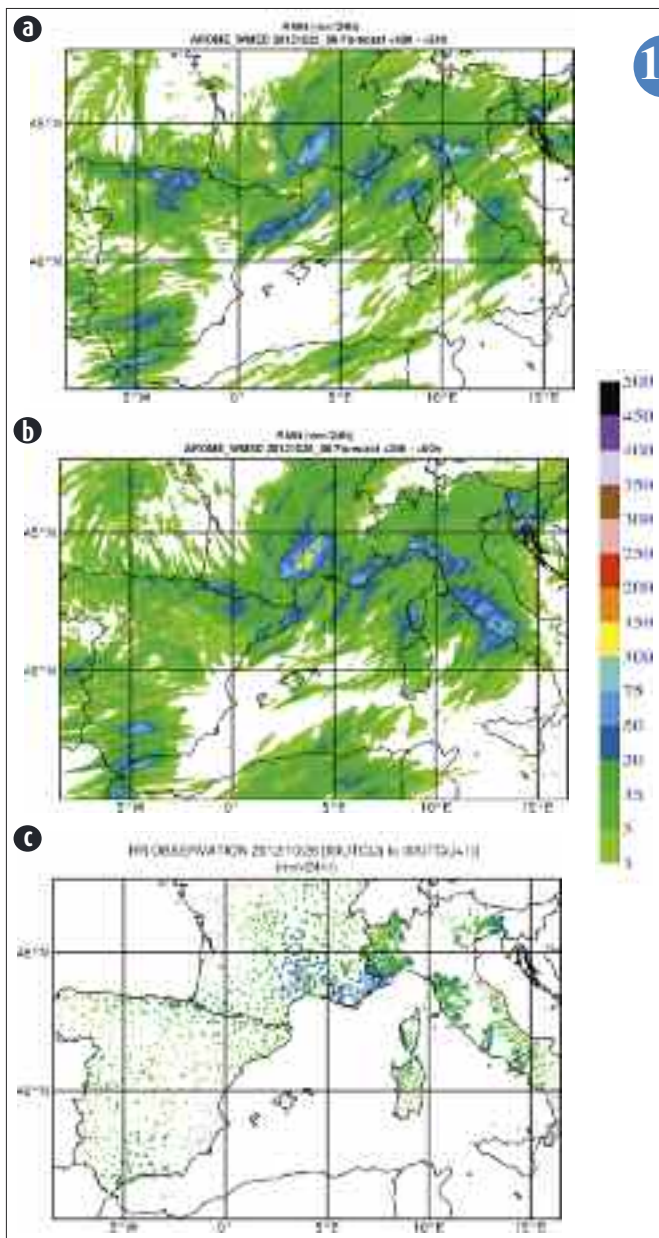
ALTIUS (Atmospheric Limb Tracker for the Investigation of the Upcoming Stratosphere) is a project of spectro-imager capable of measuring atmospheric concentration profiles of trace gases in the upper atmosphere. Developed by the Belgian Institute for Space Aeronomie (IASB), this atmospheric instrument will be embarked on a microsatellite intended for the observation of the stratospheric ozone and the other gaseous components since a heliosynchronous orbit to obtain the vertical distribution profiles of these gases. It consisted of a set of three spectral cameras making use of AOTFs (Acousto Optic Tunable Filter) in 3 channels UV (250nm in 400nm), Visible (400nm in 800nm) and Infrared (800nm in 1800nm).

A prototype of the visible channel of this instrument having similar optical characteristics (FOV, opening) but based on a linear design (lenses instead of mirrors) was realized with standard components. The test flight made by SAFIRE (French airborne environment research service) in January 2012 aboard the METEO FRANCE ATR managed to test the various modes of observations of the atmosphere (limb scattering, solar and stellar occultations) to highlight the possibilities of this instrument and prepare a possible operational campaign.

14

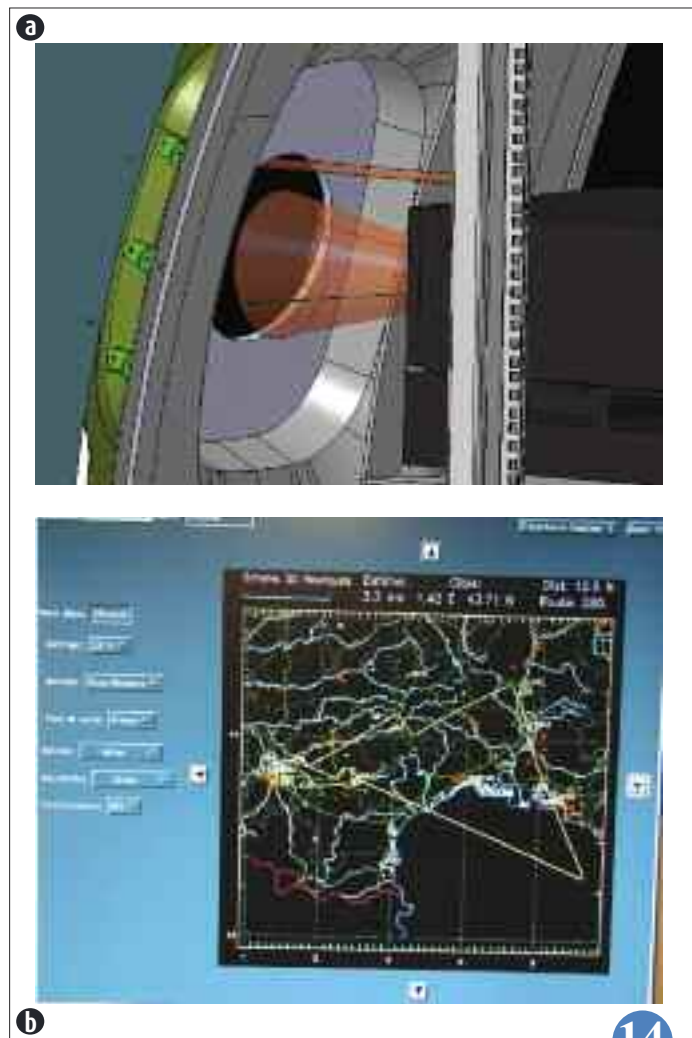






12

(a): Field of view of the spectral camera through the airplane window. Simulation under CatiaV5 made before integration of the instrument in the aircraft ATR operated by SAFIRE.  
(b): Real trajectory during the test flight made in January 2012: 1st phase: in circles above Toulouse to detect gases due to pollution. 2nd phase: straight and perpendicular to the sunset to analyse atmosphere during solar occultation.

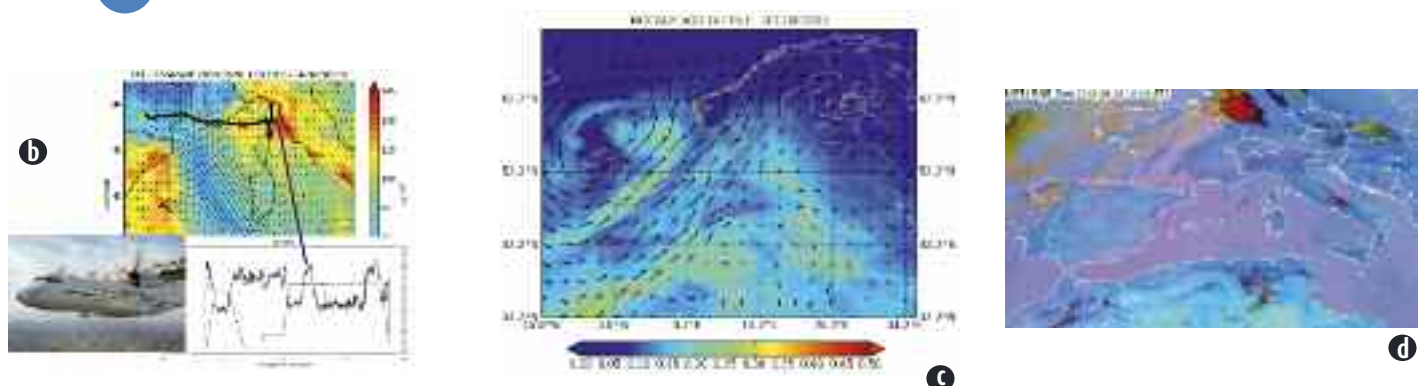


14

24 hour rain rate (mm) predicted by the AROMEWMED model at the 48 hour range (a) from the 25 October 2012 analysis, at the 24 hours range from the 26 October 2012 (b) and 24 hour rainfall rate observed the 26 October 2012 with rain gauges (c).

a) Ozone as measured by drifting balloons for 06 July 2012. Below, a photo of a drifting balloon during its launch at Martigues;  
b) Ozone field as given by MACC for 26 June 2012. The solid black line corresponds to the trajectory of the ATR-42 aircraft (photo). Below, the corresponding measurements where a maximum of ozone is detected in agreement with modelling outputs over the Gulf of Genoa;  
c) Aerosol Optical Depth as given by MOCAGE-aerosol on 29 June 2012, and  
d) METEOSAT RGB composites dust on 29 June 2012.

13



# Climate

---

After a period of intensive preparation and realization of new climate simulations within the context of the CMIP5 international project, a basis of the next IPCC report, time has come for the results analysis. These analyses have already led to about fifteen submitted papers, in particular for a special issue of Climate Dynamics prepared in collaboration with IPSL. The themes are covering in particular the detection/attribution of climate changes, the validation and projections of intra-seasonal variability and of cold spells over Europe, the simplified modeling of global coupling, ... Other studies using these simulations have also been initiated as one on the evaluation of the ability of models to reproduce clouds over Western Africa, or one on the contribution of Greenland melting on sea level.

In the field of climate regionalization, the important new fact is our participation to the international simulation exercise CORDEX. For this exercise, we have performed all the uncoupled simulations with a 50km resolution concerning Africa and the Mediterranean region. In the field of impact and adaptation to climate change, to note two new analyses relative to extreme events: the monitoring of dry spells in the Mediterranean region and a study concerning the Parisian sprawl dealing with the 2003 heat wave.

The year 2012 was also the one of the launch of the new configuration of the eurosip seasonal forecast system used operationally at Météo-France (system 4). The scores of this system reveal to be more often better than those of the previous system. Another study on the Arctic sea ice extent seasonal predictability also gives very promising results with In particular a good potential predictability of the anomaly at the end of summer. The theme of seasonal forecast regionalization was also tackled through a study of the predictability of water resources in metropolitan France.

1

---

## Climate and climate change studies

### Epicea Project: Adaptation of the City of Paris to climate change

The main objective of the project EPICEA, multidisciplinary study of the impacts of climate change at scale in the Paris area, was to evaluate the evolution of the climate of Paris in the context of climate change, and to establish quantitative relationships between urban development and climate related.

The use of an innovative methodology, incorporating a real representation of the city, helped refine climate projections leading ultimately to an increase of 2 to 4°C, depending on the rate of urbanization, of the temperature in Paris at the end of the 21st century and an increase of the number of heatwaves, 10 to 25 per year in Paris instead of one per year today.

Then, high resolution simulations (250m) of the 2003 heat wave in Paris, have modeled an urban heat island (UHI) late at night between the dense center and surrounding areas, around 4 to 7°C, and even within intramural Paris, 2 to 4°C. An “urban plume” has also occurred during this episode, warming to 2°C adjacent boroughs and municipalities around the direction of the wind.

Integrated into the adaptation component of the Climate Plan of the City of Paris, EPICEA helped give benchmarks on a theoretical level about the extent of changes in the intensity of ICU induced by actions on urban parameters (radiative properties of roofs and walls, vegetation watered and roadway mois-

tened). For instance, combining urban scenarios of large scale, the intensity of ICU would decrease by 1 to 2°C during a heat wave like that of 2003, with a maximal decrease of temperatures about 6°C at a time given.

2

---

## Influence of human activities on land surface evapotranspiration

Land surface evapotranspiration is a key component of the soil moisture budget. Yet, its multi-decadal evolution is still poorly understood, mainly due to the lack of observations. An original study conducted at CNRM-GAME has seen researchers reconstruct the global variations of annual mean evapotranspiration over the second half of the 20th century and attribute part of them to human emissions of greenhouse gases and aerosols.

Variations of evapotranspiration in space and time have been first estimated from 1950 to 2005 using a land surface hydrological model

driven by bias-corrected atmospheric reanalyses. Ensembles of 20th century climate simulations have been then achieved considering all or part of the observed radiative forcings: natural (NAT: volcanic aerosols and variations in solar activity), anthropogenic (ANT: greenhouse gases and aerosols due to human activities), natural and anthropogenic (ALL). These simulations indicate that the reconstructed variations of land surface evapotranspiration show space and time singularities (including increasing values in the mid-and-high latitudes of the Northern Hemisphere) which cannot be accounted for

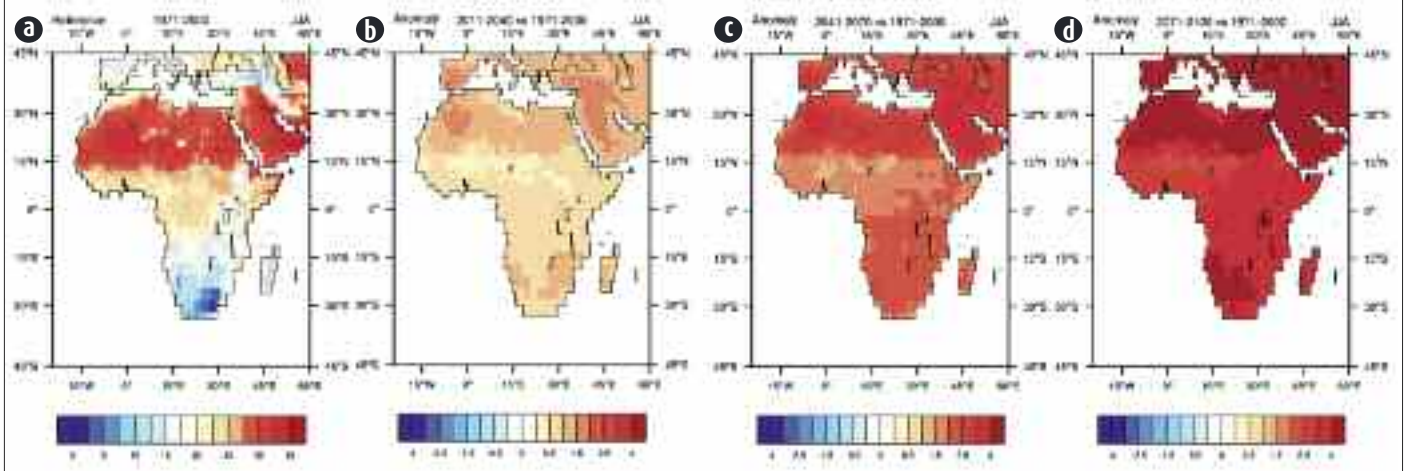
without invoking the anthropogenic forcings. It is the first time that the human influence on global evapotranspiration is thus objectively distinguished from other possible sources of multi-decadal variability. These results also emphasize that the long-term evolution of soil moisture cannot be understood only on the basis of precipitation variations.

3

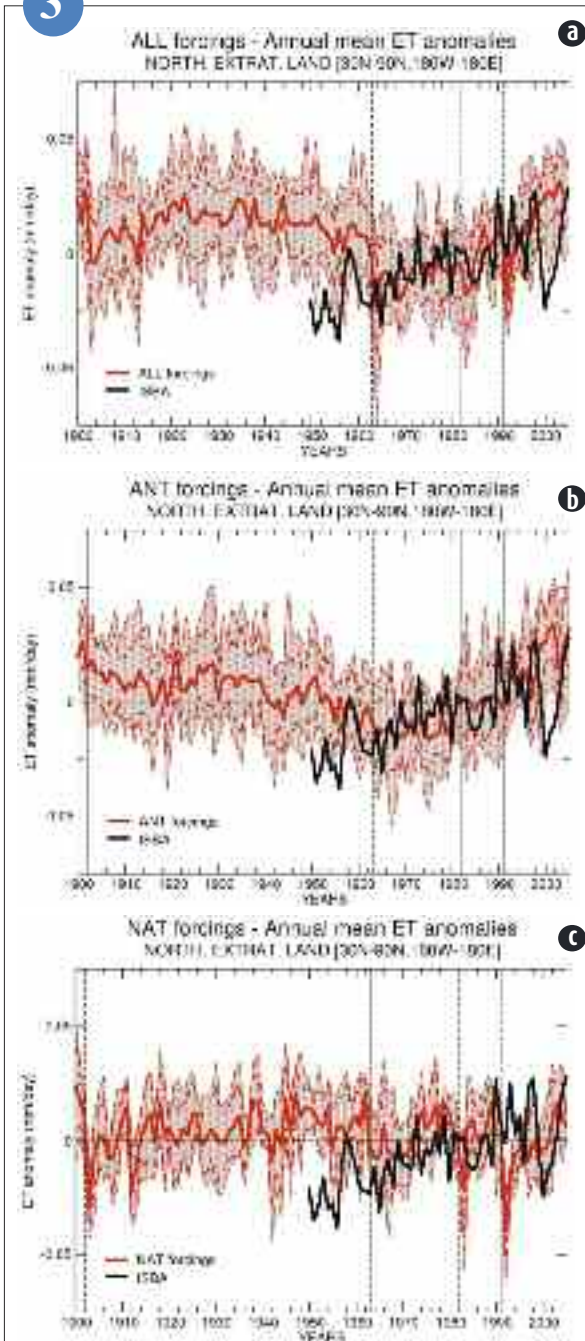


1

# CNRM – ALADIN – AFR 44 – RCP8.5 – Near Surface Air Temperature (deg C)

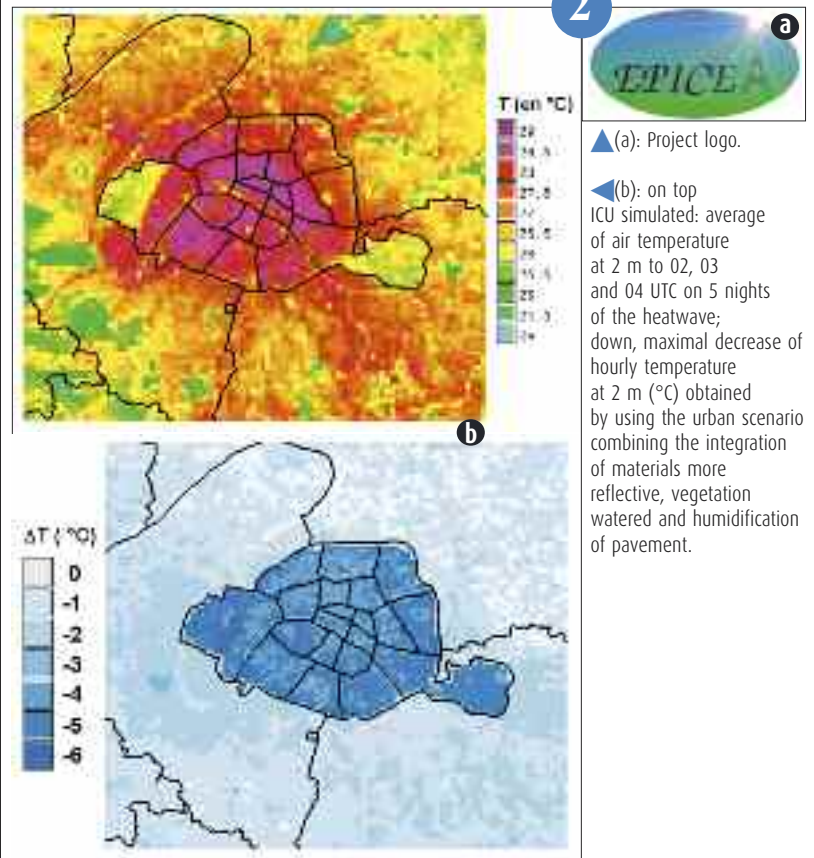


3



Near surface summer (June-July-August) temperature in a CORDEX-Africa simulation performed at CNRM with the ALADIN-Climat model driven with the CNRM-CM5 global model, for recent climate and RCP8.5 scenario: average over the period 1971-2100 (top left) and anomalies relative to this average for three different periods (2011-2040, top-right; 2041-2070, bottom-left ; 2071-2100, bottom-right).

2



(a): Project logo.

(b): on top ICU simulated: average of air temperature at 2 m to 02, 03 and 04 UTC on 5 nights of the heatwave; down, maximal decrease of hourly temperature at 2 m (°C) obtained by using the urban scenario combining the integration of materials more reflective, vegetation watered and humidification of pavement.



Evolution of annual mean evapotranspiration anomalies (relative to the 1971-2000 climatology) averaged over the Northern Hemisphere extra-tropical land areas, reconstructed (in black) from an off-line simulation of the ISBA land surface model driven by observed atmospheric forcings, and simulated (in red) in ensemble climate simulations of CNRM-CM5 driven by observed radiative forcings:  
 (a): ALL (all forcings),  
 (b): ANT (anthropogenic forcings only),  
 (c): NAT (natural forcings only).  
 The thick line denotes the ensemble mean anomalies, the dashed lines the ensemble mean  $\pm 1$  standard deviation, the shading the deviation between the minimum and maximum anomalies among the members of the ensemble.

## Impact of global climate change on cold spells in Europe

In line with a negative phase of the North Atlantic Oscillation, Europe has experienced particularly cold temperatures during the three last winter seasons, which raised some questions about the fate of such cold events in a warming climate.

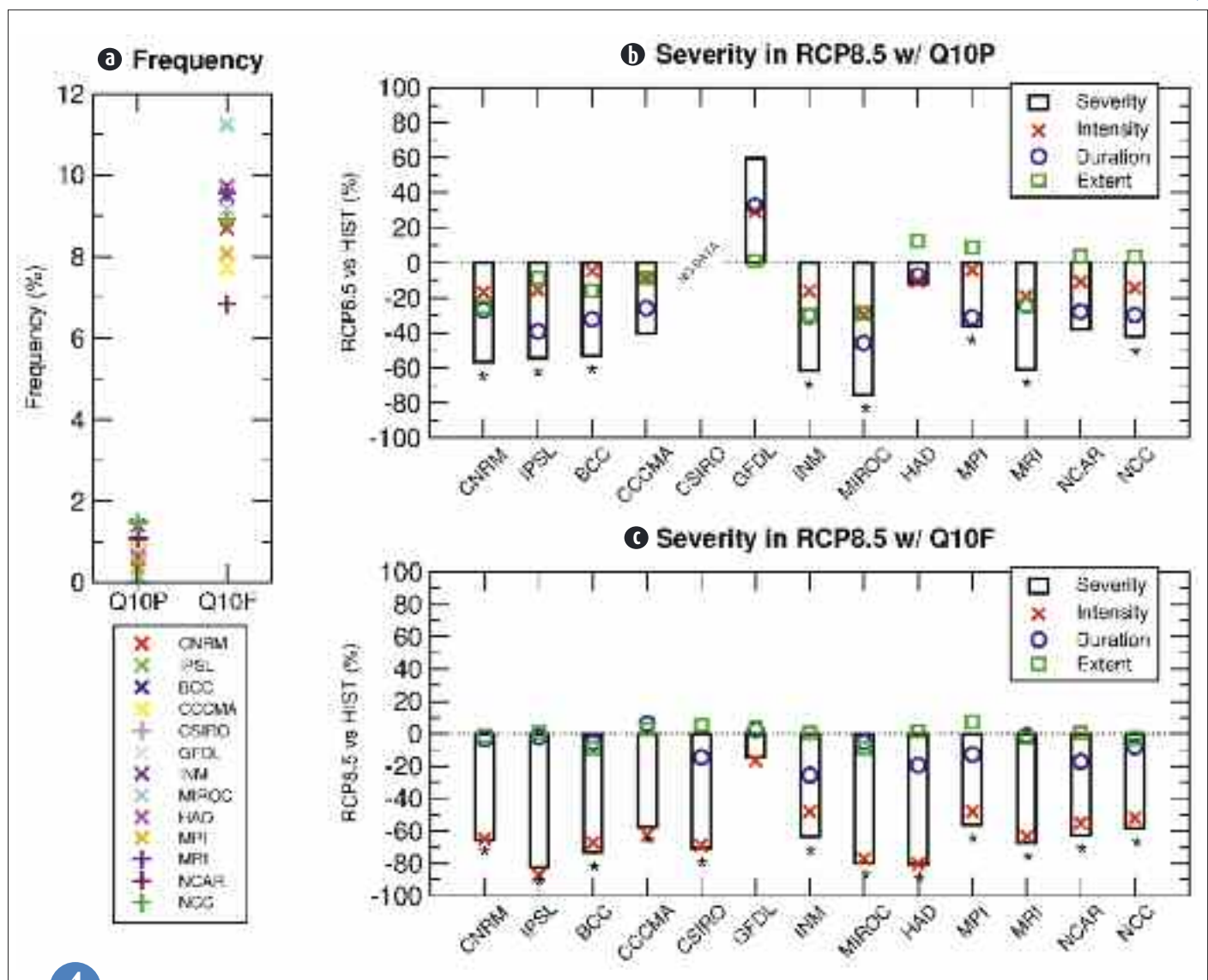
A recent study at CNRM-GAME has analysed the wintertime daily minimum temperature (Tmin) outputs from a subset of CMIP5 global climate models. Both model biases and responses in a warming climate have been discussed using historical simulations and the RCP8.5 scenario. A percentile-based index (10th percentile of Tmin, Q10) with duration and spatial extent criteria has been used to define cold spells. In line with the projected rise of mean temperature, cold spells derived from the present-day (1979-2008) Q10 are projected to be much less frequent and, except in one model, less severe at the end of the RCP8.5 scenario. When cold spells are defined from the future (2070-2099) Q10, all models simulate a decrease of their intensity

linearly related to the seasonal mean warming. Beyond the ensemble mean response, there is however a significant inter-model spread in the magnitude of the cold spell response, which is partly due to uncertainties in the snow-albedo feedback and in the response of the North Atlantic large-scale atmospheric circulation.

In summary, though some projections suggest a trend towards a negative phase of the North Atlantic Oscillation, all models predict a decrease in the frequency and/or severity of cold spells over Europe at the end of the 21st century, which is mainly due to a shift in the daily temperature distribution that is more or less pronounced according to the selected concentration scenario.

4

- (a): Frequency of cold spell days over western Europe in winter (DJFM) using a Q10 threshold estimated over 1979-2008 (Q10P) and 2070-2099 (Q10F) respectively;  
 (b): Response of 2070-2099 cold spell statistics for Q10P in RCP8.5 simulations, expressed as the departure from present-day climate (%). Stars indicate the 90% confidence level for severity differences based on a Student t-test;  
 (c): Same as b but for the Q10F threshold. Cold spell severity is diagnosed as the product of duration and intensity weighted by the spatial extent.



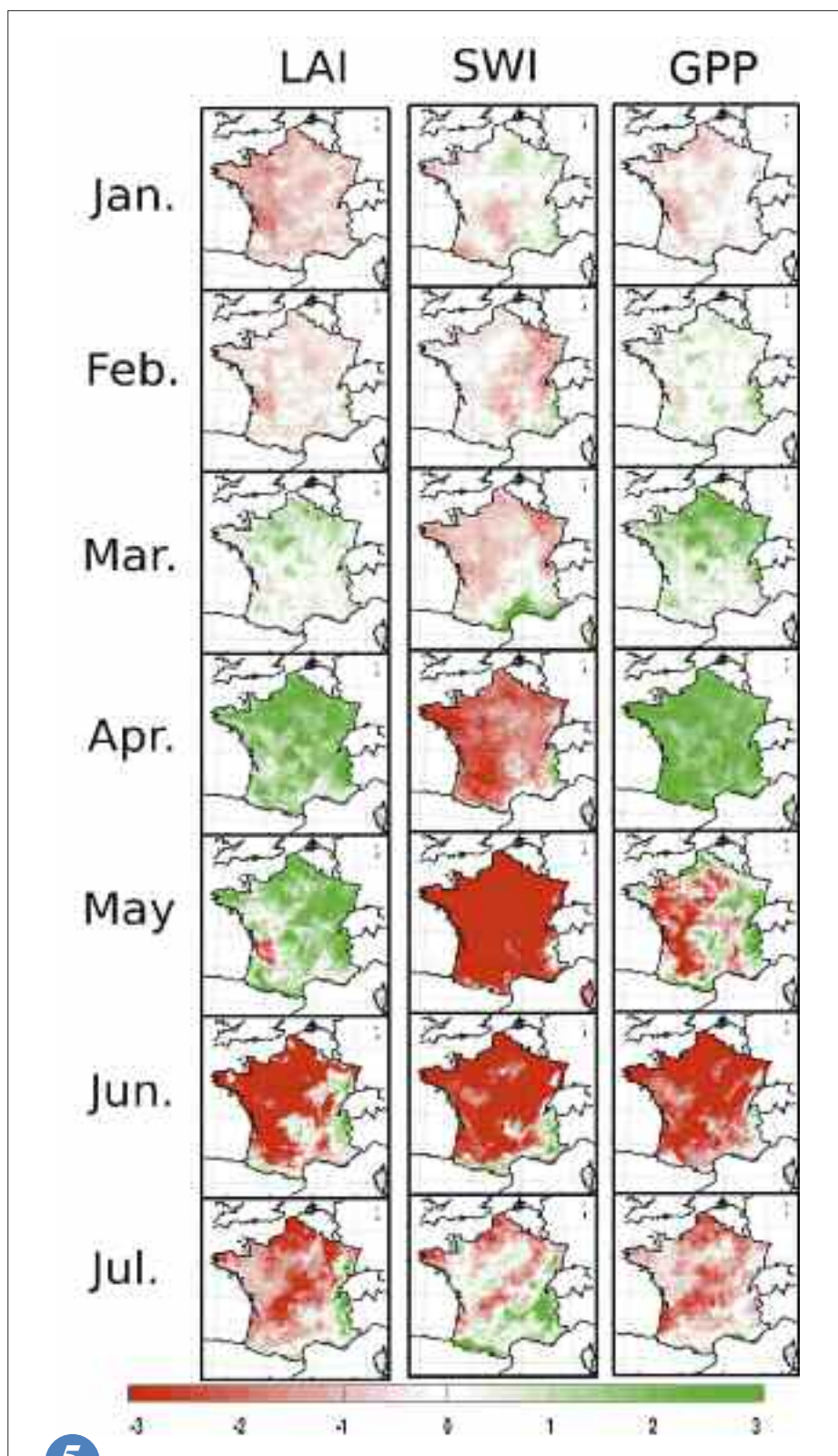


## Drought monitoring for the Euro-Mediterranean domain using land surface models and remotely sensed data

Can modelled land biophysical variables and river discharge, together with satellite data, help characterize drought events over the Euro-Mediterranean area?

In order to answer this question, coupled simulations of the ISBA-A-gs land surface model and of the TRIP hydrological model were performed for the 1991-2008 period. ISBA-A-gs was driven by surface atmospheric variables provided by the ECMWF ERA-Interim reanalysis. A soil moisture and LAI climatology was built, together with river discharge. The ERA-Interim data were first evaluated over France using a high-resolution atmospheric reanalysis. The impact of precipitation uncertainties on river discharge and vegetation variables was quantified. The soil moisture and LAI simulations produced by ISBA-A-gs were compared with in situ and satellite observations, and with the IPSL ORCHIDEE model outputs. The simulations reproduced the inter-annual variability observed by satellite products. In particular, the soil moisture anomalies presented significant correlations with LAI anomalies at key periods, more extensively with the model than with the observations. Using ISBA-A-gs together with TRIP improved the low water discharge simulations. The impact of extreme events on LAI was captured by the satellite products, for example during the 2003 summer drought. The models were able to simulate this anomaly but tended to overestimate the length of the negative anomaly: in October, the simulated anomaly was still markedly negative while the observations showed a regrowth of the vegetation. Future model upgrades may help solve this problem.

5



5

Scaled monthly anomalies of LAI from May to October 2003 over the Euro-Mediterranean area, simulated by ISBA-A-gs and ORCHIDEE, and observed from space by satellites (GEOLAND2 product based on SPOT-VGT). Warm colours correspond to negative anomalies (LAI values lower than the 1991-2008 climatology).

## Characterization of clouds observed and simulated in CMIP5 and of their radiative feedbacks in West Africa

Convection is the main source of long life clouds in the tropics. Their contribution to the energy balance via their radiative impact is important, but poorly understood. Vertical and meridian distribution of cloud occurrence and their seasonal evolution have been documented by analyzing the measurements of a radar (CloudSat) and a lidar (CALIPSO) belonging to the A-Train spatial constellation.

The observations highlight the expected presence of many convective clouds associated with rain (cumulonimbus and squall lines) and low level cloud layer on the continent during the monsoon season. However, this region is also characterized by the presence of cirrus and mid-level clouds, especially above the Sahara. If the presence of this type of cloud was inferred in the 80 by using geostationary satellite measurements, the new available sensors allow characterizing with a greater accuracy their physical properties. Above the ocean, a layer of Stratocumulus is observed.

Clouds and associated feedbacks are important regulators of climate. This is why the representation of clouds in models participating in the inter-comparison exercise CFMIP has been evaluated. It appears that most of the models capture to some extent the observed cloud structure. The maximum in cloud fraction related to the deep convective systems is collocated with the mean inter-tropical position. None of the models manages to reproduce the observed amount, even if some of them (CanAM4, IPSL-CM5B-LR, MIROC5) partly capture their occurrence. The stratocumulus over the Gulf of Guinea are also challenging for most of the models, as they are often not deep enough when they occur.

Fluxes and in particular the surface fluxes respond directly to the cloud occurrence, but they also undergo the influence of stratification of aerosols and thermodynamic properties of the

atmosphere. The solar flux in this region is characterized by a strong meridional gradient. These variations are not accurately simulated, with departure from observations larger than several tens of  $\text{W m}^{-2}$ . Over the Guinea coast, a large number of models underestimate the incoming solar flux in response to a too thin and reflective cloud layer. Over the Sahara, on the contrary, most of the models overestimate this radiative flux in response to lack of mid-level clouds and also in connection with a possible inadequate processing of aerosols in this region.

The south-north gradient infrared flux is weaker and most models have a reasonable representation of it. However, further north (Sahara) bias in incoming thermal flux increases significantly and reaches comparable values to those obtained for solar radiation, with an underestimation in most models. Again the lack of mid-level clouds is at least partially responsible for this bias.

If bias in the representation of clouds and associated feedbacks has been identified in the models, their explanation remains to be perfected. This explanation requires a simultaneous analysis:

- of observational data sets (ground-based, airborne or satellite) to be able to better document the involved processes in the lifecycle of the various cloud types and their impact;
- of numerical simulations to better understand the origin of drawbacks and then propose improvements in physical parameterizations.

6

## An estimation of Future Global Sea Level Rise Due to Greenland Ice Sheet Melting

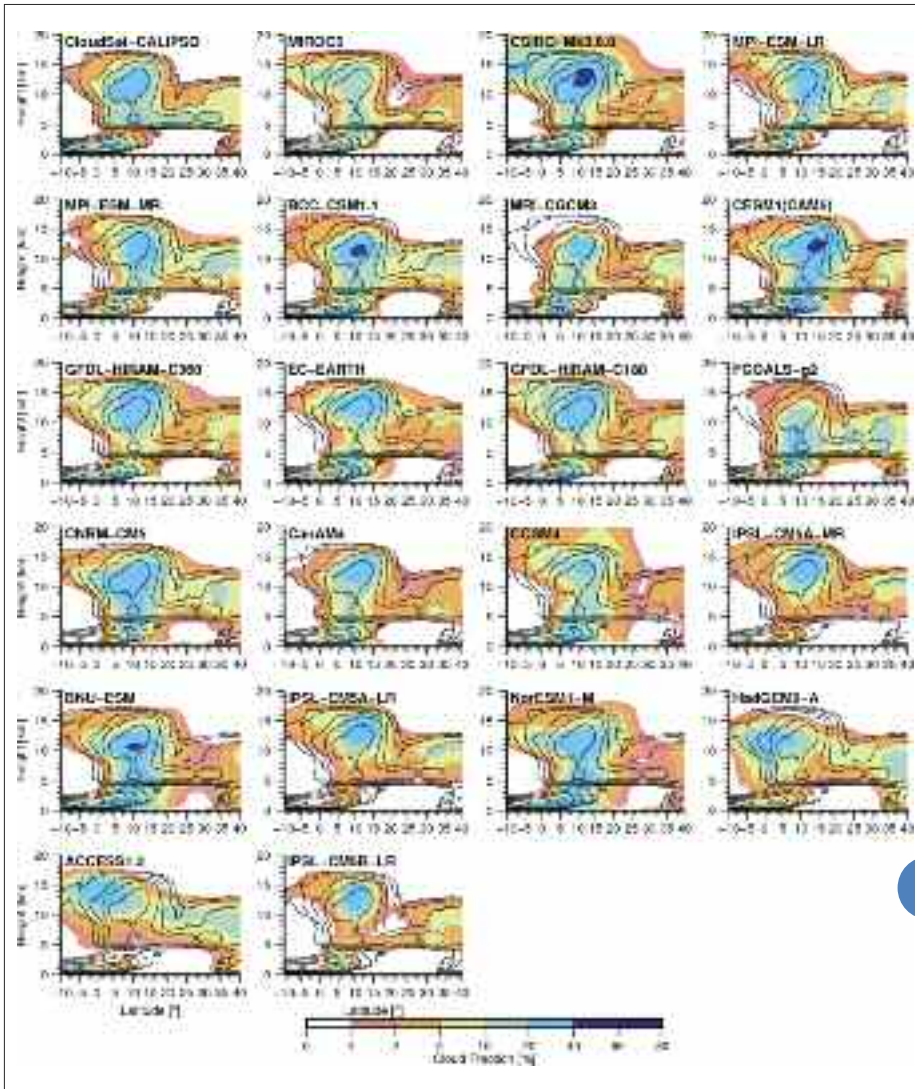
Neglecting dynamics and basal melt, the difference between future and pre-industrial surface mass balance of the Greenland ice sheet can provide a reasonable estimate of its future contribution to global sea level rise rate until 2100.

To estimate this contribution, climate simulations performed with CNRM-CM5.1 in the framework of CMIP5 (as the base of the upcoming IPCC 5th assessment report) were used for 1850-2100. The model has a horizontal resolution of about 150km, and two scenarios RCP4.5 and RCP8.5 were considered for 2006-2100. The surface mass balance was evaluated in two different ways: directly as simulated by CNRM-CM5.1 or by using the hybrid snow model CROCUS driven by surface atmospheric forcing provided by CNRM-CM5.1. A statistical technique was developed to downscale the surface mass balance to a resolution of 15km.

For the present climate, the simulated sea level rise rate, at +0.27mm/year, is slightly too low compared to known contemporary values. The total contribution of the Greenland ice sheet melting to future sea level rise in the 21st century is respectively +5cm (RCP4.5) and +6.5cm (RCP8.5). It should be noted that for the RCP8.5 scenario, in contrast to RCP4.5, the melting rate of Greenland is expected to accelerate very rapidly after the 21st century. This acceleration phenomenon is amplified both by the significant temperature increase over the Greenland ice sheet and also by topographic changes induced by the shrinking of the ice sheet.

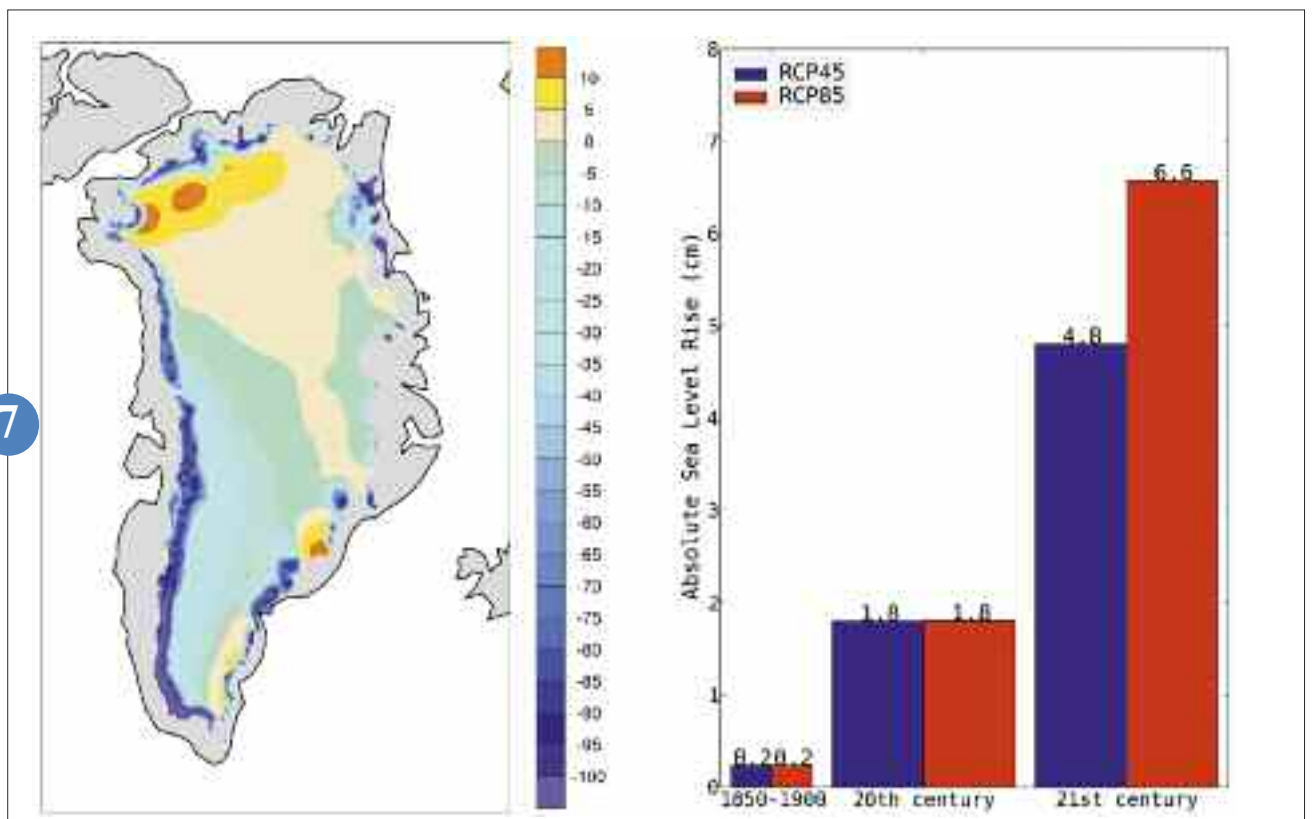
7





6 Scaled monthly anomalies of LAI from May to October 2003 over the Euro-Mediterranean area, simulated by ISBA-A-gs and ORCHIDEE, and observed from space by satellites (GEOLAND2 product based on SPOT-VGT). Warm colours correspond to negative anomalies (LAI values lower than the 1991-2008 climatology).

Greenland ice thickness change (m) for the end of the 21st century for RCP8.5 scenario (left) and the contribution to global sea level rise for 1850-1900, 20th and 21st centuries (right).



---

## Seasonal and climate forecasts

### A new model for seasonal forecasting in Eurosip system

Since 2008, Météo-France contribution to Eurosip, a seasonal forecasting consortium including ECMWF, Met-Office and NCEP, is produced with system 3. This system is characterized by ARPEGE-climat v4 with horizontal resolution 320 km coupled with OPA v8, an ocean model from CNRS with horizontal resolution 2°.

Since early 2010, CNRM has prepared a new system, starting from the model used for our new IPCC simulations: ARPEGE-climat v5 at 160 km coupled with NEMO at 1° resolution. Specific adaptations to ECMWF computer have been brought, and Mercator-Océan has prepared a new assimilation scheme. The main progress is the horizontal resolution doubling. The constraint on ocean re-analyses imposes the hind casts to start in 1991, versus 1979 for system 3. But the ensemble size increases from 11 to 15 members (41 to 51 members in real-time production. With such a short common evaluation period (22 years), one must restrict to average scores over very large domains. Figure “a” shows correlation for surface temperature over 60S-30S (HS), 30S-30N (TR) and 30N-60N (HN). Figure “b” shows the same for precipitation. One can see a general improvement with system 4, except for northern mid-latitude precipitation in winter.

System 4 has switched to operational production in August 2012, and has replaced system 3 in the multi-model since October 2012 forecasts.

8

### Seasonal predictability of the Arctic sea ice

The recent decline of the summer Arctic sea ice cover is one the most obvious indicators of climate change. In September 2012, sea ice extent set a new record minimum since satellite observations began in 1979. Was such a sea ice anomaly predictable a few months in advance?

In order to try to answer to this question, seasonal forecasts of the September sea ice cover have been replayed over the period 1990-2009 with the CNRM-CM5.1 atmosphere-sea ice-ocean global coupled model. Every year, on May 1st, the coupled model is initialized close to the observed state of the system: to do so, an ocean-sea ice reconstruction has been produced using the ocean-sea ice component of CNRM-CM5.1, NEMO-GELATO. With this reconstruction, it is possible to initialize sea ice thickness, which is not known from satellite observations over the whole period.

Forecast skills for September sea ice extent are significantly high. This implies that sea ice can be reasonably predicted from initial conditions, especially from spring sea ice volume.

Similar seasonal forecasts of March sea ice cover have been run, initialized on November 1st every year. Forecast skill scores for these predictions are comparable to those of September forecasts. They suggest that predictability of March sea ice conditions arises from the ocean initial state in the Fall, especially in the marginal seas that are initially ice free.

9

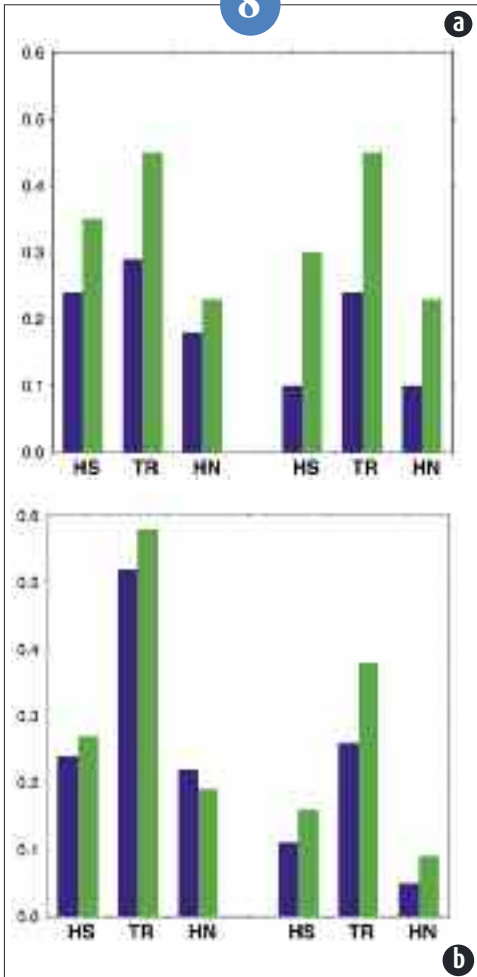
### Feasibility study of a seasonal forecasting of water resources in mainland France

Management of water resources has become a major issue in some French regions, especially during the summer when the needs of agriculture are important. Efforts for the monitoring of the resource (especially for shallow soils) have been realized in recent years by the development and operational implementation of the hydro-meteorological chain Safran-Isba-Modcou. This chain consists of a fine-scale meteorological analysis system, a surface module and a hydrological model across France (the latter being developed in cooperation with Mines Paris-Tech).

Different sources of predictability of the hydrological system, as well as the contribution of seasonal forecasting in relation to climate prediction, were evaluated for the spring season. Scores were significant downstream mountain areas or in the Paris basin, the initial state of the snowpack and the main aquifers are the main sources of predictability (initial soil moisture is playing a significant role in some isolated areas). The use of meteorological seasonal forecasts improves the scores in the north of France, whether for soil moisture or river flows, while the results are degraded in the south of France. The study of the summer season showed results consistent with the spring season (predictability related to the snowpack in this case being limited to areas downstream of the highest mountains). These studies will be pursued by works on the sources of uncertainty associated with meteorological forecasts and the study of cases studies with pilot users.

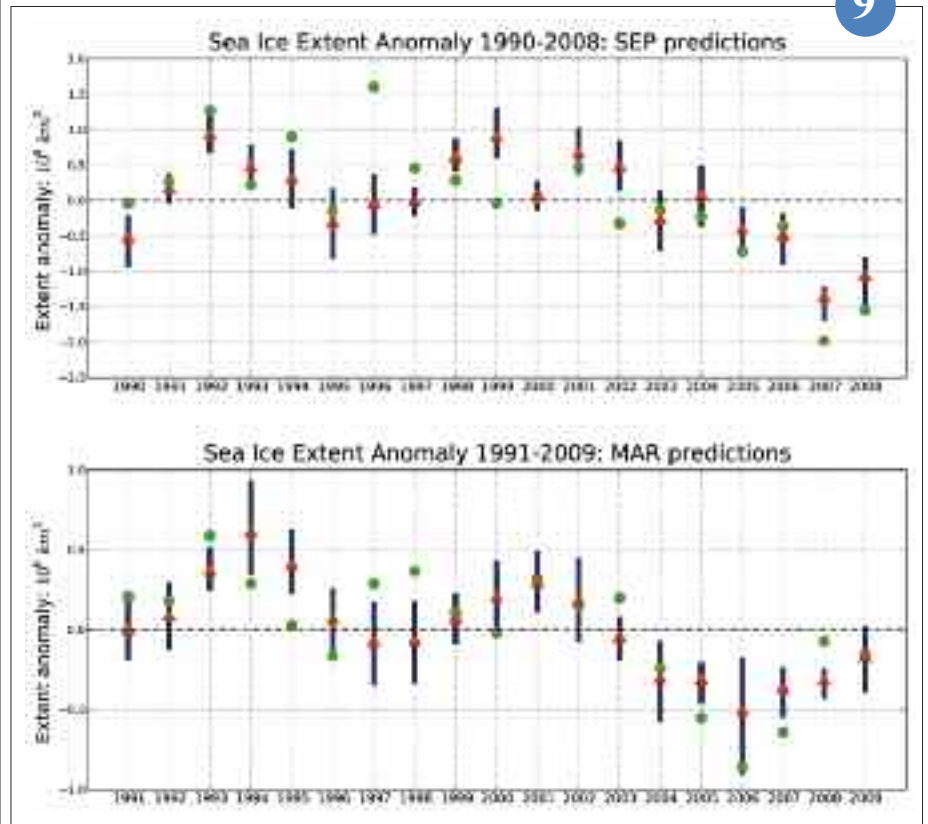
10

8



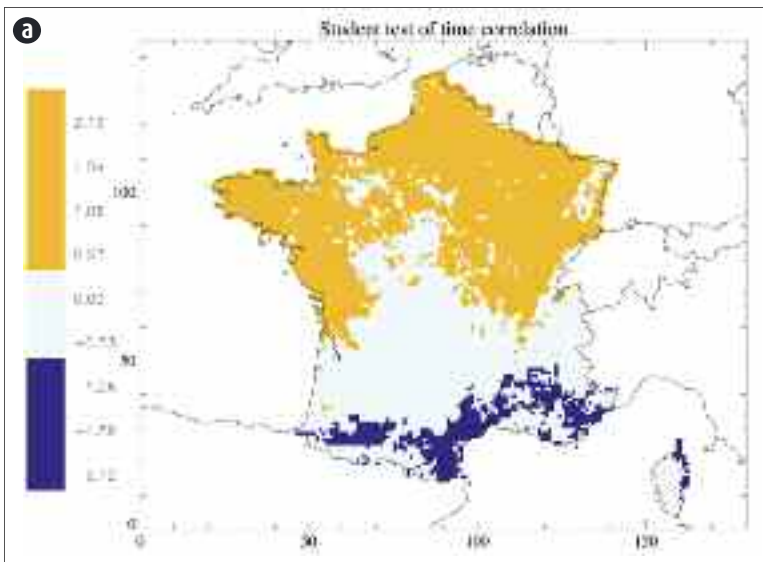
(a): Correlation for 3 latitude bands 90S-30S, 30S-30N and 30N-90N for surface temperature forecasts in DJF (left) and JJA (right); start dates are November (resp. May) 1st for 1993-2007; system 3 in blue, system 4 in green.  
(b): As Fig. "a" for precipitation.

9

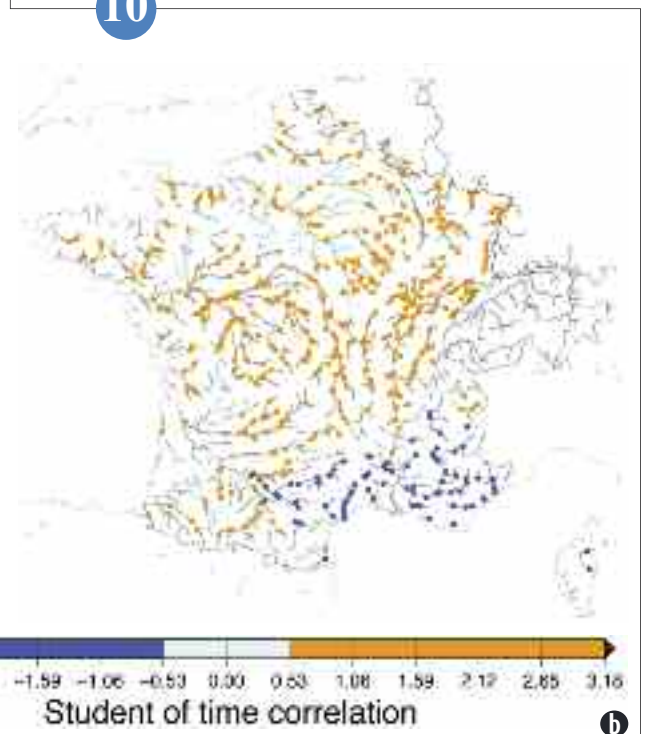


Forecast Arctic sea ice extent anomalies for September (top) and March (bottom). Red triangles: predicted anomalies (gray bars: ensemble standard deviation). Green dots: observed anomalies (NSIDC).

10



(a): Impact of the use of seasonal forecasts for the forecasting of soil moisture in spring (measured by a test on the differences in inter-annual correlations)  
Yellow: the scores are significantly improved by the use of seasonal weather forecasting. Dark blue: significant degradation scores.  
(b): Impact of the use of seasonal forecasts for the forecasting of river flows in spring (measured by a test on the differences in inter-annual correlations)  
Yellow: the scores are significantly improved by the use of seasonal weather forecasting. Dark blue: significant degradation scores.





# Chemistry, aerosols and air quality

In the field of atmospheric chemistry, the most notable fact is our first participation to the international inter-comparison exercise ACC-MIP (Atmospheric Chemistry and Climate). Led with the MOCAGE model including the whole atmospheric chemistry, this exercise complement the CCM-Val exercise performed again recently with the new CNRM-CCM model. Also to note climate change impact studies on air quality led within the context of the European project IMPACT2C. At the regional scales, two studies were achieved, the first concerning the impact of aerosols on the Mediterranean climate and the second the CO<sub>2</sub> simulation over the Parisian region.

Also in the field of air quality, the measurement field experiment TRAQA, aiming at quantifying the pollutant transport and mixing processes in the low Mediterranean troposphere, took place during summer 2012. Seven intense observing periods with surface, balloons and plane measurements were performed and the first analyses were initiated.

The year 2012 was also marked by important progresses accomplished in the context of MACC-II project. This concerns in particular the publication of the work performed on the characterization of the stations representative for ozone ensemble forecast, a method used daily. Moreover, the results of a first long simulation with the IFS model including MOCAGE chemistry, realized within the context of this project, shows a good stability of the code and a realistic representation of chemical variables.

1

## The ACCMIP Project

The ACCMIP (Atmospheric Chemistry & Climate Model Intercomparison Project) international project is complementary to the CMIP5 Climate Model Intercomparison Project. By documenting the long-term changes in atmospheric composition, it will contribute to the IPCC (Intergovernmental Panel on Climate Change) Fifth Assessment Report.

ACCMIP gathers about fifteen models, including Météo-France's MOCAGE model. Every participating team is asked to perform simulations describing the evolution of the atmospheric chemical components. These simulations consist of decadal time slice experiments on past and future.

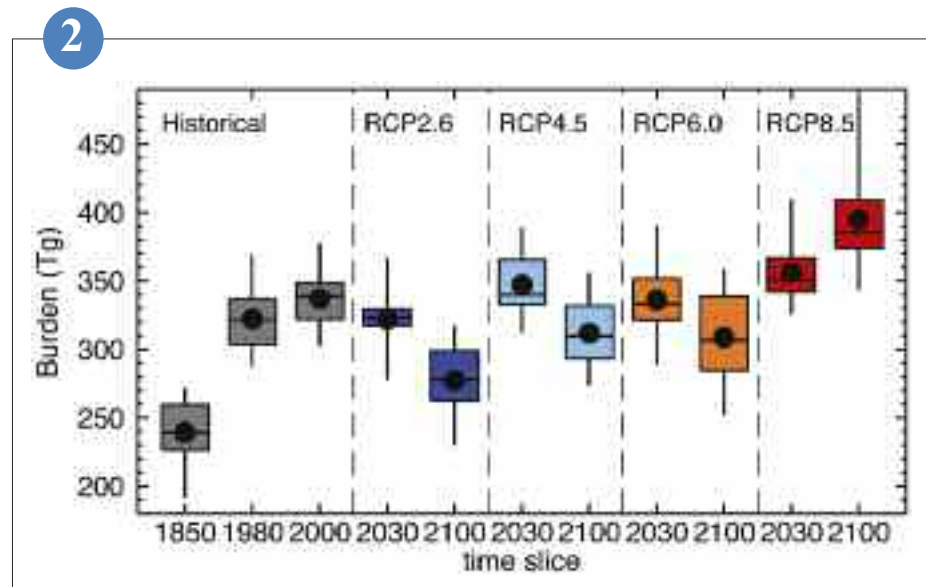
The historical period goes from the pre-industrial (1850) era to present-day (2000). The analysis of the historical period is done by evaluating how coherent and dispersive the models are. The ensemble results are then compared to the available observations. The robustness of diagnostics is then deduced, as well as the impact of human activities on the current atmospheric chemical composition.

For the future period, projection simulations follow different scenarios, for both pollutant emissions and climatic trends. These scenarios, from the most optimistic one to the most pessimistic one, are based on the "Representative Concentration Pathways". The purpose is here

to give an estimation of the range of influences that eventual emission reduction policies could induce.

ACCMIP applications go beyond the strictly geophysical scope and aim at an interdisciplinary approach. Analysis work began in 2012 and covers a wide range of applications, from the additional radiative forcing caused by a modified chemical composition of the atmosphere, to the impact of the degradation of air quality on health or crops.

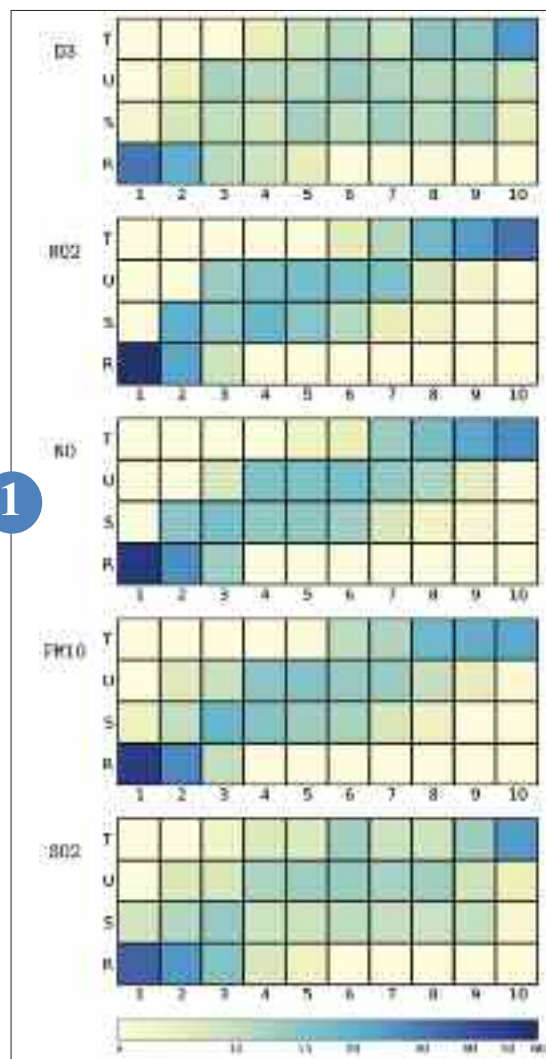
2



Modelled tropospheric ozone burdens for the different scenarios and time slices. The box, whiskers, line and dot show the interquartile range, full range, median and mean burdens. From Young and al, 2012: P. J. Young, A. T. Archibald, K. W. Bowman, J.-F. Lamarque, V. Naik, D. S. Stevenson, S. Tilmes, A. Voulgarakis, O. Wild, D. Bergmann, P. Cameron-Smith, I. Cionni, W. J. Collins, S. B. Dalsøren, R. M. Doherty, V. Eyring, G. Faluvegi, L. W. Horowitz, B. Josse, Y. H. Lee, I. A. MacKenzie, T. Nagashima, D. A. Plummer, M. Righi, S. T. Rumbold, R. B. Skeie, D. T. Shindell, S. A. Strode, K. Sudo, S. Szopa, and G. Zeng : Pre-industrial to end 21st century projections of tropospheric ozone from the Atmospheric Chemistry and Climate Model Intercomparison Project (ACCMIP), Atmos. Chem. Phys. Discuss., 12, 21615-21677, 2012, doi:10.5194/acpd-12-21615-2012.

European air quality monitoring networks are quite heterogeneous. In order to assess the spatial representativeness of the measurements (greater for a rural site far from emission sources than for a polluted site perturbed by nearby emissions sources), a classification of European monitoring sites has been achieved. For each pollutant (considered separately), monitoring sites have been classified using an automated and "objective" procedure based on their passed measurements (Joly and Peuch, 2012). For each pollutant, the classes obtained (abscissa: from 1 to 10) are here confronted to the "subjective" metadata that characterize the sites (ordinate: R=rural, S=sub-urban, U=urban, T= traffic). The colour scale shows for each type of site the distribution of the different classes, in percentage. This objective classification of European monitoring sites is used in the framework of the MACC project, for the validation of the models, and for the in situ data analysis.

1



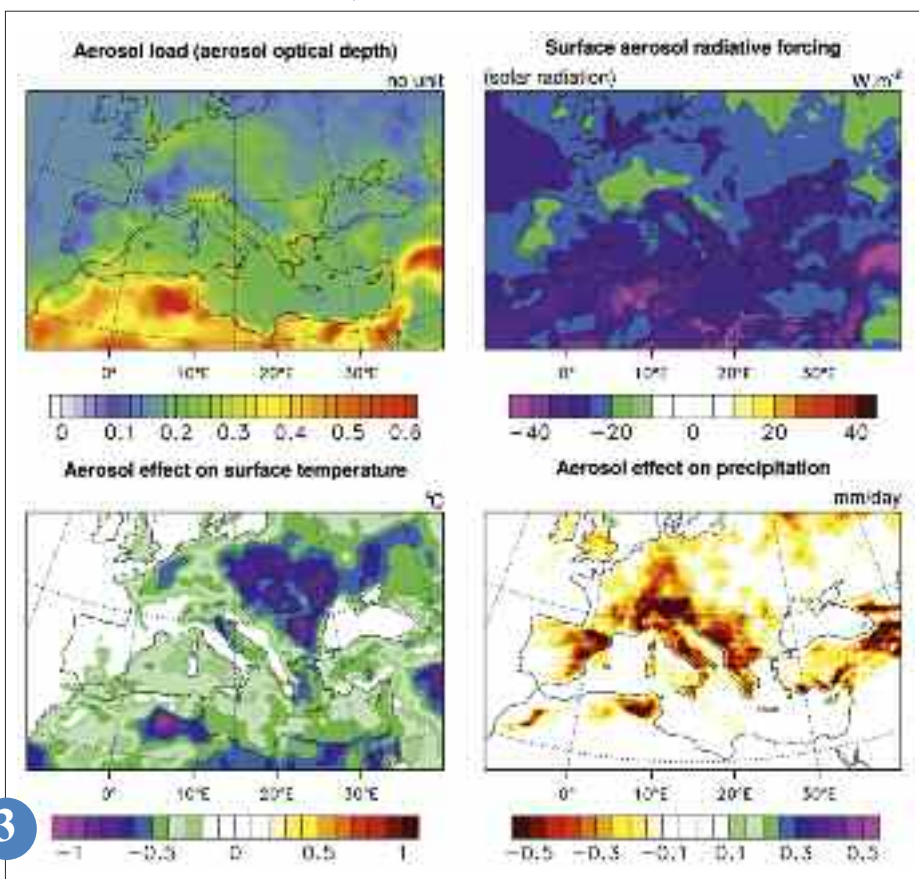
## Aerosol impact on the regional climate

Aerosols, which show a high spatial and temporal variability, can modify the radiative budget and climate. Studies at the regional scale can enable us to better estimate their effects.

The Mediterranean basin is affected by strong aerosol loads, coming from various sources (desert dust from the Sahara, sea salts, industrial pollution and biomass burning from Europe, forest fires, ...). Simulations have been carried out using a regional climate system model (ALADIN-Climat for the atmosphere, NEMOMED8 for the ocean and TRIP for the rivers). These different aerosols are included through realistic climatologies, deriving from both satellite products and chemistry models. The figure presents the mean effects for summer (when the aerosol load is maximal), in terms of radiative forcing, surface temperature and precipitation.

Aerosols absorb and scatter the incoming solar radiation, causing not only a decrease in surface radiation and temperature (direct effect), but also changes in the atmospheric circulation. Ocean-atmosphere coupling enables us to highlight the decrease in sea surface temperature due to aerosols, and its consequences on the hydrological cycle (reduction in evaporation and precipitation). This study in the framework of the ChArMEx project confirms the importance of aerosols in the Mediterranean climate variability, and will be extended with the addition of an interactive aerosol scheme in ALADIN-Climat.

Average summer aerosol effects simulated with the regional climate system model: aerosol load (aerosol optical depth, top left), aerosol surface radiative forcing ( $W.m^{-2}$ , top right), aerosol effect on temperature ( $^{\circ}C$ , bottom left) and precipitation ( $mm/day$ , right). Bottom maps represent differences between simulations with and without aerosols.



3

## Numerical modelling study of European air quality in current and future climates

In order to study the impacts of climate change on regional air quality, atmospheric chemistry models rely on global or regional climate models. In order to interpret air quality simulations in a future climate, it is a prerequisite to assess how realistic air quality hind-casts are when driven by forcings from climate models for the current period.

Three six-year simulations for the current climate 2000-2010 have been run with the model of Météo-France, MOCAGE. These simulations differ by the meteorological forcings used, either operational meteorological analyses or outputs from climate simulations. The changes in meteorology on atmospheric fields (temperature, etc...) and in emissions and deposition processes (deposition velocities, volatile organic compound emissions, etc...) that depend upon meteorology affect the horizontal and vertical distributions of species. Reliable skill indicators have been estimated for the simulations run with climate forcings (mean bias, mean normalized bias, RMSE, deviation standards, number of exceedance days). They can thus be used to interpret simulations for future periods.

In the 2030s and 2050s, the changes in meteorological parameters affect the quantities and distributions of pollutants in the atmosphere, but the future evolutions in European and global emissions also play a significant role. Faced with climate change and increased emissions in some countries in the world, the impacts of European policies for reducing anthropogenic emissions are mitigated, depending on the regions and the pollutants due to the respective influence of local emissions and of long-range transport of pollutants.

4

## Simple modelling of transient climate response to increasing atmospheric carbon dioxide

Determining the response of the climate system to an imposed external perturbation is a major challenge in climate science. The global and annual mean surface temperature response is a useful metric to determine the magnitude of a climate change. Coupled atmosphere-ocean general circulation models are the most comprehensive tool to study this response but they are computationally expensive. Alternatively, energy-balance models can be used to emulate the response of a coupled model.

Recently, we have shown that the response of the global surface air temperature has two time scales, and that response can be viewed as the result of a two-layer simple model, the first layer representing the atmosphere and the upper ocean and the second the deep ocean. In this study, we show that it is possible

to calibrate the few parameters (radiative forcing, global feedback, ...) of this energy-balance model in order to reproduce the responses of all coupled models participating in CMIP-5. The framework described in this work is a new method for estimating the global parameters of climate sensitivity of the coupled models.

The use of this framework can allow tackling a fundamental issue: quantify the relative part of each parameter in the spread of the responses of the climatic models and contribute thus to estimate the uncertainty associated with the climatic projections.

5

## CO<sub>2</sub> dispersion modelling over Paris region

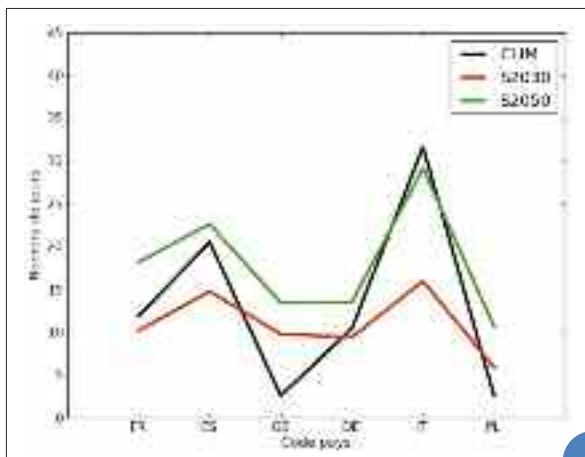
Accurate simulation of the spatial and temporal variability of tracer mixing ratios over urban areas is essential in order to utilize CO<sub>2</sub> measurements in an atmospheric inverse framework to better estimate regional CO<sub>2</sub> fluxes.

The meso-scale atmospheric model Meso-NH has run at 2km horizontal resolution during one a year period over the Ile-de-France province, coupled with the Town-Energy Balance (TEB) urban canopy scheme and with the Interactions between Soil, Biosphere and Atmosphere CO<sub>2</sub>-reactive (ISBA-A-gs) surface scheme. It has been evaluated during the March field campaign of the CO<sub>2</sub>-MEGAPARIS project, in order to analyze the impacts of urban heat island and urban-rural contrasts on the CO<sub>2</sub> dispersion. Boundary layer heights (BLH) at urban, sub-urban and rural sites are well captured by the model, especially the onset time of the BLH increase and its growth rate in the morning, that are essential for tall tower CO<sub>2</sub> observatories (Fig. a).

Hence, at Eiffel tower, the observed spikes of CO<sub>2</sub> maxima (in black, Fig. b) occur every morning exactly at the time at which the boundary layer growth reaches the measurement height (310m). These spikes have a very short duration as the BLH grows quickly, favouring the rapid mixing of pollutant on a deeper layer. The modelled concentrations (blue curve) can be seen to agree very well with observations in terms of timing and temporal evolution, meaning that the predicted BLH reaches 310m at the right time. In terms of intensity, there are small biases on CO<sub>2</sub> concentrations, that could be linked to the misrepresentation of the anthropogenic emissions, as the Eiffel site is at the heart of traffic emission sources. The remove of urban scheme (red curve, Fig. a) induces mainly a underestimation of the nocturnal BLH.

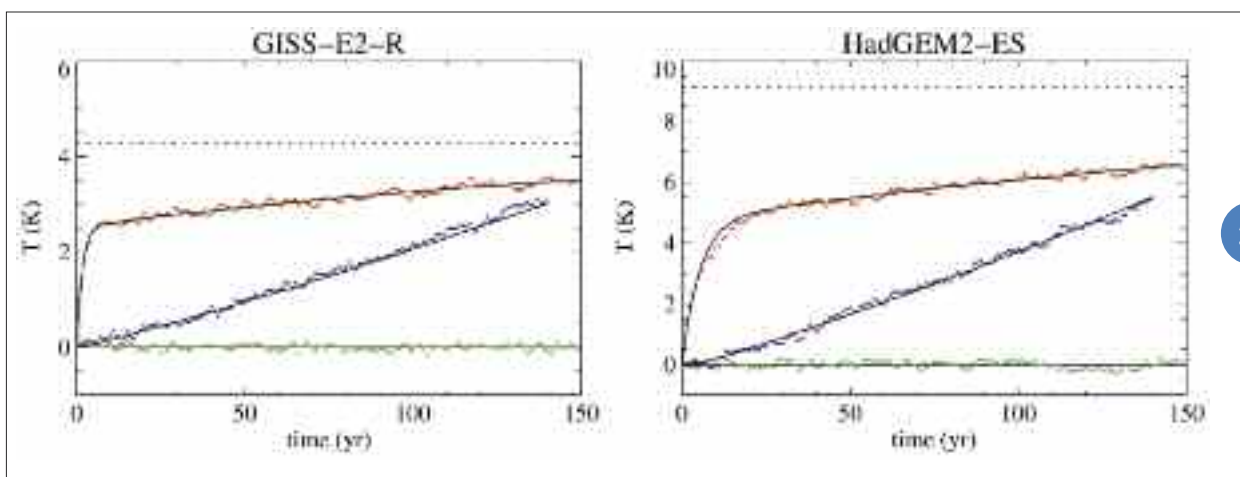
6



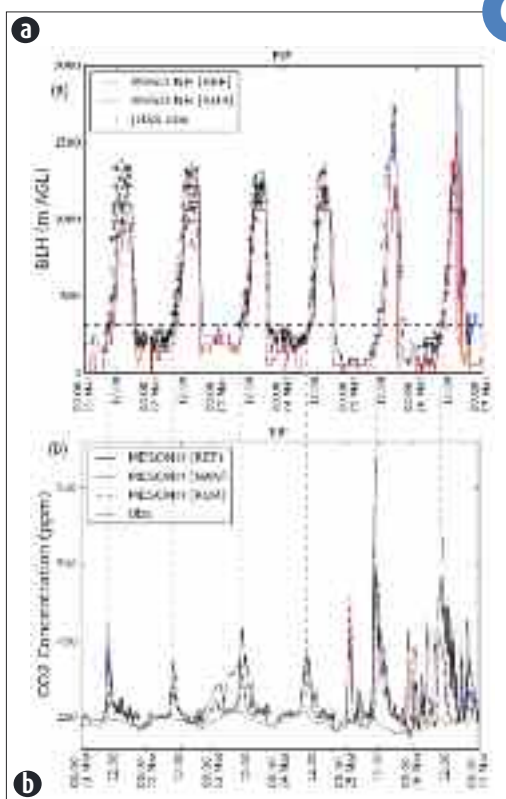


One of the indicators used to interpret the results of simulations of the future evolution of European air quality is the number of days of exceedance of daily maximum 8-h average concentrations (Mx8h) of ozone. The threshold of  $120 \mu\text{g}\cdot\text{m}^{-3}$  is computed over France (FR), Spain (ES), Germany (DE), England (GB), Italy (IT) and Poland (PL) for the summertime (June, July, August and September) and for CLIM (black line), S2030 (red line) and S2050 (green line) simulations. CLIM refers to the present climate (period of 2000-2010). S2030 and S2050 refer to 2030 and 2050 time slices respectively.

4



5



6

Time series of global and annual mean surface air temperature change in response to the abrupt 4xCO<sub>2</sub> (red), the 1%/y CO<sub>2</sub> (blue) and the control experiment (green) CMIP5 experiments for GISS and HadGEM models and the corresponding energy-balance model analytical temperature evolutions (black). For each model, the black dotted line indicates the estimated equilibrium temperature response, for a quadrupling of carbon dioxide.

(a): Time series of boundary layer heights predictions at Eiffel and observations at Jussieu (black) (in meters above ground level) for the reference simulations (blue) and the simulations without TEB (red). (b): Time series of observed and predicted CO<sub>2</sub> concentrations (in ppm) at Eiffel Tower for the reference simulations (blue), the simulations without TEB (red) and the simulations without anthropogenic emissions (green). The vertical dashed lines correspond to the time in the morning at which observed boundary layer heights reach 310m.

# Snow

---

Snow and avalanche research revolves around three main axes: snow-atmosphere interactions, remote sensing applied to the snowpack and study of the physical properties of snow.

The first axis focuses on the mountain meteorology and snow atmosphere interactions. The work carried out this year allowed advances in fine-scale modelling of snow transport by the wind in relief area. Several studies have shown also the potentialities of the AROME model for avalanche risk forecasting application.

Concerning remote sensing of snow, the work conducted in 2012 focused on exploitation of visible and micro-wave satellite images to access certain properties of the snowpack and comparison with simulations produced by SURFEX/Crocus. One has also characterized sensitivity of satellite microwave products to precipitation, which paves the way to their assimilation in AROME in order to improve the simulation of precipitation over the reliefs.

In the field of the snow physical properties, more progress has been made in the study of the snow at the micro-scale, in observation and determination of physical properties of three dimensional snow samples like permeability for instance. Complemented by larger scale observations on various websites (in particular in the Col de Porte as shown in the figure), these works are being translated into improvements of the SURFEX/Crocus snow model through the introduction of new characteristic variables of the snow and the redesign of the optical scheme.

1

---

## Estimation of the snow permeability from its microstructure

The ability of air to flow through snow is represented by its intrinsic permeability. This variable, which governs the transport phenomena within the snowpack (mechanism of “wind-pumping”, air convection in the pores...), is particularly important for studies related to snow-atmosphere exchanges or to snow metamorphism, for example.

In this context, the permeability tensor was calculated from 3D images of snow microstructures obtained by X-ray tomography (Figure a). The 35 images used span a wide range of snow types from fresh snow to melt forms.

The results of computations show that, for some snow samples, the permeability is anisotropic, i.e. the intensity of the flow varies significantly depending on the considered direction of the sample. Figure b illustrates this phenomenon by showing a sample of depth hoar where permeability is higher in the vertical direction than in the horizontal one. Moreover, this study indicates that the permeability is strongly correlated with the density and the specific surface area (SSA) of snow, which allowed us to propose a regression between these three variables. The fit obtained, tested with data from the literature

and compared with other existing parameterizations, is probably the best currently available relationship to estimate the permeability of snow from its SSA and its density, two variables measurable in the field.

The regression can be used directly or integrated in snowpack models such as the Crocus model, to estimate the evolution of the permeability profile with time.

2

---

## Evaluation of integrated and profile of snow physical properties (density and specific surface area) of SURFEX/ISBA-Crocus at the col de Porte site

Many scientific applications require a detailed description the vertical profile of the physical properties of snow, including avalanche hazard warning activities which are operationally carried out by Météo-France.

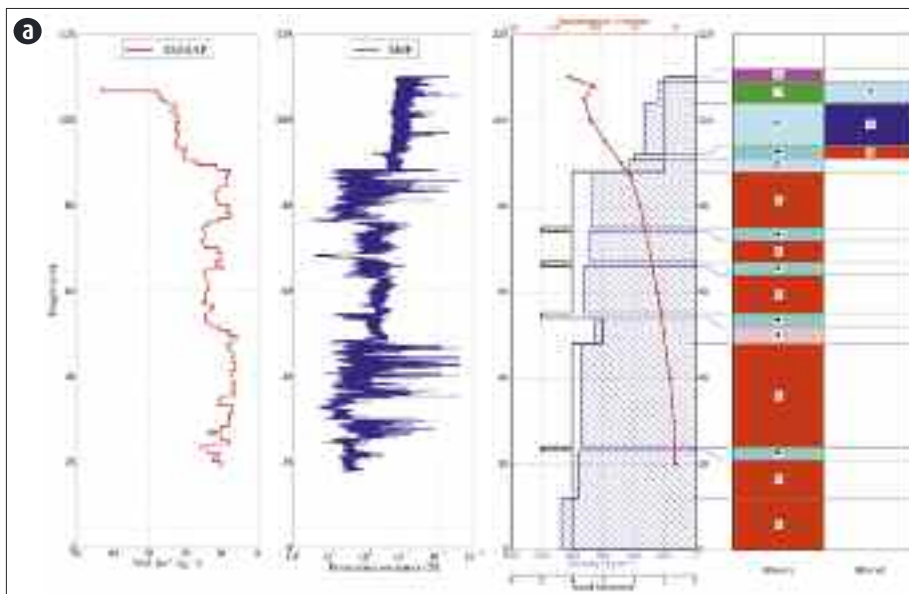
The detailed snowpack model Crocus simulated the physical properties of up to 50 numerical layers, and represents snow metamorphism, i.e. the microstructure transformations of snow over time. Crocus has recently been introduced as a snow scheme of the land surface model ISBA in the SURFEX interface.

Replacing the original version of Crocus by SURFEX/ISBA-Crocus in the operational chain of models SAFRAN – Crocus – MEPR (SCM) is planned for 2013, pending full evaluation and validation of the new components of the model. Among other tests, SURFEX/ISBA-Crocus was evaluated against snow measurements carried out in 2009 – 2010 at col de Porte (1325 m altitude, Chartreuse mountain range near Grenoble).

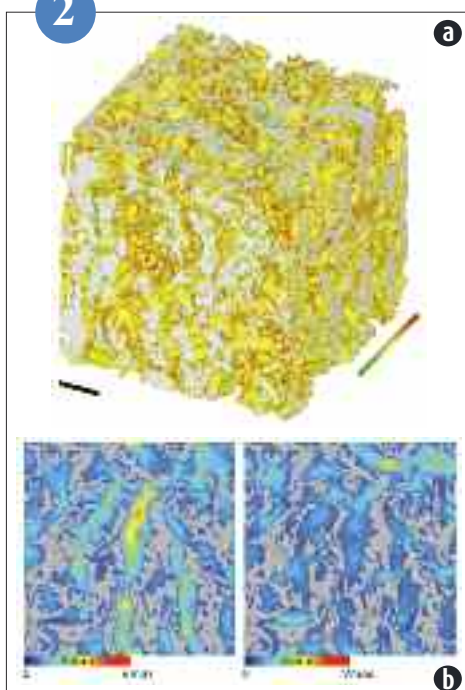
The total snow height is well simulated (bias and root mean square deviation of -5.1cm and 7.6cm, respectively). Vertical profiles of

the specific surface area (quantitative proxy for snow metamorphism) and density compare favorably to observations (see Figures “a” and “b”). Work is in progress to extend the evaluation of SAFRAN - SURFEX/ISBA-Crocus – MEPR (S2M) to a larger number (above 100) of observation sites in the Alps and the Pyrenees.

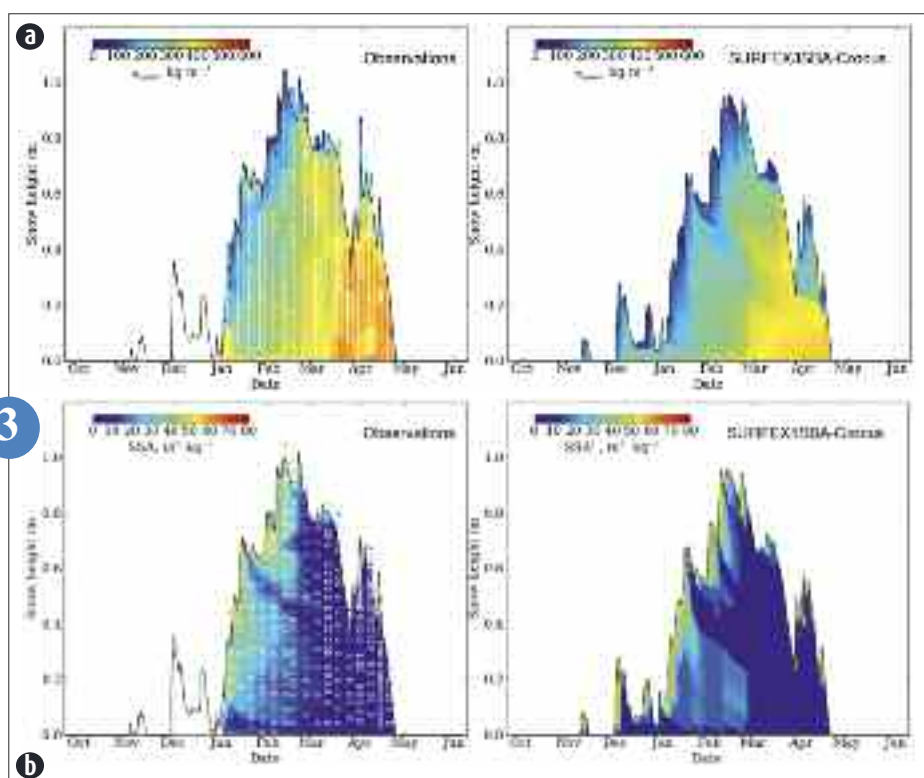
3



(a): Example of measurements to the Col de Porte site for February, 6th 2012: On the right are the variables observed in a classical manual vertical sounding of the snowpack: temperature, density, snow hardness, grain type (this last parameter is visually determined by the observer). The two profiles on the left are automatic observations of specific surface area (proportional to the inverse of the optical radius) of snow (in red) and penetration resistance (in blue) carried out at the same place using dedicated sensors. These new observations, regularly carried out at the Col de Porte for two years, allow quantifying snow properties now so far inaccessible in routine in the field. They pave the way to a finer modelling of the physical properties of snow.  
(b): Measurement of the snow specific surface area with the ASSSAP sensor (collaboration GAME-LGGE).



(a): Three-dimensional visualization of a sample of depth hoar. The scale is indicated by the 1 mm length bar. The color code represents the degree of curvature of the air-ice interface: red for convexities, green for concavities, and yellow for flat areas. The tomographies which provided the 35 images used in this study were performed at the ESRF or 3S-R laboratory.  
(b): Vertical cross-sections of the 3D image shown in figure a. The ice is depicted in gray. The color scale corresponds to the fluid velocity in pores computed for a pressure gradient of  $2 \times 10^{-2}$  Pa in the vertical (on top) and horizontal (down) directions and for a dynamic viscosity of the air of  $1.8 \times 10^{-5}$  Pa s<sup>-1</sup>. The color bar corresponds to 3 mm. We see that the flow constrained by the vertically elongated microstructure, which is characteristic of this snow type, is larger in the vertical than in the horizontal direction.



(a): Comparison of the time evolution of the vertical profile of density observations (left) and SURFEX/ISBA-Crocus simulations (right) at col de Porte during the 2009 – 2010 snow season.  
(b): Comparison of the time evolution of the vertical profile of specific surface area (SSA) observations (left) and SURFEX/ISBA-Crocus simulations (right) at col de Porte during the 2009 – 2010 snow season.



## Monitoring snowpack properties using passive microwave remote sensing data

Remote sensing microwave measurements are almost not sensitive to clouds and have the ability to penetrate several layers of snow to detect any internal property changes, such as Snow Water Equivalent (SWE), in almost all weather conditions. The electromagnetic radiation emitted from the ground under the snowpack is attenuated and scattered by snow crystals whose effect varies depending on their size, vertical distribution, ...

Snowpack property retrieval from microwave measurements is therefore a very challenging issue given the complexity of this environment. We study the snow signature on observations using a wide range of remote sensing instruments (AMSU-A, AMSU-B, SSM/I and SSMI/S). These observations are studied in conjunction with the snowpack model CROCUS coupled to the ISBA-DF model and forced by ERA-interim reanalyses. We show that relevant information on the SWE can be extracted from combinations of microwave observations. The attached figure shows maps for the

1st of December 2009 with (a) differences in surface emissivities from AMSU-A, (b) the Tbs gradient from SSM/I between 19 GHz and 37GHz together with (c,d) time series of these variables versus the SWE simulated by CROCUS near a synoptic station. The comparison shows a very good correlation between CROCUS simulated SWE and microwave retrievals. It should be noted that CROCUS does not assimilate any snow depth data from synoptic stations. Other comparisons were conducted with VIS/IR observations and SWE analysis from GlobSnow highlighting the added-value of microwave data. This work is a step towards the assimilation of these observations in the CROCUS snow model.

4

## Using MODIS data to study snow surface properties

The imaging spectroradiometer MODIS is on board two satellites Terra and Aqua since 2000. Each of these sensors provides one image per day over the Alps with a time shift of a few hours. Among MODIS spectral bands, the two visible bands (250m spatial resolution) and five visible and near-infrared bands (500m spatial resolution) are especially useful for snow study.

Indeed, these bands are sensitive to different properties of the snowpack. The visible bands give some information on the impurity content of the surface snow whereas in the near-infrared, the reflectances are mainly influenced by the surface grain size values (optical radius).

MODIS data are processed with a method adapted to mountainous areas, e.g. taking into account multiples reflections on slope.

Once processed, MODIS data allow the retrieval of snow albedo, i.e. the fraction of solar energy reflected by the snowpack, of surface grain size (cf. figure) and of impurity content. Thus, on one hand, these data are a crucial tool to evaluate the distributed simulation of the snowpack. On the other hand, the snowpack simulation does not take into account real snowpack observations neither for operational nor research applications. The simulation error is then cumulated over the whole winter season. MODIS data can be assimilated into the snowpack in order to modify, suitably with the observations, the estimates of the snow properties predicted by the model.

5

## Impact of vegetation on snow albedo of sub-arctic ecosystems during SNORTEX

SNORTEX (Snow Reflectance Transition Experiment) objective is to characterize snow-melting patterns at a landscape scale using a multi-scale strategy supported by multi-angular and multi-spectral remote sensing information. The experiment took place in a 100 km<sup>2</sup> flat European taiga of Finnish Lapland during a 3-years campaign (2008, 2009 and 2010). Measuring snow Bi-directional Reflectance Distribution Function (BRDF) and albedo along with key properties (grain size, roughness, and impurity) is at the core of the investigation.

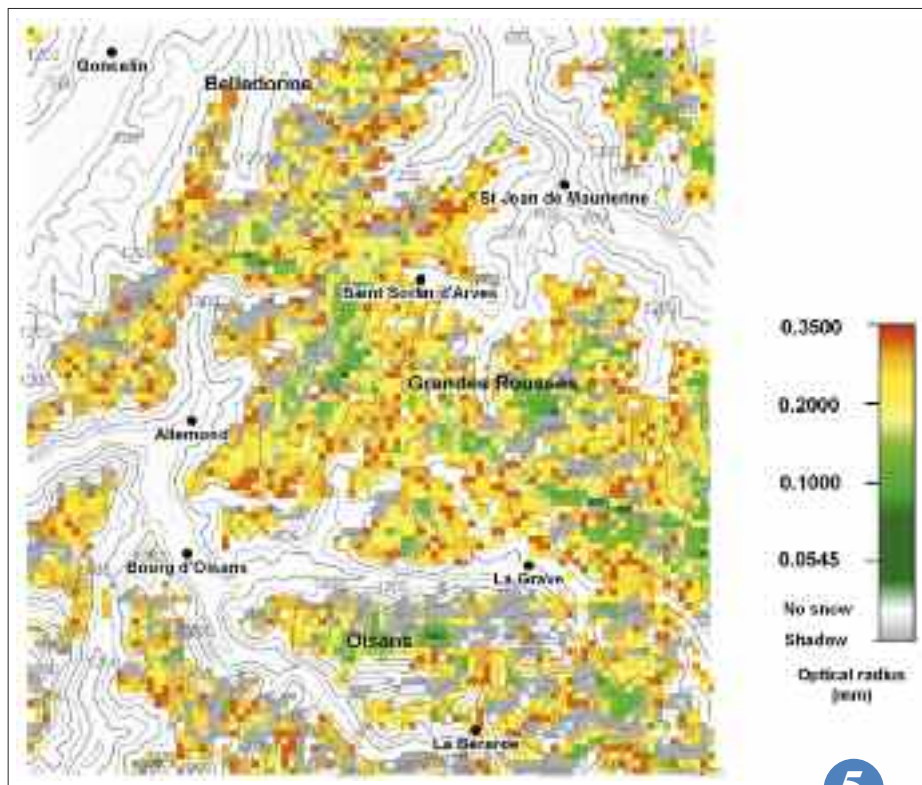
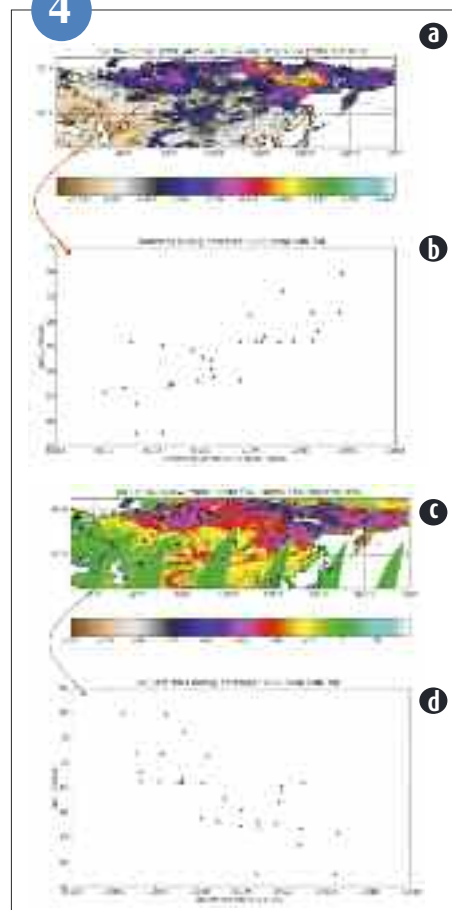
Snow-melting study of boreal ecosystem from ground level to remote sensing data validation combined various means of observations (ground-based, airborne, satellite) and modelling effort. CNRM managed the project in partnership with the Finnish Meteorological Institute, and also flew OSIRIS (air-POLDER) sensor for measuring from helicopter meter-scale directional and polarized reflectance in visible and solar infrared bands.

Conifer forest composes about one third of the study area and cast sizeable shadows. Forward light scattering peak arising from snow underneath the trees marks OSIRIS BRDF. Alternating of narrow bands of heightened poor herbaceous cover and large-scale snow ditch feature wetlands. This second major landscape unit shows in contrast to conifer backward light scattering based on analysis of OSIRIS BRDF. The onset of snow-melt is also conspicuous over wetlands, which was particularly the case in 2009 due to the persistence of liquid water in winter beneath snow. Snow albedo from near infrared BRDF is close to 0.4 for forest and 0.6 for wetlands in mid-March, with fast decrease then for wetlands. Land cover distribution is then crucial for seasonal albedo and regional snow metamorphosis.

6

(a): emissivity difference (AMSU-A 23GHz -31 GHz) and  
(b): SSM/I brightness temperature  
gradient December 1st 2009 and  
(c, d): daily series of these variables near a synoptic  
station during the month of December 2009 as a function  
of snow water equivalent simulated by CROCUS.

4

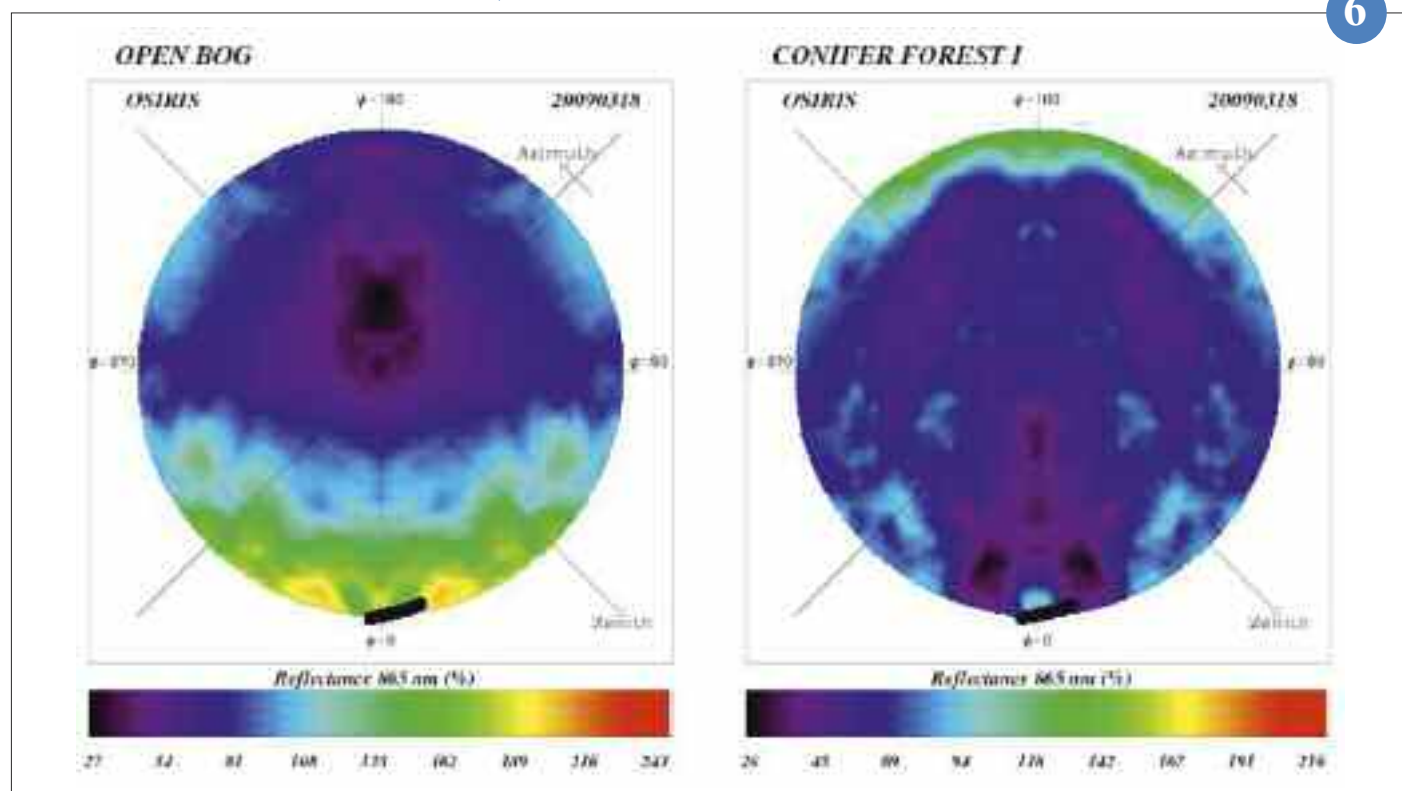


5

Optical radius of surface snow retrieved over one part of the Alps from MODIS data  
on 2009-03-21 at 10:40 UTC.

Anisotropy factor of the near infrared reflectance for wetland (left) and conifers (right) from about 1 million of OSIRIS  
samples at mid-March 2009. Black dots delineate the angular sun position during flight lines, which indicates backward  
and forward scattering.

6



# Oceanography

---

The research activities on the air-sea interactions and the activities on observations at sea for Météo-France and the scientific community purposes have been continued in 2012 at CMM.

The specific research actions concern the influence of the ocean on the atmospheric boundary layer (in particular the waves impacts on fluxes) and the improvement of the parametrization of turbulent fluxes in Numerical Weather Prediction (NWP) models. One part of the research activities is dedicated to improve observations at sea, via software or instrumental development, and to participate in national or international scientific programs. Observations at sea (drifting buoys, moored buoys, ships) are conducted either for operational needs of Météo-France or EUMETNET (E-SURFMAR operational service) or as a contribution to the operational coastal oceanography, or for scientific purposes (support to research). In this context, too, Météo-France supports maintaining the network of moored buoys PIRATA in the tropical Atlantic Ocean.

The year 2012 was marked by the preparation and participation in the HyMeX project with reinforcing the scientific equipment of the two moored buoys in Mediterranean Sea and with the deployment of drifting buoys. The network of E-SURFMAR drifting buoys is currently more than 100 buoys operating in the North Atlantic. Coordinated by CMM, since its beginning E-SURFMAR will celebrate its tenth anniversary in early 2013.

1

---

## Contribution of operational ocean forecasting systems to oceanic drift prediction

Since 2007, the operational oil spill and adrift object model MOTHY operated by Météo-France uses as additional forcing data currents provided by oceanographic forecasting systems such as Mercator-Océan. It allows integrating the prediction of large-scale currents and gyres that are not modelled by MOTHY.

The purpose of this new study is to better understand and identify the most important oceanic processes to compel drift application from numerical models that attempt to reproduce observed trajectories of drifting buoys (the oceanic general circulation model NEMO combined with a Lagrangian transport tool and the MOTHY model). Targeted forecasting scales are about three days because they are the most useful for operational. Study data come from two in real condition drift experiment with satellite-tracked drifters released along the Azur Coast (Western Mediterranean) and near the mouth of the Congo River (Angola). They provide accurate cases-study related to specific drift regimes.

Some trajectories of Mediterranean experience were for instance influenced by Mistral during their passage in front of the Gulf of Lion and driven offshore. In this situation, the forecasts from NEMO surface currents alone are unsatisfactory and it has been shown that the key processes for this case comes from additional wave-induced transport term and direct drag by the wind. The addition of these contributions to the surface current of NEMO allows improving average prediction scores by 41% (Figure 1). These processes are parameterized in MOTHY current computing, which provides similar results when currents from NEMO are added.

It is also stressed the importance of very coastal processes not taken into account in MOTHY, such as the role of river plumes on the surface velocities. Changes in the velocity field are induced offshore by the spread of freshwater released, but also directly near the mouth by the river outflow itself. Not supplying the plume in the Angola forecasts leads to increase the error of some drift simu-

lations by 44%. Finally, for trajectories trapped by coastal currents, the horizontal resolution of models plays a key role in the flow position and associated structures for the Angola current and the Ligurian-Provençal current, although additional and unrealistic recirculation can also be introduced at very small scale by high resolution modelling.

This study suggests that taking into account the interaction of high-frequency continuum atmosphere-ocean-wave are important for oceanic drift application, which leads to future work on coupled systems that may offer complete solution for drift applications. Taking into account local processes such as the Congo plume is also crucial for drifts expertise.

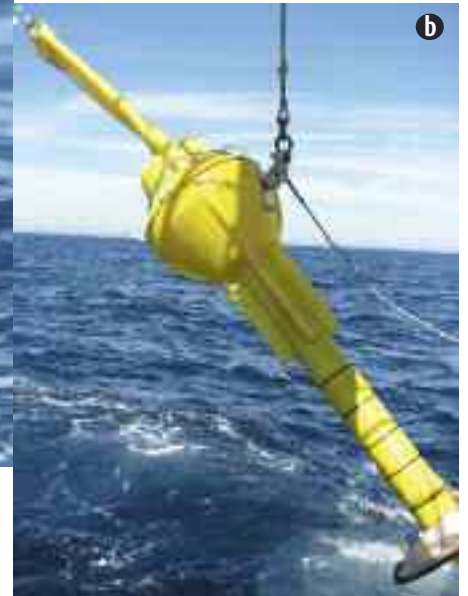
2



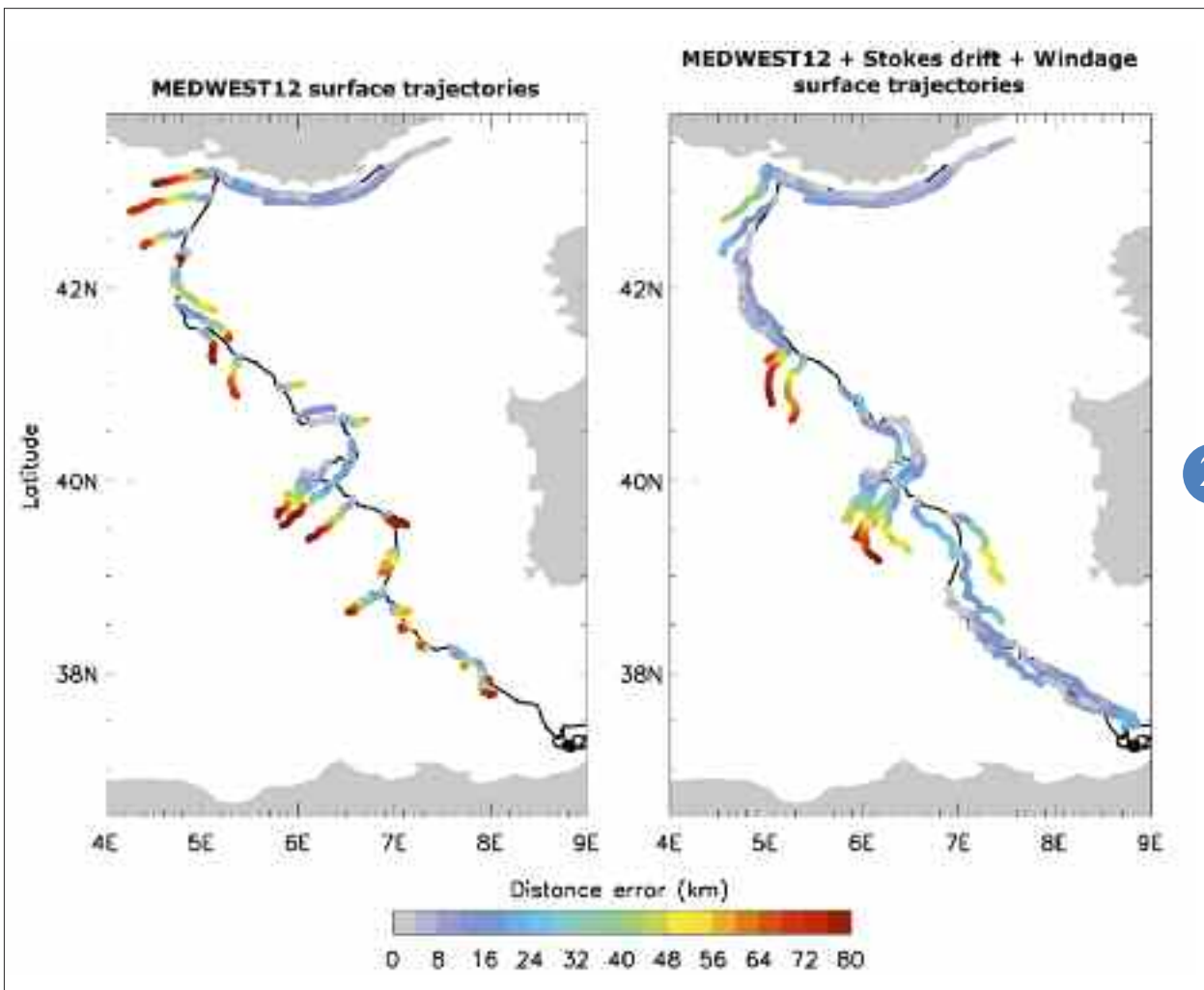
1



(a): Deployment of a salinity drifter for HyMeX.  
(b): Deployment of a Marisonde drifting buoy for HyMeX.



Average three days long trajectories computed every day from the surface currents of the Mediterranean regional  $1/12^\circ$  configuration for one observed buoy (black trajectory). Computed drift forecasts are colored to score the distance error to observation, from 0 km (grey) to 80 km (red). Consideration of the Stokes drift (from Wave Watch wave model) and a windage (1% of 10 m wind) on the right figure, not consideration on the left.



2

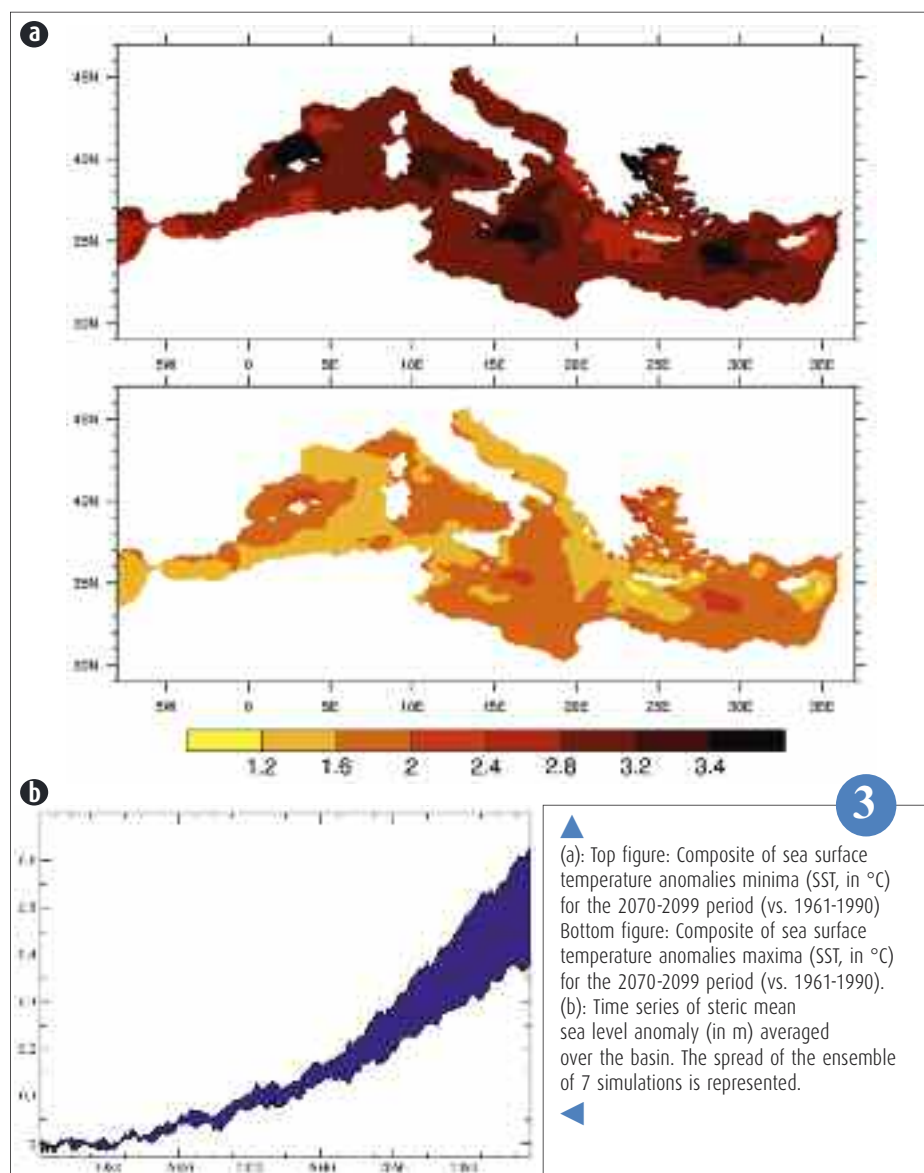
## High resolution modelling of the Mediterranean Sea

Acting as a mini-ocean, the Mediterranean basin is a suitable location for studying the impact of climate change on the ocean. The residence time of Mediterranean water is much lower than in the wide ocean so that a faster response to coming changes is expected. Besides, the Mediterranean region has been identified as one of the most responsive regions to climate change.

Global climate simulations are too coarse to give an adequate representation of currents and water masses in the Mediterranean, therefore a high resolution regional model is required for climate studies over this area. For this purpose, a regional Mediterranean configuration of the ocean model NEMO at  $1/8^\circ$  (NEMO-MED8 developed at CNRM) is used to assess the climatic change over this region. An ensemble of 7 simulations has been run over the 2001-2099 period to estimate the sensitivity of the oceanic response to the choice of (i) the scenario and (ii) the boundary forcings (Atlantic, rivers and atmosphere).

All simulations display a warming of sea surface temperatures by the end of the 21st century. The related uncertainty reaches  $2^\circ\text{C}$  in some sub-regions (fig. a) and is linked to the choice of the scenario. The choice of the boundary conditions especially influences the circulation of the water masses and thus impacts the vertical redistribution of the surface warming through the water column. This vertical distribution of the heat anomaly is found in the steric component of mean sea level averaged over the basin, which displays a large spread (fig. b). Ongoing simulations coupled with an atmospheric regional model and accounting for a better representation of Atlantic conditions should provide a more accurate estimate of the climate change impact on the basin.

3



## The E-SURFMAR Programme

The E-SURFMAR programme of EUMETNET, which aims to coordinate, optimize and progressively integrate European activities in matter of weather and oceanographic observations at the sea surface, will celebrate its tenth anniversary in early 2013. Coordinated by the CMM, the programme has permitted:

- The funding and the centralized management of a network of drifting buoys (100 buoys in operation continuously),
- the dramatic reduction in the cost of telecommunications for buoys and ships, thanks to the use of more appropriate means,
- the support of the automation of measurements onboard ships which led to issue a call for tender for the procurement of automatic stations,
- the development of quality control monitoring tools, and of a metadata database for ships, made available to the international community on the Web.

Following this success, the Assembly of EUMETNET ELG has renewed its confidence in Météo-France to manage the programme over the next five years. The programme becomes Operational Service of EUMETNET from 1 January 2013.

4

## Observing the ocean-atmosphere interface during HyMeX

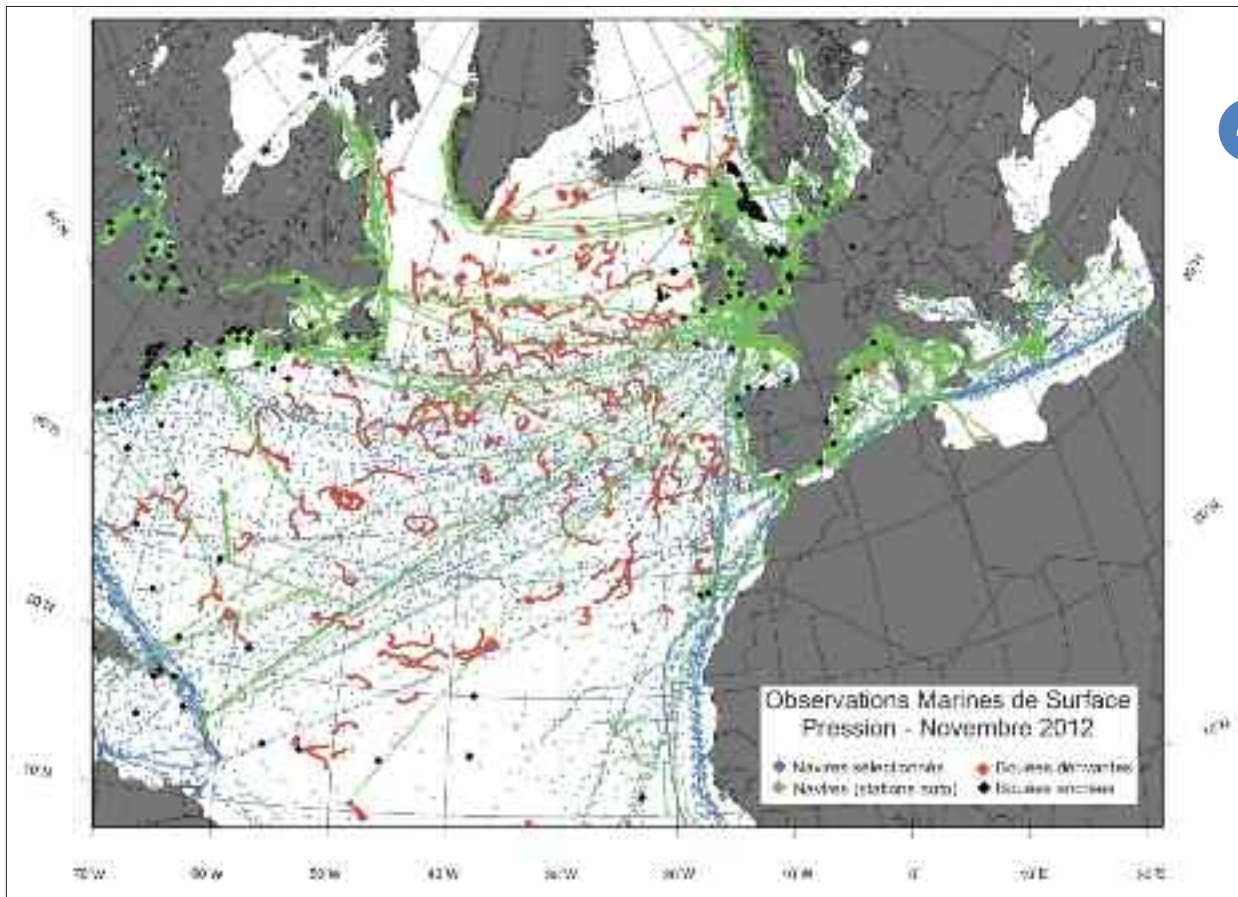
The CMM actively participated in surface hydrological and atmospheric observation during the HyMeX SOP1, with the scientific objective of documenting ocean-atmosphere exchanges in the Gulf of Lion. This area is crossed by most of the convective systems resulting in high precipitating events regularly impacting the south-east of France in autumn.

Surface drifters were deployed offshore Toulon at the beginning of September. Five of them are Marisonde drifters measuring and transmitting in real time wind speed and direction, atmospheric pressure, sea surface temperature and water temperature down to 300m. Five SVP drifters were transmitting atmospheric pressure, sea surface temperature and water temperature down to 80m or surface salinity. GMEI contributed to the installation of meteorological stations measuring and transmitting automatically atmospheric and surface oceanic parameters (SEOS) onboard the cargo ship Marfret-Niolon and the port tender Le Provence (Phares et Balises), which has been chartered during intense observation periods at sea (IOPs). During these IOPs of 2 to 3 days each radiosoundings and temperature and salinity profiles in the oceanic mixed layer were performed every 3h. Turbulent and radiative heat fluxes, as well as atmospheric parameters and wave spectra were monitored continuously.

5

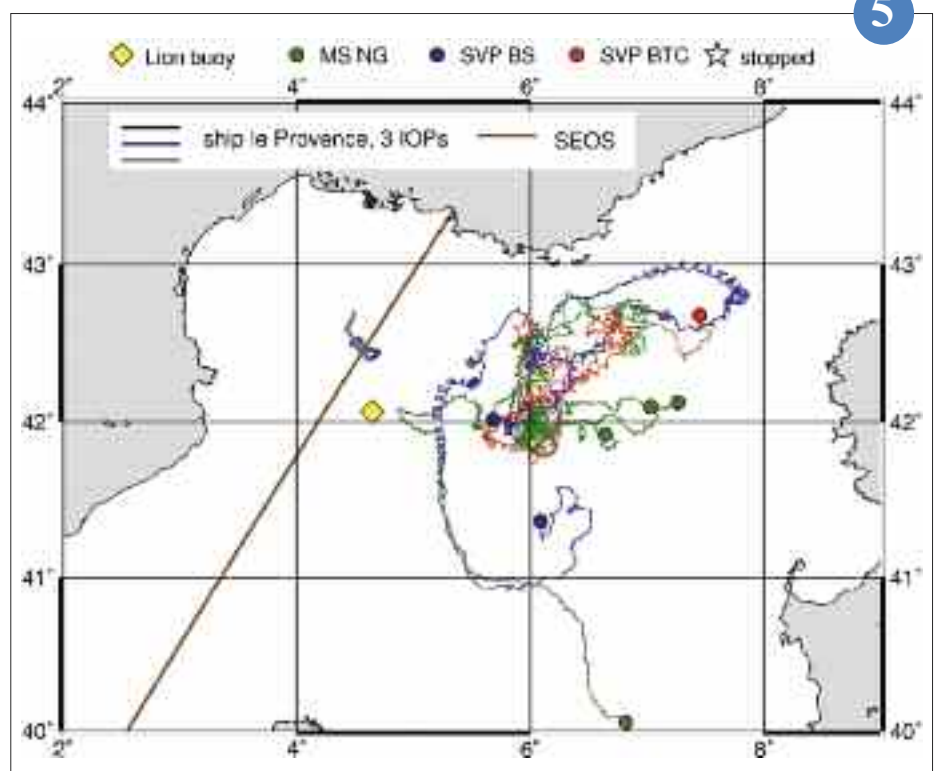


4



Surface marine observations in October 2012. Each dot represents an observation of drifting (red) or moored buoy (black), conventional ship (blue) or shipborne automatic weather station (green).

5



Map of the surface observations at sea during the HyMeX SOP1 (September-October 2012), with ship trajectories (solid lines, brown, Marfret-Niolon with the SEOS station, black, blue and grey, Le Provence), the Lion moored buoy (yellow) and the trajectories of Marisondes drifters (green), SVP salinity drifters (blue), and SVP temperature drifters (red). Stars indicate drifters stopped before the end of the SOP1.



# Observation engineering

---

The research activities on the air-sea interactions and the activities on observations at sea for Météo-France and the scientific community purposes have been continued in 2012 at CMM.

The specific research actions concern the influence of the ocean on the atmospheric boundary layer (in particular the waves impacts on fluxes) and the improvement of the parametrization of turbulent fluxes in Numerical Weather Prediction (NWP) models. One part of the research activities is dedicated to improve observations at sea, via software or instrumental development, and to participate in national or international scientific programs. Observations at sea (drifting buoys, moored buoys, ships) are conducted either for operational needs of Météo-France or EUMETNET (E-SURFMAR operational service) or as a contribution to the operational coastal oceanography, or for scientific purposes (support to research). In this context, too, Météo-France supports maintaining the network of moored buoys PIRATA in the tropical Atlantic Ocean.

The year 2012 was marked by the preparation and participation in the HyMeX project with reinforcing the scientific equipment of the two moored buoys in Mediterranean Sea and with the deployment of drifting buoys. The network of E-SURFMAR drifting buoys is currently more than 100 buoys operating in the North Atlantic. Coordinated by CMM, since its beginning E-SURFMAR will celebrate its tenth anniversary in early 2013.

1

---

## Visibility Monitoring using Conventional Roadside Cameras

In order to prevent traffic supervision and then leading to a fast intervention in the event of an accident, cameras have been settled in most part of high roads. Thanks to the image processing improvement, benefits can be used for meteorology.

During a PhD thesis work ("Visibility Monitoring using Conventional Roadside Cameras" April 11th 2012) led by the IFSTTAR in collaboration with Météo France and IGN, Raouf Babari developed the idea to evaluate the meteorological visibility using such cameras. The calculation of the visibility estimator is based on the gradient magnitude selected by

applying Lambert's law with respect to changes in lighting conditions. The advantage is that the contrast of Lambertian's surfaces only depends on visibility. Knowing the scene targets distribution, a mathematic relation can be found between visibility and the luminance gradient magnitude. The method has been tested on the meteorological observatory of Trappes thanks to different visibility sensors: collected data have been compared to results from the novel visibility estimator algorithm. At the moment, the methodology presented here is only robust on daylight periods.

The first results show the relevance and the reproducibility of the approach in a large variety of lighting conditions. The next step consists on validating the method on several meteorological observatories during the next winter (2012) and spring (2013).

2

---

## Remote detection of fog by a scanning lidar

Predicting fog is a key issue for many human activities. In France, the fog forecasting system for airports is based on a "column" numerical model named COBEL. COBEL deals a single spatial coordinate and assumes relevant processes are acting mostly on the vertical axis. Operational at Roissy Charles-de-Gaulle, Orly and Lyon St-Exupéry airports, COBEL is ill-adapted to advection fogs for horizontal advection is then a key process. In 2012, the Groupe de Météorologie Expérimentale et Instrumentale of CNRM conducted an experiment aimed at testing the ability of a scanning lidar to detect advection fogs kilo-

meters away and thus predict its arrival on a site several tens of minutes before it actually affects it. The experiment was supported by the French armament agency and the French Navy.

A scanning lidar was purchased and deployed on the Navy base of Lanvéoc. There it was operated from June to October 2012. At an elevation angle of 1 to 2 degrees, scans made of 15 10-second steps in 15 azimuths (from 80 deg. to 220 deg.) were repeated every 6 minutes. During the period, 14 fog cases were observed. Eleven of them were detected at least 45 minutes in advance. Of the three remaining

cases, two are thin or broken fogs. As for the last, a careful examination of the signals show it is detected 10 minutes before its arrival because of a very low cloud ceiling (70m). The ability of scanning lidar to detect advection fogs is thus confirmed. An operational application seems feasible but will require the development of detection algorithms and the provision of lidars with lighter maintenance.

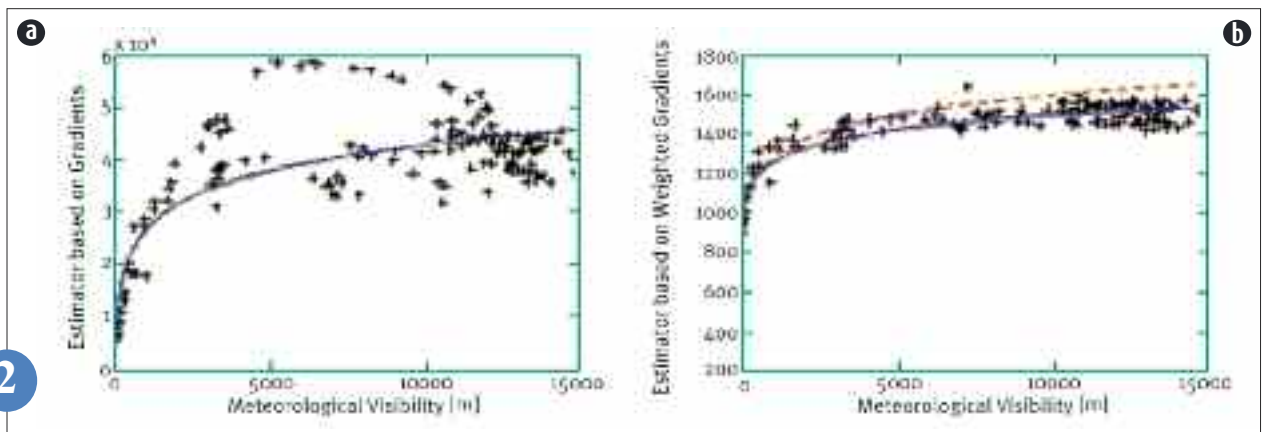
3



Backscatter lidar units tested by Météo-France in preparation of the future operational backscatter lidar network for the detection of volcanic ashes. The three "RMAN" units were operated side by side for several weeks and inter-compared. Several ceilometers were also deployed on the same site to study their potential complementarity with the lidars.

Logarithmic model fitting of the plot of the estimators as a function of reference visibilities.

(a): sum of the module of the luminance gradient in the entire image.  
(b): sum of the module of the luminance gradient weighted by the confidence of pixels to belong to Lambertian surfaces (blue line) and sum of the module of the luminance gradient weighted by the confidence of pixels to belong to Lambertian surfaces and with weighted fit for low visibility distances (dashed red line).



(a): Photography of the lidar deployed and operated at Lanvéoc air base in the frame of an experiment aimed at testing the ability of a lidar to detect advection fogs in advance. The lidar was deployed on the control tower, at about 17 meters above the ground.  
(b): Azimuth angles of the lidar during the experiment at Lanvéoc. The line-of-sight of the lidar was successively directed towards the 15 directions represented by the red lines on the figure. The length of the lines is 5km. The maximum range of the lidar was about 10km.



## A lidar inter-comparison study in the framework of aerosol detection

The 2010 Eyjafjallajökull eruption (Icelandic volcano) showed a serious lack of volcanic ash observations. Within this context, objectives of better management of the impacts of volcanic ashes come with the scope of the 2012-2016 Météo-France objectives and performance agreements. The current Lidars Aérosols project plans to install a dozen lidars evenly located in France (overseas territory excluded).

An inter-comparison study was carried out during the 2012 spring and summer period in order to assess the lidar and ceilometers ability to detect aerosols. Lidars have different characteristics: some of them use an infrared wavelength (VAISALA – CL31 and CL51, JENOPTIK – CHM15k Nimbus), other a visible wavelength (SIGMASPACE – Mini MPL and MPL, CIMEL – CE370) or an ultraviolet wavelength (LEOSPHERE – RMAN510).

Only Saharan aerosols detection was considered because no volcanic ash cloud occurred in the vicinity of Toulouse. Volcanic ashes have roughly similar characteristics compared with desert aerosols. In addition, they are strongly aspherical, therefore they strongly depolarise the light (depolarisation rate: 35 % with a 355 nm wavelength).

This study helps in showing that ceilometers are unable to meet this need at high altitude. Moreover, in this frame of detection and identification of aerosols and especially volcanic ashes, the light polarisation measurement appears to be highly necessary.

4

## ERAD2012 Conference: the international weather radar community meets in Toulouse

From 25 to 29 July 2012, the International Conference Centre (ICC) of Météo-France hosted the 7th ERAD Conference (European Conference on Radar in Meteorology and Hydrology). The initial intent of ERAD, which has been perpetuated since its first edition in 2000, was to create an open forum between students, academics, engineers, end users and operational radar operators working with or using weather radars and weather radar data. The goal of ERAD is to facilitate mutual understanding between data producers and data users and to help young generations of scientists accessing state-of-the-art knowledge on radars.

Co-organized by the DSO, CNRM and CIC team, this new edition of ERAD has been a great success with more than 400 participants from 32 countries. A high level program, alternating oral and poster sessions,

was designed to make a state of the art of all current and future weather radar applications. In addition to traditional sessions on radar QPE, hydrology and microphysics, new research subjects were investigated through sessions devoted to air-traffic control, as well as birds and insects detection. Significant efforts were also made to encourage student participation.

This conference was also an opportunity for Météo France to highlight its radar network and products, as well as to share its expertise in data processing, polarimetric radar combination - gauges, operating X-band radars, radar data assimilation in the numerical model, ...

6

## Boundary Layer Observation: some progress and prospects

In the atmosphere, turbulence is usually estimated from airborne measurements, remote sensing devices or instrumented masts. Recently the CNRM -GAME have settled and validated an in-situ measurement pod carried by a tethered balloon dedicated to the turbulence estimation throughout the boundary layer. Used during the BLLAST experimental campaign, this platform may be used as a reference in order to validate other turbulence observation techniques.

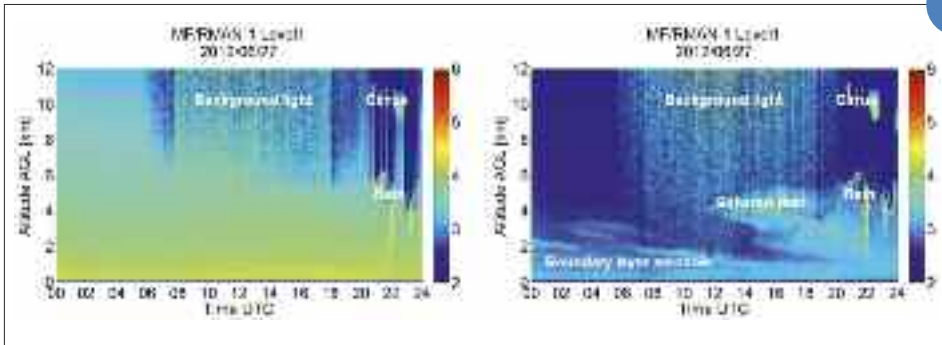
The CNRM-GAME operates also a stratified water flume which is a quasi-unique infrastructure specially designed to study stable boundary layers at high Reynolds number. A new experiment on the stable boundary layer has been performed in 2012. Results validate the use of this approach to study the stable boundary layer. Their analysis, in collaboration with Wageningen University, contributes to improve performance of weather forecast model in the lower atmosphere.

Atmospheric turbulence study from observations relies also on new analysis techniques of fast measurements based on random media reconstruction methods. These stochastic engineering techniques developed by the CNRM-GAME rely on Markovian models of measurement processes or turbulence. New probabilistic estimation algorithms have been developed to build these models. During 2012 efforts were done to apply these tools to real data, in particular Doppler lidar data from the BLLAST campaign. Our next goal is to develop a numerical system reconstructing locally the turbulent boundary layer with a high spatial and temporal resolution.

5



4



Vertical profiles (decimal logarithm of the signal corrected from the square decrease with height) observed above Toulouse on June, 27th 2012 with RMAN510 #1 (355nm wavelength).  
Left panel: co-polarisation channel.  
Right panel: cross-polarisation channel.

CNRM-GAME large stratified water flume (upper-right corner: optical measurements of velocity, giving access to a resolution equivalent in the atmosphere of about 1m and an acquisition frequency of about a hundred hertz).



5

ERAD 2012 group picture.



6

## **KuROS (Ku Band Radar for Observations of Surfaces): a new airborne radar**

China (CNSA) and France (CNES) have jointly established a satellite mission designed primarily to monitor the ocean surface in order to measure which is commonly called by oceanographers as "sea state": wind direction, amplitude and wavelength of the waves. This mission is named CFOSAT (Chinese-French Oceanic SATellite) and was started in 2008.

As part of this mission, the ATR 42 from Météo France, operated by the French Airborne Environment Research Service (SAFIRE), flew the new Ku-band radar named Kuros, designed and developed by LATMOS to prepare and validate the CFOSAT mission. The first measurement campaign was led over three weeks (April-May 2012) from Toulouse Matabiau airport with flights over Atlantic Ocean and Mediterranean Sea. On a technical side, the first tests campaign has

improved many of the defects on the instrument. Scientifically, it is still premature to make an assessment, but the results of the 10 degrees antenna seem very encouraging and reflect the performance in terms of wave spectrum modulation, Doppler information and link budgets. With regard to the 40 degrees antenna, the preliminary results do not meet the exact specifications in terms of link budget. The defect has been identified and works to optimize and improve this method are in process.

7

## **The EUFAR project: 12 years of coordination of the European network of instrumented aircraft for environmental and geosciences**

The EUFAR project is an FP7 Integrating Activity of the European Commission, bringing together 32 European legal entities, i.e. 14 operators of airborne facilities operating 20 instrumented aircraft and providing access to 6 specialised instruments and 18 institutions expert in airborne research, involved in 9 Networking Activities, Transnational Access to 26 installations and 3 Joint Research Activities. To provide a wide range of scientists (cf. figure) with easy access to the most complete range of research infrastructures, EUFAR (i) develops transnational access to national infrastructures; (ii) reduces redundancy and fills the gaps; (iii) improves the service by strengthening expertise through exchange of knowledge, development of standards and protocols, constitution of databases and joint instrumental research activities; (iv) promotes the use of research infrastructures, especially for young scientists from countries where such facilities are lacking.

Coordinated by CNRM since its constitution in 2000 with 9 partners under FP5, the evolution of the EUFAR network in size, activity and budget (0,64 M€ in FP5, 5 M€ in FP6 and 8 M€ in FP7) suggests that it has reached its nominal configuration for offering access to a large and comprehensive fleet of diverse aircraft and airborne instruments. The constitution of a sustainable structure, as already envisaged in the Memorandum of Understanding signed by the COPAL project members, remains a challenging issue in support of the long-term management of the EUFAR Office, to be addressed in the next EC funded project beyond September 2013.

9

## **Drones take off to study the atmosphere**

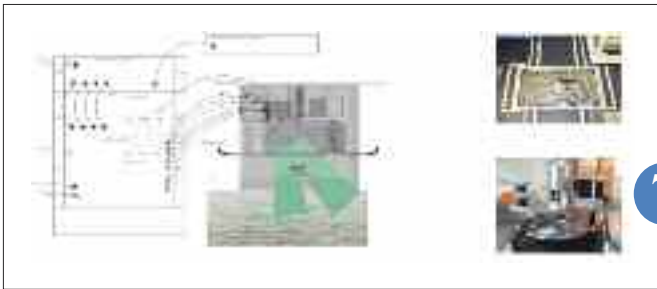
The use of unmanned aerial systems (UAS) for civilian applications is booming. Combined with the miniaturization of environmental sensors and advances in electronics and navigation systems, UAS offer new and exciting opportunities in atmospheric science. A project funded by ANR, titled VOLTIGE: Vecteurs d'Observation de La Troposphère pour l'Investigation et la Gestion de l'Environnement, focuses on UAS for scientific and civilian applications. "Voltige" is a French word for aerobatics or stunt flying.

VOLTIGE strives to fill a niche for UAS by developing autonomous profiling capability and coordinated observations to observe the major parameters related to fog cycles via an integrated network of sensors. The project has two major objectives: increase our scientific capacity to observe the atmosphere and surface of the Earth; and engage students on recent technological advances in meteorology and aeronautics.

The occurrence of fog events are of great concern for the transportation industry and airport operators; however, forecasting of fog events is still a major challenge as numerical simulations lack sufficient information to predict or reproduce fog events using classical meteorological models. Most fog studies are limited to ground-based measurements that utilize remote sensing techniques to explore the vertical structure. VOLTIGE will deploy multiple ultra-light UAS simultaneously to measure key parameters of fog to better understand its development and evolution.

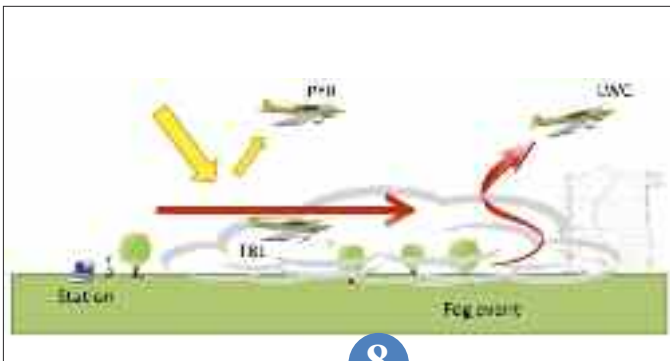
VOLTIGE couples novel technology with innovative science and engages scientists, engineers and students at the Centre National de Recherches Météorologique (CNRM), École Nationale de Météorologie (INP-ENM) and École Nationale de l'Aviation Civile (ENAC).

8



KuROS radar details.

7

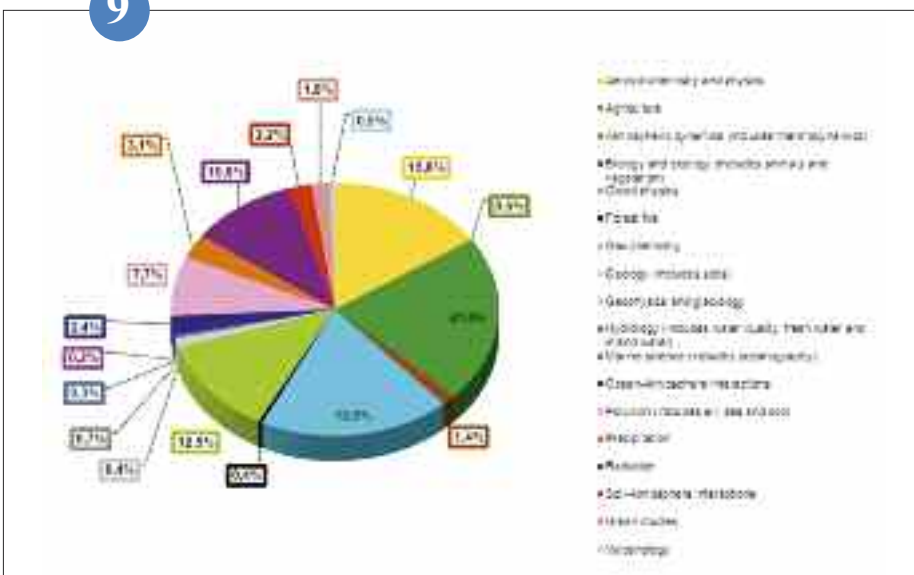


(a): Multiple platforms illustrate the observational capacity to study fog events.  
(b): UAS instrumented with meteorological sensors.

8



9



Distribution of airborne research publications from the EUFAR database per type of science (with respect to a total of 3893 peer-reviewed publications from 1998 to 2012).



# Research for aeronautics

CNRM actively contributes to the Single European Sky (SES) initiative within the framework of the SESAR technological program. The following papers illustrate these contributions with: the analysis of gust wind interactions with the airport infrastructures simulated in the CNRM water tunnel to identify areas of enhanced winds; the development of filtering tools for the calculation of the optimal aircraft trajectory; implementation of a novel low level wind shear detection technique to improve safety during approach ; development of a very high resolution version of the AROME limited area forecast model to initialize turbulence models of wave vortex propagation.

A close dialogue between MET services and ATM users thus allows identifying and clarifying requirements, hence further adapting Météo-France observation and forecasting products to very specific ATM applications. Within SESAR and upstream research programs of the European Commission, diverse Météo-France teams cooperate for the development of innovative solutions. In 2013, the first demonstration of the expected benefits of the new MET services will be performed with the support of Brussels Airlines, the French Air Navigation Service Provider DSNA and Thales over the French territory and Trans-African flights.

1

## Mathematics and meteorology for air traffic management (SESAR)

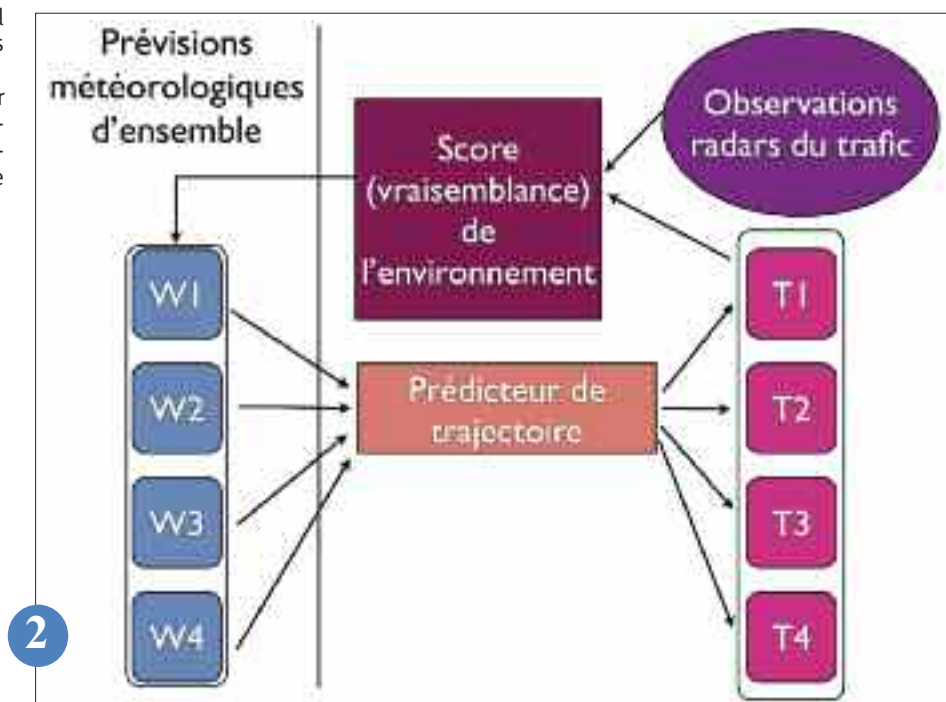
Météo-France is a recognized actor of the European R&D in civil aviation. Météo-France has been involved in the SESAR program since 2008. SESAR is the R&D effort launched by the European Union in the frame of its unique sky initiative. New challenges have emerged for the meteorological community, but the program also turned out to be a good opportunity to demonstrate to our partners our know-how in the forecast and observation domains. In 2012, we developed innovative stochastic estimation methods and algorithms in order to optimize the meteorological information used by the air traffic management systems in Europe. The developed probabilistic algorithms optimally combine the meteorological parameter uncertainties with the aircraft trajectory prediction systems. These methods make use of meteorological Ensemble Forecasts, aircraft trajectory predictors and real time observations such as aircraft radar tracks or airborne meteorological data.

The learning method use non-linear filters or Bayesian estimation techniques. The estimation of probability density functions estimations has no analytical solution. Therefore, the

resolution is given by probability densities approximated by particles approximations. The advantage of the learning method interest resides in its ability to combine different approaches. For instance, Kalman estimators can be used where they are optimal that is, on the linear parts of the problem. These upstream works will continue to evaluate the capability of our algorithms to be used in more and more real environments.

2

Example of learning algorithm for the meteorological forecast uncertainty. We estimate the meteorological forecast likelihood with respect to the air-traffic prediction errors by using radar traffic observations and trajectory prediction system. Thus we weight the members of the ensemble meteorological forecast, and then considering the atmosphere as a random medium structured by these weights we will optimize air traffic.





1

First workshop MET/ATM at Météo-France (4-5 October 2012) between 11.2 project partners and aeronautical users: SESAR JU, Eurocontrol, ANSPs (DSNA, AENA, NATS, Belgo control), airline companies (Air France, Lufthansa Regional Airlines, Novair, BBA, European Cockpit Association) and industries (Airbus, Dassault Aviation, Thales, Selex, INDRA, Honeywell, Frequentis, Safran).

## Fine-scale zoning of the wind over Roissy-CDG airport

To continue embarking and disembarking passengers, safely and during storms: in order to reach this ambitious goal which involves major economic consequences for the airlines, Météo-France designed an original study aiming to describe gusts at the scale of each passengers boarding bridge.

Considerable facilities have been implemented together: fine wind-measurements near the terminals, numerical simulations on computer and hydraulic simulations in a flume. The Group of experimental and instrumental meteorology (GMEI) of the CNRM-GAME was in charge to coordinate this study and to perform it, except for numerical simulations. CERFACS, as an expert in the use of Computational Fluid Dynamics models (CFD) was our partner for this.

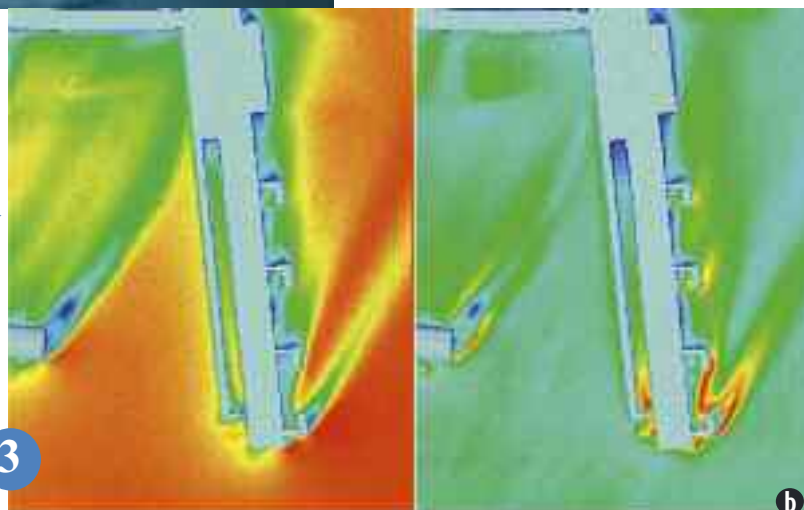
Starting in July 2010 by installing six fast wind-sensors in Roissy-CDG, this study consisted also in two experimental phases of hydraulic simulation on two models, one at the 1/3000th scale early 2011, the other at 1/400th early 2012. The numerical meshing of the airport, then the CFD simulations were performed from late 2010 to late 2011.

The report was officially delivered to the French Civil Air Authority DGAC in September 2012. It shows that some boarding bridges are protected according to the wind direction. It gives a relation between the velocity at these points and at the one measured on the runway, the only airport reference until then. Besides from improvements of the service to civil aviation, this innovative study should also have scientific consequences based on the original comparison between numerical simulations on one hand and flume hydraulic simulations on the other hand, including the benefit of accurate in-field reference measurements.



a

(a): Photo CNRM/GMEI/SPEA J.-C. Canonici  
Laser measurements (LDV techniques)  
near terminal 2F.  
(b): Document CERFACS  
Wind field calculated by CERFACS through computational fluid dynamics code (CFD) right average wind left RMS.



3

b



## Development and evaluation of a nation-wide low-level wind-shear mosaic

Wind-shear is a difference in wind speed or direction over a relatively short distance in the atmosphere. Its horizontal component is commonly observed in the low levels within severe phenomena caused by thunderstorms, like gust fronts or meso-cyclones.

An algorithm for the detection of horizontal wind-shear in the low levels has been developed, from radial velocity data (wind component parallel to the radar beam axis) of all radars of ARAMIS network. This mosaic, which is produced every 5 minutes over metropolitan France, has a 1km<sup>2</sup> resolution. The product gives an estimation of the maximum horizontal wind-shear detected in the low levels between 0 and 2km above ground.

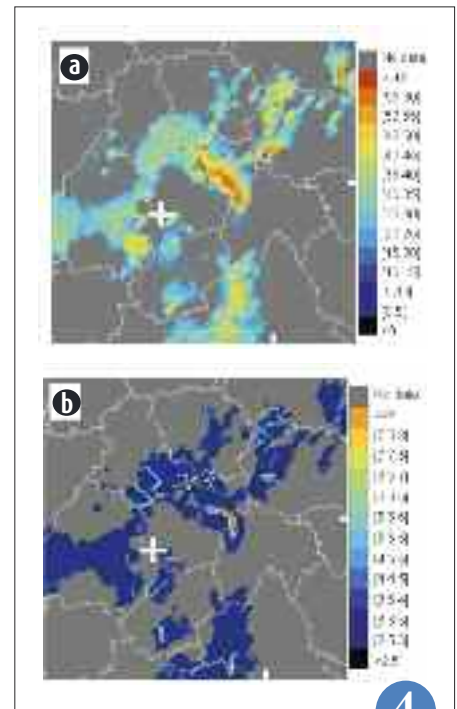
The examination of the wind-shear mosaic on different cases has shown that the product is able to retrieve small scale wind-shear signatures that can be linked to convergence lines ahead of convective cells indicative of gust fronts.

A statistical evaluation of the wind-shear mosaic has also been performed, by comparing the horizontal wind-shear values observed inside the area defined by convective objects with the gusts recorded along their trajectory by weather stations. This comparison has shown a link between the low-level horizontal wind-shear observed by the radar network and the gusty winds associated with thunderstorms.

The forecasters wished therefore to have the wind shear mosaic available and the product is soon going to be produced in an operational environment. It will be used as new information to improve the description of the gusts risk associated to thunderstorms, together with the storm relative “helicity” or the storm velocity.

4

Meso-scale system observed in the Limousin region on 12 July 2011: reflectivity mosaic in dBZ (a) and wind-shear mosaic in m s<sup>-1</sup> km<sup>-1</sup> (b) observed at 1950 UTC. The white cross indicates the position of Grèzes radar. The white lines indicate the French “départements” boundaries.



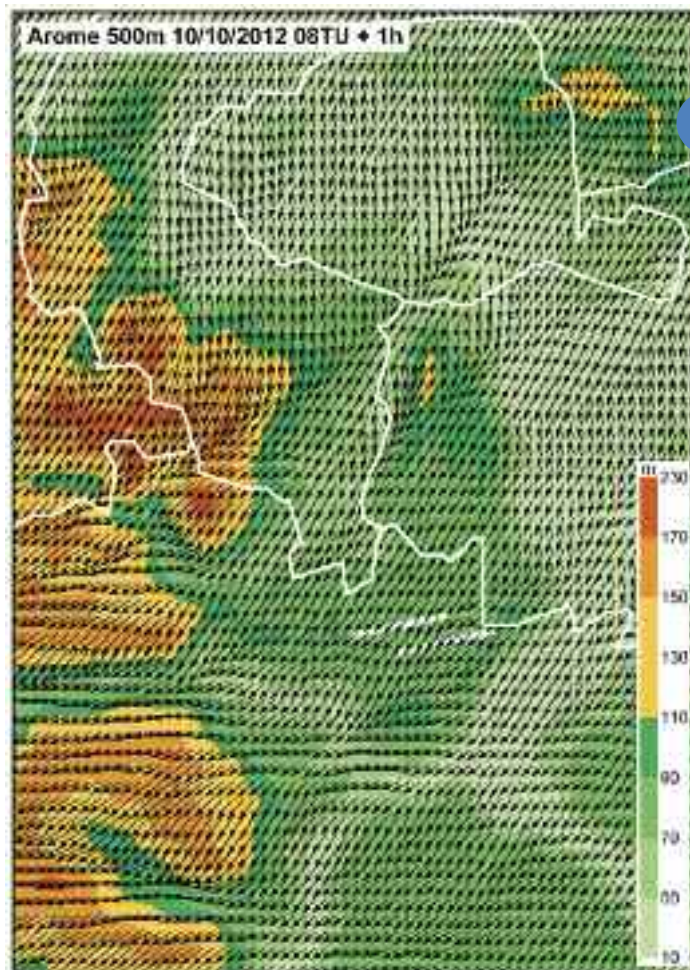
4

## An experimental suite: AROME-airport for aviation weather hazards

The AROME-airport model is a version of the AROME model that produces high resolution simulations around sensitive areas such as airports.

In the context of the European R&D programme SESAR (Single European Sky ATM Research) this model is used to make forecasts for different parameters around the CDG airport during a two-month period during autumn 2012. The configuration that was set up is composed of an hourly assimilation of observations over the north west of France at a 2.5km resolution, followed by a forecast on a 100km by 100km model at a 0.5km resolution. The model runs every hour with a first-guess taken from the AROME-France operational suite, the forecast range is 5 hours. Different settings have been tested. The meteorological output fields are temperature, humidity, wind, turbulent kinetic energy and the eddy dissipation rate. The meteorological fields from this model feed a wake-vortex model designed by the Université catholique de Louvain (UCL) whose final goal is to allow a dynamical adjustment of take-off and landing delays.

5



The figure shows an example of an AROME-airport simulation zoomed over the south-west part of the domain, around the Orly airport materialized by the white lines. The coloured field is the orography; the arrows represent wind at 10m in full resolution after one hour forecast.



# Appendix

## 2012 Scientific papers list

### Papers published in peer-reviewed journals (impact factor > 1)

- Barré J., V.-H. Peuch, J.-L. Attié, L. El Amraoui, W. A. Lahoz, B. Josse, M. Claeysman and P. Nédélec, 2012 : Stratosphere-troposphere ozone exchange from high resolution MLS ozone analyses, *Atmos. Chem. Phys.*, Volume: 12, Pages: 6129-6144, Doi: 10.5194/acp-12-6129-2012, Published: JUL 2012.
- Batté L. and M. Déqué, 2012: A stochastic method for improving seasonal predictions. *Geophysical Research Letters*, Volume: 39, Article Number: L09707, Doi: 10.1029/2012GL051406, Published: MAY 4 2012.
- Baumgardner D., L. Avallone, A. Bansemer, S. Bormann, P. Brown, U. Bundke, P. Chuang, D. Collins, D. Cziczo, P. Field, M. Gallagher, J.-F. Gayet, A. Heymsfield, A. Korolev, M. Krämer, G. McFarquhar, S. Mertes, O. Möhler, S. Lance, P. Lawson, M. Petters, K. Pratt, G. Roberts, D. Rogers, O. Stetzer, J. Stith, W. Strapp, C. Twohy, and M. Wendisch, 2012: In Situ, Airborne Instrumentation: Addressing and Solving Measurement Problems in Ice Clouds, *Bulletin of the American Meteorological Society*, Volume: 93, Issue: 2, Pages: E529-E534, Doi: 10.1175/BAMS-D-11-00123.1. Published: FEB 2012.
- Begue N., P. Tulet, J.-P. Chaboureaud, G. Roberts, L. Gomes, and M. Mallet, Long-range transport of Saharan dust over Northern Europe during EUCAARI 2008 campaign: Evolution of dust optical properties by scavenging. *Journal of Geophysical Research-Atmospheres*, Volume: 117, Article Number: D17201, Doi: 10.1029/2012JD017611. Published: SEP 5 2012.
- Bellon G., B. Stevens, 2012: Using the Sensitivity of Large-Eddy Simulations to Evaluate Atmospheric Boundary Layer Models. *Journal of Atmospheric Sciences*, Volume: 69, Issue: 5, Pages: 1582-1601, Doi: 10.1175/JAS-D-11-0160.1. Published: MAY 2012.
- Belviso S., I. Masotti, A. Tagliabue, L. Bopp, P. Brockmann, C. Fichot, G. Caniaux, L. Prieur, J. Ras, J. Uitz, H. Loisel, D. Desailly, S. Alvain and N. Kasamatsu, 2012: DMS dynamics in the most oligotrophic subtropical zones of the global ocean. *Biochemistry*, Volume: 110, Issue: 1-3, Special Issue: SI, Pages: 215-241, Doi: 10.1007/s10533-011-9648-1. Published: SEP 2012.
- Besson L., C. Boudjabi, O. Caumont, J. Parent du Châtelet, 2011: Links between weather phenomena and characteristics of refractivity measured by precipitation radar. *Boundary-Layer Meteorology*, Volume: 143, Issue: 1, Special Issue: SI, Pages: 77-95, Doi: 10.1007/s10546-011-9656-7. Published: APR 2012.
- Beuvier J., K. Béranger, C. Lebeaupin-Brossier, S. Somot, F. Sevault, Y. Drillet, R. Bourdallé-Badie, N. Ferry and F. Lyard, 2012: Spreading of the Western Mediterranean Deep Water after winter 2005: time scales and deep cyclone transport. *Journal of Geophysical Research-Oceans*, Volume: 117, Article Number : C07022, Doi: 10.1029/2011JC007679. Published: JUL 26 2012.
- Boisier J.-P., N. DeNoblet-Ducoudré, A. J. Pitman, F. Cruz, C. Delire, B. J.J.M. van den Kurk, M. K. van der Molen, C. Müller and A. Voldoire, 2012: Attributing the biogeophysical impacts of Land-Use induced Land-Cover changes on surface climate to specific causes. Results from the first LUCID set of simulations. *Journal of Geophysical Research-Atmospheres*, Volume: 117, Article Number: D12116, Doi: 10.1029/2011JD017106. Published: JUN 30 2012.
- Bouin M.N., D. Legain, O. Traullé, S. Belamari, G. Caniaux, A. Fiandrin, F. Lagarde, J. Barrié, E. Moulin and G. Bouhours, 2012: Using scintillometry to estimate sensible heat fluxes over water: first insights. *Boundary Layer Meteorology*, Volume: 143, Issue: 3, Pages: 451-480, Doi: 10.1007/s10546-012-9707-8, Published: JUN 2012.
- Bouniol D., F. Couvreur, P.-H. Kamsu-Tamo, M. Leplay, F. Guichard, F. Favot, E. O'Connor: Diurnal and seasonal cycles of cloud occurrences, types and radiative impact over West Africa. *Journal of Applied Meteorology and Climatology*, Volume: 51, Issue: 3, Pages: 534-553, Doi: 10.1175/JAMC-D-11-051.1. Published: MAR 2012.
- Bouttier F., B. Vié, O. Nuissier, L. Raynaud, 2012: Impact of stochastic physics in a convection-permitting ensemble. *Monthly Weather Review*
- Brousseau P., L. Berre, F. Bouttier, G. Desroziers: Flow-dependent background-error covariances for a convective-scale data assimilation system. *Quarterly Journal of the Royal Meteorological Society*, Volume: 138, Issue: 663, Pages: 310-322, Doi: 10.1002/qj.920, Part: Part b. Published: JAN 2012.
- Bueno B., G. Pigeon, L. K. Norford, K. Zibouche & C. Marchadier, Development and evaluation of a building energy model integrated in the TEB scheme. *Geoscientific Model Development*, Volume: 5, Issue: 2, Pages: 433-448. Published: 2012.
- Bueno B., L. Norford, G. Pigeon & R. Britter. A resistance-capacitance network model for the analysis of the interactions between the energy performance of buildings and the urban climate. *Building and Environment*, Volume: 54, Pages: 116-125, Published: AUG 2012.
- Carmagnola C.M., F. Domine, M. Dumont, P. Wright, B. Strellis, M. Bergin, J. Dibb, G. Picard and S. Morin, 2012: Snow spectral albedo at Summit, Greenland: comparison between in situ measurements and numerical simulations using measured physical and chemical properties of the snowpack. *The Cryosphere*, tc-2012-172.
- Calonne N., C. Geindreau, F. Flin, S. Morin, B. Lesaffre, S. Rolland du Roscoat and P. Charrier: 3-D image-based numerical computations of snow permeability: links to specific surface area, density, and microstructural anisotropy, *The Cryosphere Discuss.*, 6, 1157-1180, doi: 10.5194/tcd-6-1157-2012, 2012.
- Calvet J.C., S. Lafont, E. Cloppet, F. Souverain, V. Badeau, C. Le Bas, 2012: Use of agricultural statistics to verify the interannual variability in land surface models: a case study over France with ISBA-A-gs. *Geoscientific Model Development*, Volume: 5, Issue : 1, Pages: 37-54, Doi: 10.5194/gmd-5-37-2012. Published: 2012.
- Carmagnola C., M.F. Dominé, S. Morin, L. Arnaud, G. Picard, N. Champollion, M. Bergin, J. Dibb, P. Wright and M. Dumont: Ricerche sulla neve in Groenlandia: misure e risultati della campagna alla base Summit. *Nimbus* 63-64, 5-13, 2012.
- Carrer D., S. Lafont, J.-L. Roujean, J.-C. Calvet, C. Meurey, P. Le Moigne and I. F. Trigo, 2012: Incoming Solar and Infrared Radiation Derived from METEOSAT: Impact on the Modeled Land Water and Energy Budget over France, *Journal of Hydrometeorology*, Volume: 13, Issue: 2, Pages: 504-520, Doi: 10.1175/JHM-D-11-059.1. Published: APR 2012.
- Cattiaux J., H. Douville, A. Ribes, F. Chauvin and C. Planete, 2012: Towards a better understanding of changes in wintertime cold extremes over Europe, *Climate Dynamics*, online, Doi: 10.1007/s00382-012-1436-7.
- Cattiaux J. and P. Yiou, 2012: Contribution of atmospheric circulation to remarkable European temperatures of 2011, *Bulletin of the American Meteorological Society*, in « Explaining Extreme Events of 2011 from a Climate Perspective », Volume: 93, Pages: 1041-1067, Doi: 10.1075/BAMSD-12-00021.1, Published: JUL 2012.
- Charles E., D. Idier, J. Thiébot, G. Le Cozannet, R. Pedreros, F. Ardhuin and S. Planton, 2011: Present wave climate in the Bay of Biscay: spatiotemporal variability and trends from 1958 to 2001. *Journal of Climate*, Volume 25, Issue 6, Pages: 2020-2039, Published: March 2012, Doi: 10.1175/JCLI-D-11-00086.1.
- Cheab A., C. Francois, V. Badeau, J. Boe, I. Chuine, C. Delire, E. Dufrene, E. Gritti, M. Legay, C. Page, W. Thuillier, N. Viovy, P. Leadley, 2012: Climate change impacts on tree ranges: model inter-comparison facilitates understanding and quantification of uncertainty. *Ecology Letters*, Volume: 15, Issue: 6, Pages: 533-544, Doi: 10.1111/j.1461-0248.2012.01764.x. Published: JUN 2012.
- Chevallier M. and D. Salas-Méla, 2012: The Role of Sea Ice Thickness Distribution in the Arctic Sea Ice Potential Predictability: A Diagnostic Approach with a Coupled GCM. *Journal of Climate*, Volume: 25, Issue: 8, Pages: 3025-3038, Doi: 10.1175/JCLI-D-11-00209.1. Published: APR 2012.
- Corre L., L. Terray, M. Balmaseda, A. Ribes, A. Weaver, 2011: Can oceanic reanalyses be used to assess recent anthropogenic changes and low-frequency internal variability of upper ocean temperature? *Climate Dynamics*, Volume: 38, Issue: 5-6, Pages: 877-896, Doi: 10.1007/s00382-010-0950-8. Published: MAR 2012.

- Couvreur F., C. Rio, F. Guichard, M. Lothon, G. Canut, D. Bouniol and A. Gounou, 2012: Initiation of daytime local convection in a semi-arid region analysed with high-resolution simulations and AMMA observations, *Quarterly Journal of the Royal Meteorological Society*, Volume: 138, Issue: 662, Pages: 56-71, Doi: 10.1002/qj.903, Part: Part a. Published: Jan 2012.
- Dabas A., S. Remy and T. Bergot 2012: Use of a Sodar to Improve the Forecast of Fogs and Low Clouds on Airports. *Pure and Applied Geophysics*, Volume: 169, Issue: 5-6, Special Issue: SI, Pages: 769-781, Doi: 10.1007/s00024-011-0334-y. Published: MAY 2012.
- Daloz A.-S., F. Chauvin, K. Walsh, S. Lavender, D. Abbs and F. Roux, 2012: The ability of general circulation models to simulate tropical cyclones and their precursors over the North Atlantic main development region. *Climate Dynamics*, Volume: 39, Issue: 7-8, Pages: 1559-1576, Doi: 10.1007/s00382-012-1290-7. Published: OCT 2012.
- De Boissésion E., V. Thierry, H. Mercier, G. Caniaux and D. Desbroyères, 2012: Origin, formation and variability of the Subpolar Mode Water located over the Reykjanes ridge in the ORCA025-G70 simulation. *Journal of Geophysical Research*, Volume: 117, Article Number: C12005, Doi: 10.1029/2011JC007519, Published: DEC 8 2012.
- De Munck C., G. Pigeon, V. Masson, F. Meunier, P. Bousquet, B. Tréméac, M. Merchat, P. Pœuf, C. Marchadier, 2012: How much can air conditioning increase air temperatures for a city like Paris, France? *International Journal of Climatology*, Doi: 10.1002/joc.3415. Sous presse.
- De Noblet-Ducoudre N., J.P. Boisier, A. Pitman, G.B. Bonan, V. Brovkin, F. Cruz, C. Delire, V. Gayler, B.J.J.M. Van den Hurk, P.J. Lawrence, M.K. Van der Molen, C. Muller, C.H. Reick, B.J. Strengers, A. Voldoire: Determining Robust Impacts of Land-Use-Induced Land Cover Changes on Surface Climate over North America and Eurasia: Results from the First Set of LUCID Experiments : *Journal of Climate*, Volume: 25, Issue: 9, Pages: 3261-3281. Published: MAY 2012.
- Decharme B., R. Alkama, F. Papa, S. Faroux, H. Douville, and C. Prigent, 2012: Global off-line evaluation of the ISBA-TRIP flood model, *Climate Dynamics*, Volume: 38 Issue: 7-8, Pages: 1389-1412, Doi: 10.1007/s00382-011-1054-9. Published: APR 2012.
- Déqué M., S. Somot, E. Sanchez-Gomez, C.M. Goodess, D. Jacob, G. Lenderink, O.B. Christensen, 2011: The spread amongst ENSEMBLES regional scenarios: Regional Climate Models, driving General Circulation Models and interannual variability. *Climate Dynamics*, Volume: 38, Issue: 5-6, Pages: 951-964, Published: MAR 2012. Doi: 10.1007/s00382-011-1053-x.
- Desroziers G. and L. Berre: Accelerating and parallelizing minimizations in ensemble and deterministic variational assimilations. *Quarterly Journal of Royal Meteorological Society*, Volume: 138, Issue: 667, Pages: 1599-1610, Doi: 10.1002/qj.1886. Part Part b. Published: JUL 2012.
- Dumont M., Y. Durand, Y. Araud and D. Six, 2012: Variational assimilation of albedo in a snowpack model and reconstruction of the spatial mass balance distribution of an alpine glacier. *Journal of Glaciology*, 58, 207, 151-164, Doi: 10.3189/212JoG11J163.
- Domine F., J.-C. Gallet, J. Bock and S. Morin, 2012: Structure, specific surface area and thermal conductivity of the snowpack around Barrow, Alaska. *Journal of Geophysical Research-Atmospheres*, Volume: 117, Pages: R14-R14, Doi: 10.1029/2011JD016647. Published: MAR 15 2012.
- Douville H., A. Ribes, B. Decharme, R. Alkama, J. Sheffield, 2012: Anthropogenic influence on multidecadal changes in reconstructed global evapotranspiration, *Nature Climate Change*, online, Doi: 10.1038/NCLIMATE1632.
- Dubois C., S. Somot, F. Sevault, M. Déqué, B. Lheveder, L.Li, A. Carillo, A. Dell'Aquila, A. Elizalde-Arellano, D. Jacob, E. Scoccimarro, P. Oddo and S. Gualdi, 2012: Future projections of the surface heat and water budgets of the Mediterranean sea in an ensemble of coupled atmosphere-ocean regional climate models, *Climate Dynamics*, Volume: 39, Issue: 7-8, Pages: 1859-1884, Doi: 10.1007/s00382-011-1261-4, Published: OCT 2012.
- Duvel J.-P., H. Bellenger, G. Bellon and M. Remaud, 2012: An event-by-event assessment of tropical intraseasonal perturbations for general circulation models, *Climate Dynamics*, online, Doi: 10.1007/s00382-012-1303-6.
- Flaounas E., P. Drobinski, M. Borge, J.-C. Calvet, G. Delrieu, E. Morin, G. Tartari and R. Toffolon: Assessment of gridded observations used for climate model validation in the Mediterranean region: the HyMeX and MED-CORDEX framework. *Environement Research Letters*, Volume: 7, Issue: 2, Article Number: 024017, Doi: 10.1088/1748-9326/7/2/024017, Published: APR-JUN 2012.
- Getirana A. C. V., A. Boone, D. Yamazaki, B. Decharme, F. Papa and N. Mognard, 2012: The Hydrological Modeling and Analysis Platform (HyMAP): evaluation in the Amazon basin. *J. Hydrometeor.*, in press, Doi: 10.1175/JHM-D-12-021.1.
- Guedj S., F. Karbou and F. Rabier, 2012: Land surface temperature estimation to improve the assimilation of SEVIRI radiances over land. *Journal of Geophysical Research*, Vol.116, D14107, 18 PP., Doi: 10.1029/2011JD015776.
- Grandpeix J.-Y. and J.P. Lafore, 2012: Reply to "Comments on 'A Density Current Parameterization Coupled with Emanuel's Convection Scheme. Part I: The Models'". *Journal of the Atmospheric Sciences*, Volume: 69, Issue: 6, Pages: 2090-2096, Doi: 10.1175/JAS-D-11-0127.1. Published: JUN 2012.
- Guérémy J.-F., N. Laanaia and J.-P. Céron, 2012: Seasonal forecast of French Mediterranean heavy precipitating events linked to weather regimes, *Nat. Hazards Earth Syst. Sci.*, 12, 2389-2398, doi: 10.5194/nhess-12-2389-2012. Published: JUL 2012.
- Haase J.S., J. Maldonado-Vargas, F. Rabier, P. Cocquerez, M. Minois, V. Guidard, P. Wyss, A.V. Johnson. A proof-of-concept balloon-borne Global Positioning System radio occultation profiling instrument for polar studies. *Geophysical Research Letters*, Volume: 39, Article Number: L02803, Doi: 10.1029/2011GL049982. Published: JAN 21 2012.
- lacono-Marziano G., V. Marécal, M. Pirre, F. Gaillard, J. Arteta, B. Scaillet and N. T. Arndt, 2012: Gas emissions due to magma-sediment interactions during flood magmatism at the Siberian Traps: gas dispersion and environmental consequences. *Earth and Planetary Science Letters*, Volume: 358, Pages: 308-318, Doi: 10.1016/j.epsl.2012.09.051, Published: DEC 2012.
- Hilton F., R. Armante, T. August, C. Barnet, A. Bouchard, C. Camy-Peyret, V. Capelle, L. Clarisse, C. Clerbaux, P.-F. Coheur, A. Collard, C. Crevoisier, G. Dufour, D. Edwards, F. Fajjan, N. Fourié, A. Gambacorta, M. Goldberg, V. Guidard, D. Hurtmans, S. Illingworth, N. Jacquinet-Husson, T. Kerzenmacher, D. Klaes, L. Lavanant, G. Masiello, M. Matricardi, A. McNally, S. Newman, E. Pavelin, S. Payan, E. Péquignot, S. Peyridieu, T. Phulpin, J. Remedios, P. Schlüssel, C. Serio, L. Strow, C. Stubenrauch, J. Taylor, D. Tobin, W. Wolf and D. Zhou: Hyperspectral Earth Observation from IASI: Five Years of Accomplishments. *Bulletin of the American Meteorological Society*, Volume: 93, Issue: 3, Pages: 347-+, Doi: 10.1175/BAMS-D-11-00027.1. Published: MAR 2012.
- Jaumouillé E., S. Massart, A. Piacentini, D. Cariolle and V.-H. Peuch, 2012: Impact of a time-dependent background error covariance matrix on air quality analysis, *Geosci. Mod. Dev.*, 5, 1075-1090.
- Joly M. and V.-H. Peuch, 2012: Objective classification of air quality monitoring sites over Europe. *Atmospheric Environment*, Volume: 47, Pages: 111-123, Published: FEB 2012.
- Jorda G., D. Gomis, E. Alvarez-Fanjul, S. Somot, 2012: Atmospheric contribution to Mediterranean and nearby Atlantic sea level variability under different climate change scenarios. *Global and Planetary Change*, Volume: 80-81, Pages: 198-214, Doi: 10.1016/j.gloplacha.2011.10.013. Published: JAN 2012.
- Kocha C., J.-P. Lafore, P. Tulet and Y. Seity: High-resolution simulation of a major West African dust-storm: comparison with observations and investigation of dust impact. *Quarterly Journal of Royal Meteorological Society*, Volume: 138, Issue: 663, Pages: 455-470, Doi: 10.1002/qj.927. Part: Part b. Published: JAN 2012.
- Krysztofiak G., V. Catoire, G. Poulet, V. Marécal, M. Pirre, F. Louis, S. Canneaux and B. Josse Detailed modeling of the atmospheric degradation mechanism of very-short lived brominated species. *Atmospheric Environment*, Volume: 59, Pages: 514-532, Doi: 10.1016/j.atmosenv.2012.05.026. Published: NOV 2012.
- Kukkonen J., T. Olsson, D. M. Schultz, A. Baklanov, T. Klein, A. I. Miranda, A. Monteiro, M. Hirtl, V. Tarvainen, M. Boy, V.-H. Peuch, A. Poupkou, I. Kioutsioukis, S. Finardi, M. Sofiev, R. Sokhi, K. E. J. Lehtinen, K. Karatzas, R. San José, M. Astitha, G. Kallos, M. Schaap, E. Reimer, H. Jakobs and K. Eben: A review of operational, regional-scale, chemical weather forecasting models in Europe. *Atmospheric Chemistry and Physics*, Volume: 12, Issue: 1, Pages: 1-87, Doi: 10.5194/acp-12-1-2012. Published: 2012.
- Kurzeneva E., E. Martin, Y. Batrak and P. Le Moigne, 2012: Climate data for parameterisation of lakes in Numerical Weather Prediction models. *TELLUS Series A-Chemical and Physical Meteorology*, Volume: 64, Article Number: 17226, Doi: 10.3402/tellusa.v64i0.17226. Published: 2012.
- L'Heveder B., L. Li, F. Sevault and S. Somot, 2012: Interannual variability of deep convection in the Northwestern Mediterranean simulated with a coupled AORCM. *Climate Dyn.*, Doi: 10.1007/s00382-012-1527-5.
- Lacroix P., J.-R. J. Grasso, J. Roulle, G. Giraud, D. Goetz, S. Morin and A. Helmstetter, 2012: Monitoring of snow avalanches using a seismic array: Location, speed estimation and relationships to meteorological variables, *Journal of Geophysical Research-Earth Surface*, Volume: 117, Article Number: F01034, Doi: 10.1029/2011JF002106. Published: MAR 24 2012.
- Lafont S., Y. Zhao, J.-C. Calvet, P. Peylin, P. Ciais, F. Maignan and M. Weiss, 2012: Modelling LAI, surface water and carbon fluxes at high-resolution over France: comparison of ISBA-Ags and ORCHIDEE. *Biogeosciences*, Volume: 9, Issue: 1, Pages: 439-456, Doi: 10.5194/bg-9-439-2012. Published: 2012.
- Lahoz W.A., V.-H. Peuch, J. Orphal, J.-L. Attié, K. Chance, X. Liu, D. Edwards, H. Elbern, J.-M. Flaud, M. Claeysman and L. El Amraoui, 2012: Monitoring air quality from space: the case for the geostationary platform, *Bull. Am. Meteorol. Soc.*, Volume: 93, Issue: 2, Pages: 221-233, Doi: 10.1175/BAMS-D-11-00045.1, Published: FEB 2012.
- Lagouarde J.P., A. Henon, M. Irvine, J. Voogt, G. Pigeon, P. Moreau, V. Masson, P. Mestayer: Experimental characterization and modelling of the nighttime directional anisotropy of thermal infrared measurements over an urban area: Case study of Toulouse (France). *Remote Sensing of Environment* volume: 117, Pages: 19-33, Doi: 10.1016/j.rse.2011.06.022, Published: FEB 15 2012
- Marécal V., M. Pirre, G. Krysztofiak, P. D. Hamer and B. Josse, 2012: What do we learn about bromoform transport and chemistry in deep convection from fine scale modelling? *Atmospheric Chemistry and Physics*, Volume: 12, Issue: 14, Pages: 6073-6093, Doi: 10.5194/acp-12-6073-2012. Published: 2012.
- Massart S., A. Piacentini and O. Pannekoucke: Importance of using ensemble estimated background error covariances for the quality of atmospheric ozone analyses. *Quarterly Journal of Royal Meteorological Society*, Volume: 138, Issue: 665, Pages: 889-905, Doi: 10.1002/qj.971. Part: Part b. Published: APR 2012.

- Mattar C., J.-P. Wigneron, J.A. Sobrino, N. Novello, J.-C. Calvet, C. Albergel, P. Richaume, A. Mialon, D. Guyon, J.C. Jimenez-Munoz and Y. Kerr: A combined optical-micro-wave method to retrieve soil moisture over vegetated areas, *IEEE Transaction on Geoscience and Remote Sensing*, Volume: 50, Issue: 5, Special Issue: SI, Pages: 1404-1413, Doi: 10.1109/TGRS.2011.2179051, Part: Part 1. Published: MAY 2012, doi: 10.1109/TGRS.2011.2179051, 2012.
- Ménégoz M., A. Voldoire, H. Teyssedre, D. Salas y Melia, V.H. Peuch and I. Goutevin, 2012: How does the atmospheric variability drive the aerosol residence time in the Arctic region? 2012: *TELLUS Series B-Chemical and Physical Meteorology*, Volume: 64, Article Number: 11596, Doi: 10.3402/tellus.v64i0.11596. Published: 2012.
- Menkes C. E., M. Lengaigne, P. Marchesio, N. C. Jourdain, E. M. Vincent, J. Lefèvre, F. Chauvin and J.-F. Royer, 2012: Comparison of tropical cyclogenesis indices on seasonal to interannual timescales, *Climate Dynamics*, Volume 38, Numbers 1-2, Pages: 301-321, Doi: 10.1007/s00382-011-1126-x. Published: JAN 2012.
- Meyssignac B., D. Salas y Melia, M. Becker, W. Llovel and A. Cazenave, 2012: Tropical Pacific spatial trend patterns in observed sea level: internal variability and/or anthropogenic signature? *Climate of The Past*, Volume: 8, Issue: 2, Pages: 787-802, Doi: 10.5194/cp-8-787-2012. Published: 2012.
- Michel C., G. Rivière, L. Terray and B. Joly: The dynamical link between surface cyclones, upper-tropospheric Rossby wave breaking and the life cycle of the Scandinavian blocking. *Geophysical Research Letters*, Volume: 39, Article Number: L10806, Doi: 10.1029/2012GL051682. Published: MAY 18 2012.
- Michel Y., 2012: Estimating deformations of random processes for correlation modelling: methodology and the one-dimensional case. *Q.J.R. Meteorol. Soc.* doi: 10.1002/qj.2007.
- Mohino E., S. Janicot, L. Li, H. Douville, 2011: Impact of the Indian part of the summer MJO on West Africa using nudged climate simulations. *Climate Dynamics*, Volume: 38, Issue: 11-12, Pages: 2319-2334, Doi: 10.1007/s00382-011-1206-y. Published: JUN 2012.
- Mokhtari M., L. Gomes, P. Tulet and T. Rezoug, 2012: Importance of the surface size distribution of erodible material: an improvement on the Dust Entrainment And Deposition (DEAD) Model. *Geoscientific Model Development*, Volume: 5, Issue: 3, Pages: 581-598. Published: 2012.
- Morin S., J. Erbland, J. Savarino, F. Domine, J. Bock, U. Friess, H.-W. Jacobi, H. Sihler and J.M. F. Martins, 2012: An isotopic view on the connection between photolytic emissions of NOx from the Arctic snowpack and its oxidation by reactive halogens. *Journal of Geophysical Research-Atmospheres*, Volume: 117, Article Number: D00R08, Doi: 10.1029/2011JD016618. Published: JAN 21 2012.
- Morin S., F. Domine, A. Dufour, Y. Lejeune, B. Lesaffre, J.-M. Morin, S.F. Domine, A. Dufour, Y. Lejeune, B. Lesaffre, J.-M. Willemet, C.M. Carmagnola and H.-W. Jacobi, Measurements and modeling of the vertical profile of specific surface area of an alpine snowpack, *Adv. Water Resour.*, doi: 10.1016/j.advwatres.2012.01.010, sous presse.
- Morin S., Y. Lejeune, B. Lesaffre, J.-M. Panel, D. Poncet, P. David and M. Sudul: An 18-yr long (1993–2011) snow and meteorological dataset from a mid-altitude mountain site (Col de Porte, France, 1325 m alt.) for driving and evaluating snowpack models, *Earth Syst. Sci. Data*, 4, 13-21, doi: 10.5194/essd-4-13-2012, 2012.
- Muri H., A. Berger, Q. Yin, A. Voldoire, D. Salas-Mélia and S. Sundaram, 2012: SST and ice sheet impacts on the MIS-13 climate. *Climate Dynamics*, Volume: 39, Issue: 7-8, Pages: 1739-1761, Doi: 10.1007/s00382-011-1216-9. Published: OCT 2012.
- Nabat P., F. Solmon, M. Mallet, J. F. Kok and S. Somot: Dust emission size distribution impact on aerosol budget and radiative forcing over the Mediterranean region: a regional climate model approach, *Atmos. Chem. Phys.*, 12, 10545-10567, doi: 10.5194/acp-12-10545-2012, 2012.
- Nikulin G., C. Jones, P. Samuelsson, P. Giorgi, M.B. Sylla, G. Asrar, M. Büchner, R. Cerezo-Mota, O.B. Christensen, M. Déqué, J. Fernandez, A. Hänsler, E. van Meijgaard, L. Sushama, 2012: Precipitation Climatology in An Ensemble of CORDEX-Africa Regional Climate Simulations. *Journal of Climate*, Volume: 25, Issue: 18, Pages: 6057-6078, Doi: 10.1175/JCLI-D-11-00375.1. Published: SEP 15 2012.
- Oger N., O. Pannekoek, A. Doerenbecher and P. Arbogast: Assessing the trajectory influence in adaptive observation Kalman filter sensitivity method. *Quarterly Journal of Royal Meteorological Society*, Volume: 138, Issue: 664, Pages: 813-825, Doi: 10.1002/qj.950, Part: Part a. Published: APR 2012.
- Olivie D.J.L., D. Cariolle, H. Teyssedre, D. Salas, A. Voldoire, H. Clark, D. Saint-Martin, M. Michou, F. Karcher, Y. Balkanski, M. Gauss, O. Dessens, B. Koffi and R. Sausen, 2012: Modeling the climate impact of road transport, maritime shipping and aviation over the period 1860-2100 with an AOGCM 2012: *Atmospheric Chemistry and Physics*, Volume: 12, Issue: 3, Pages: 1449-1480, Doi: 10.5194/acp-12-1449-2012. Published: 2012.
- Oruba L., G. Lapeyre and G. Rivière: On the Northward Motion of Midlatitude Cyclones in a Barotropic Meandering Jet. *Journal of the Atmospheric Sciences*, Volume: 69, Issue: 6, Pages: 1793-1810, Doi: 10.1175/JAS-D-11-0267.1. Published: JUN 2012.
- Oueslati B. and G. Bellon, 2012: Tropical precipitation regimes and mechanisms of regime transitions: contrasting two aquaplanet general circulation models. *Climate Dynamics*, Doi: 10.1007/s00382-012-1344-x. See here.
- Papadopoulos V.P., S. Josey, A. Bartzokas, S. Somot, S. Ruiz, P. Drakopoulou, 2012: Large scale atmospheric circulation favoring deep and intermediate water formation in the Mediterranean Sea. *Journal of Climate*, Volume: 25, Issue: 18, Pages: 6079-6091, Doi: 10.1175/JCLI-D-11-00657.1, Published: SEP 15 2012.
- Parrens M., E. Zakharova, S. Lafont, J.-C. Calvet, Y. Kerr, W. Wagner and J.-P. Wigneron: Comparing soil moisture retrievals from SMOS and ASCAT over France, *Hydrology and Earth System Sciences*, Volume: 16, Issue: 2, Pages: 423-440, Doi: 10.5194/hess-16-423-2012. Published: 2012.
- Pedinotti V., A. Boone, B. Decharme, J.-F. Crétau, N. Mognard, G. Panthou and F. Papa, 2012: Characterization of the hydrological functioning of the Niger basin using the ISBA-TRIP model. *Hydrology and Earth System Sciences*, Volume: 16, Issue: 6, Pages: 1745-1773, Doi: 10.5194/hess-16-1745-2012. Published: 2012.
- Peings Y., D. Saint-Martin and H. Douville, 2012: A numerical sensitivity study of the Siberian snow influence on the Northern Annular Mode. *Journal of Climate*, Volume: 25, Issue: 2, Pages: 592-607, Doi: 10.1175/JCLI-D-11-00038.1, Published: JAN 15 2012.
- Rabier F, S. Cohn, P. Cocquerez, A. Hertzog, L. Avallone, T. Deshler, J. Haase, T. Hock, A. Doerenbecher, J. Wang, V. Guidard, J.N. Thépaut, R. Langland, A. Tangborn, G. Balsamo, E. Brun, D. Parsons, J. Bordereau, C. Cardinali, F. Danis, J.P. Escarnot, N. Fourrié, R. Gelaro, C. Genthon, K. Ide, L. Kalnajs, C. Martin, L.-F. Meunier, J.-M. Nicot, T. Pertulla, N. Potts, P. Ragazzo, D. Richardson, S. Sosa-Sesma, A. Vargas: The Concordiasi field experiment over Antarctica: first results from innovative atmospheric measurements. *BAMS meeting summary*, Doi: 10.1175/BAMS-D-12-00005.1.
- Raynaud L., L. Berre, G. Desroziers: Accounting for model error in the Météo-France ensemble data assimilation system. *Quarterly Journal of Royal Meteorological Society*, Volume: 138, Issue: 662, Pages: 249-262, Doi: 10.1002/qj.906. Part: Part a. Published: JAN 2012.
- Raynaud L. and O. Pannekoek: Heterogeneous filtering of ensemble-based background-error variances. *Quarterly Journal of Royal Meteorological Society*, Volume: 138, Issue: 667, Pages: 1589-1598, Doi: 10.1002/qj.1890. Part: Part b. Published: JUL 2012.
- Rémy S., O. Pannekoek, T. Bergot and C. Baehr. Adaptation of a particle filtering method for data assimilation in a 1D numerical model used for fog forecasting. *Quarterly Journal of Royal Meteorological Society*, Volume: 138, Issue: 663, Pages: 536-551, Doi: 10.1002/qj.915. Part: Part b. Published: JAN 2012.
- Ricard D, V. Ducrocq and L. Auger: A Climatology of the Mesoscale Environment Associated with Heavily Precipitating Events over a Northwestern Mediterranean Area. *Journal of Applied Meteorology and Climatology*, Volume: 51, Issue: 3, Pages: 468-488, Doi: 10.1175/JAMC-D-11-017.1. Published: MAR 2012.
- Ricard D., P. Arbogast, F. Crépin, A. Joly: Relationship between convection over Central America and the intensity of the jet stream bearing on the 1999 December European storms. *Quarterly Journal of Royal Meteorological Society*, Volume: 138, Issue: 663, Pages: 377-390, Doi: 10.1002/qj.931. Part: Part b. Published: JAN 2012.
- Ringeval B., B. Decharme, S. L. Piao, P. Ciais, F. Papa, N. de Noblet-Ducoudré, C. Prigent, P. Friedlingstein, I. Gouttevin, C. Koven, and A. Ducharme, 2012: Modelling sub-grid wetland in the ORCHIDEE global land surface model: evaluation against river discharges and remotely sensed data. *Geosci. Model Dev.*, Volume: 5, Pages: 941-962, Doi: 10.5194/gmd-5-941-2012, Published: JUL 2012.
- Rio C., J.-Y. Grandpeix, F. Hourdin, F. Guichard, F. Couvreux, J.-P. Lafore, A. Fridlind, A. Mrowiec, S. Bony, N. Rochetin, R. Roehrig, A. Idelkadi, M.-P. Lefebvre, I. Musat, 2012: Control of deep convection by sub-cloud lifting processes: The ALP closure in the LMDZ5B general circulation model. *Climate Dynamics*, online, Doi: 10.1007/s00382-012-1506-x.
- Rousselot M., Y. Durand, G. Giraud, L. Mérindol, I. Dombrowski-Etchevers, M. Déqué and H. Castebrenet, 2012: Statistical adaptation of ALADIN RCM outputs over the French Alps – application to future climate and snow cover, *Cryosphere*, Volume: 6, Issue: 4, Pages: 785-805, Doi: 10.5194/tc-6-785-2012, Published: 2012.
- Rivière G., P. Arbogast, G. Lapeyre, and K. Maynard: A potential vorticity perspective on the motion of a mid-latitude winter storm. *Geophysical Research Letters*, Volume: 39, Article Number: L12808, Doi: 10.1029/2012GL052440. Published: JUN 30 2012.
- Saccone P., S. Morin, C. Colomb, F. Baptist, J.-M. Bonnevill, M. P. Colace, F. Dolome, M. Faure, R. Geremia, J. Lochet, F. Poly, S. Lavorel and J.-C. Clément: The effects of snowpack properties and plant strategies on litter during winter in subalpine meadows. *Plant and Soil*, Doi: 10.1007/s11104-012-1307-3, 2012.decomposition.
- Séférian R., L. Bopp, M. Gehlen, J. Orr, C. Ethé, P. Cadule, O. Aumont, D. Salas y Melia, A. Voldoire and G. Madec, 2012: Skill assessment of three earth system models with common marine biogeochemistry. *Climate Dynamics*, online, Doi: 10.1007/s00382-012-1362-8.
- Séférian R., D. Iudicone, L. Bopp, T. Roy and G. Madec, 2012: Water Mass Analysis of Effect of Climate Change on Air-Sea CO2 Fluxes: The Southern Ocean. *Journal of Climate*, Volume: 25, Issue: 11, Pages: 3894-3908, Doi: 10.1175/JCLI-D-11-00291.1, Published: JUN 1 2012.
- Singla S., J.-P. Céron, E. Martin, F. Regimbeau, M. Déqué, F. Habets, and J.-P. Vidal, 2012: Predictability of soil moisture and river flows over France for the spring season, *Hydrology and Earth System Sciences*, Volume: 16, Issue: 1, Pages: 201-216, Doi: 10.5194/hess-16-201-2012. Published: 2012.



Solé J., S. Ruiz, A. Pascual, S. Somot and J. Tintoré, 2012: Ocean color response to wind forcing in the Alboran Sea: a new forecasting method. *Journal of Marine Systems*, Volume: 98-99, Pages: 1-8, Doi: 10.1016/j.jmarsys.2012.02.007. Published: SEP 1 2012.

Szczypka C., B. Decharme, D. Carrer, J.-C. Calvet, S. Lafont, S. Somot, S. Faroux and E. Martin, 2012: Impact of precipitation and land biophysical variables on the simulated discharge of European and Mediterranean rivers, *Hydrol. Earth Syst. Sci.*, 16, 3351-3370, Doi: 10.5194/hess-16-3351-2012

Thierion C., L. Longuevergne, F. Habets, E. Ledoux, P. Ackerer, S. Majdalani, E. Lebouis, S. Lecluse, E. Martin, S. Queguiner and P. Viennot, 2012: Assessing the water balance of the Upper Rhine Graben hydrosystem *Journal of Hydrology*, Volume: 424, Pages: 68-83, Doi: 10.1016/j.jhydrol.2011.12.028. Published: MAR 6 2012.

Thouren O., Brenguier J.-L. and F. Burnet, 2012: Supersaturation calculation in large eddy simulation models for prediction of the droplet number concentration, *Geosci. Model Dev.*, 5, 761-772, Doi: 10.5194/gmd-5-761-2012. Published: 23 May 2012

Tremeac B., P. Bousquet, C. de Munck, G. Pigeon, V. Masson, C. Marchadier, M. Merchat, P. Poëuf, F. Meunier: Influence of air conditioning management on heat island in Paris air street temperatures. *Applied Energy*, Volume: 95, Pages: 102-110, Doi: 10.1016/j.apenergy.2012.02.015. Published: JUL 2012.

Tsimplis M. N., F. Raicich, L. Fenoglio-Marc, A. G.P. Shaw, M. Marcos, S. Somot and A. Bergamasco, 2011: Recent developments in understanding sea level rise at the Adriatic coasts. *Physics and Chemistry of the Earth, Special Issue of Physics and Chemistry of the Earth: "Venetia and Northern Adriatic Climate"*, Parts A/B/C, Volume: 40-41, Pages: 59-71, Published: 2012, Doi: 10.1016/j.pce.2009.11.007.

Vergnes J.-P., B. Decharme, R. Alkama, E. Martin, F. Habets, H. Douville, 2012: A Simple Groundwater Scheme for Hydrological and Climate Applications: Description and Offline Evaluation over France. *Journal of Hydrometeorology*, Volume: 13, Issue: 4, Pages: 1149-1171, Doi: 10.1175/JHM-D-11-0149.1. Published: AUG 2012.

Vergnes J.-P. and B. Decharme, 2012: A simple groundwater scheme in the TRIP river routing model: global off-line evaluation against GRACE terrestrial water storage estimates and observed river discharges. *Hydrology and Earth System Science*, Volume: 16, Issue: 10, Pages: 3889-3908, Doi: 10.5194/hess-16-3889-2012, Published: 2012.

Vidal J.-P., E. Martin, N. Kitova, J. Najac and Soubeyroux, J.-M.: Evolution of spatio-temporal drought characteristics: validation, projections and effect of adaptation sce-

narios, *Hydrology and Earth System Sciences*, Volume: 16, Issue: 8, Pages: 2935-2955, Doi: 10.5194/hess-16-2935-2012. Published: 2012.

Vionnet V., E. Brun, S. Morin, A. Boone, S. Faroux, P. Le Moigne, E. Martin and J.-M. Willemet: The detailed snowpack scheme Crocus and its implementation in SURFEX v7.2. *Geoscientific Model Development*, Volume: 5, Issue: 3, Pages: 773-791, Doi: 10.5194/gmd-5-773-2012. Published: 2012.

Vionnet V., G. Guyomarc'h, F.N. Bouvet, E. Martin, Y. Durand, H. Bellot, C. Bel, P. Pugliese: Occurrence of blowing snow events at an alpine site over a 10-year period: Observations and modelling, *Advances in Water Resources*, Doi: org/10.1016/j.advwatres.2012.05.004, 2012.

Voltaire A., E. Sanchez-Gomez, D. Salas y Méliá, B. Decharme, C. Cassou, S. Sényesi, S. Valcke, I. Beau, A. Alias, M. Chevallier, M. Déqué, J. Deshayes, H. Douville, E. Fernandez, G. Madec, E. Maisonnave, M.-P. Moine, S. Planton, D. Saint-Martin, S. Szopa, S. Tyteca, R. Alkama, S. Belamari, A. Braun, L. Coquart, F. Chauvin, 2012: The CNRM-CM5.1 global climate model: description and basic evaluation, *Climate Dynamic*, Doi: 10.1007/s00382-011-1259-y.

Vrac M., P. Drobinski, A. Merlo, M. Herrmann, C. Lavaysse, L. Li and S. Somot, 2012: Dynamical and statistical downscaling of the French Mediterranean climate :uncertainty assessment. *Nat. Hazards Earth Syst. Sci.*: 12, 2769-2784, doi: 10.5194/nhess-12-2769-2012.

Wigner J.-P., M. Schwank, E. Lopez-Baeza, Y.H. Kerr, N. Novello, C. Millan, C. Moisy, P. Richaume, A. Mialon, A. Al Bitar, F. Cabot, H. Lawrence, D. Guyon, J.-C. Calvet, J.P. Grant, T. Casal, P. de Rosnay, K. Saleh, A. Mahmoodi, S. Delwart, S. Mecklenburg: First evaluation of the simultaneous SMOS and ELBARA-II observations in the Mediterranean region, *Remote Sensing of Environment*, 124, 26-37, Doi: 10.1016/j.rse.2012.04.014, 2012.

Zakharova E., J.-C. Calvet, S. Lafont, C. Albergel, J.-P. Wigner, M. Pardé, Y. Kerr, M. Zribi: Spatial and temporal variability of biophysical variables in southwestern France from airborne L-band radiometry, *Hydrology and Earth System Sciences*, Volume: 16, Issue: 6, Pages: 1725-1743, Doi: 10.5194/hess-16-1725-2012 Published: 2012.

Zhao Y., P. Ciais, P. Peylin, N. Viovy, B. Longdoz, J.M. Bonnefond, S. Rambal, K. Klumpp, A. Olioso, P. Cellier, E. Maignan, T. Eglin and J.-C. Calvet: How errors on meteorological variables impact simulated ecosystem fluxes: a case study for six French sites, *Biogeosciences*, 9, 2537-2564, Doi: 10.5194/bg-9-2537-2012, 2012.

Zyryanov D., G. Foret, M. Eremenko, M. Beekmann, J.-P. Cammas, M. D'Isidoro, H. Elbern, J. Flemming, E. Friese,

I. Kioutsioutkis, A. Maurizi, D. Melas, F. Meleux, L. Menut, P. Moinat, V.-H. Peuch, A. Poupkou, M. Razingier, M. Schultz, O. Stein, A. M. Suttie, A. Valdebenito, C. Zerefos, G. Dufour, G. Bergametti and J.-M. Flaud, 2012: 3-D evaluation of tropospheric ozone simulations by an ensemble of regional Chemistry Transport Model, *Atmospheric Chemistry and Physics*, Volume: 12, Issue: 7, Pages: 3219-3240, Doi: 10.5194/acp-12-3219-2012, Published: 2012.

Barker D., H. Xiang-Yu, L. Zhiqian, Auligne, T. et al. THE WEATHER RESEARCH AND FORECASTING MODEL'S COMMUNITY VARIATIONAL/ENSEMBLE DATA ASSIMILATION SYSTEM WRFDA. *Bulletin of the American Meteorology Society*, Volume: 93, Issue: 6, Pages: 831-843, Doi: 10.1175/BAMS-D-11-00167.1, Published: JUN 2012.

Daux V., I. Garcia de Cortazar-Atauri, P. Yiou, O. Mestre and al.: An open-access database of grape harvest dates for climate research: data description and quality assessment CLIMATE OF THE PAST Volume: 8, Issue: 5, Pages: 1403-1418, Published: 2012.

Mathieu J., V.-H. Peuch, Objective classification of air quality monitoring sites over Europe. *Atmospheric Environment*, Volume: 47, Pages: 111-123, Doi: 10.1016/j.atmosenv.2011.11.025, Published: FEB 2012.

Nahmani S., O. Bock, M.-N. Bouin and al. Hydrological deformation induced by the West African Monsoon: Comparison of GPS, GRACE and loading models. *Journal of Geophysical Research-Solid Earth*, Volume: 117, Article Number: B05409, Doi: 10.1029/2011JB009102. Published: MAY 12 2012.

Olivie D.J.L., D. Cariolle, H. Teyssedre and al. Modeling the climate impact of road transport, maritime shipping and aviation over the period 1860-2100 with an AOGCM *ATMOSPHERIC CHEMISTRY AND PHYSICS* Volume: 12 Issue: 3 Pages: 1449-1480 Doi: 10.5194/acp-12-1449-2012, Published: 2012.

Venema V.K.C., O. Mestre, E. Aguilar and al. Benchmarking homogenization algorithms for monthly data. *Climate of The Past*, Volume: 8, Issue: 1, Pages: 89-115, Doi: 10.5194/cp-8-89-2012, Published: 2012.

Wang H., T. Auligne, H. Morrison. Impact of Microphysics Scheme Complexity on the Propagation of Initial Perturbations. *Monthly Weather Review*, Volume: 140 Issue: 7, Pages: 2287-2296, Doi: 10.1175/MWR-D-12-00005.1, Published: JUL 2012.

## Other scientific papers

Guichard F., L. Kergoat, C.M. Taylor, B. Cappelaere, M. Chong, J.-M. Cohard, F. Couvreur, C. Dione, A. Gounou, F. Lohou et M. Lothon, 2012 : Interactions entre surface et convection au Sahel. *La Météorologie*, Volume : N° Special AMMA, Pages : 25-32, Doi: 10.4267/2042/ 48129. Published : OCT 2012.

Brun E., V. Vionnet, S. Morin, A. Boone, E. Martin, S. Faroux, P. Le Moigne et J.-M. Willemet, 2012 : Le modèle de manteau neigeux Crocus et ses applications. *La Météorologie*, 76, 44-54.

Karbou F., F. Beucher, O. Bock, J.-P. Lafore, Z. Mumba, J.-B. Ngamini, M. Nuret, F. Rabier et J.-L. Redelsperger, 2012 : Les leçons de l'expérience AMMA en matière de Prévision Numérique du Temps. *La Météorologie*, pp 49-54, Doi: 10.4267/2042/48132.

Lafore J.P., N. Asencio, D. Bouniol, F. Couvreur, C. Flamant, F. Guichard, N. Hall, S. Janicot, C. Kocha, C. Lavaysse, S. Leroux, E. Poan P. Peyrillé, R. Roca, R. Roehrig, F. Roux, F. Saïd, 2012 : Le Système de Mousson Ouest-Africain *La Météorologie*.

Taylor C. M., R. A. M. De Jeu, F. Guichard, P. P. Harris and W. A. Dorigo, 2012: Afternoon rain more likely over drier soils. *Nature*, Volume: 489, Pages: 423-426, Doi: 10.1038/nature11377. Published: Septembre 2012.

Soubeyroux J.-M., N. Kitova, M. Blanchard, J.-P. Vidal, E. Martin et P. Dandin, Sècheresse des sols en France et changement climatique *La Météorologie*, 2012, 78, 21-30.

Eymard L., C. Baron, G. Caniaux, C. Flamant, L. Kergoat, F. Karbou, J.A Ndione, T. Pellarin, N. Martiny, J. Ramahoretra, E. Vintrou et R. Roca, 2012 : L'observation spatiale dans le programme AMMA. *La Météorologie*, pp 80-89, Doi : 10.4267/2042/48136.

Carmagnola C. M., F. Domine, S. Morin, L. Arnaud, G. Picard, N. Champollion, M. Bergin, J. Dibb, P. Wright and M. Dumont, 2012: Ricerca sulla neve in Groenlandia: misure e risultati della campagna alla base Summit. *Nimbus*, 63-64, pp 6-14.

Caniaux G., H. Giordani, J.L. Redelsperger, M. Wade, B. Bourlès, D. Bourras, G. de Coëtlogon, Y. du Penhoat, S. Janicot, E. Key, N. Kolodziejczyk, L. Eymard, J. Jouanno, A. Lazar, M. Leduc-Leballeur, N. Lefèvre, F. Marin, H. Nguyen et G. Parard, 2012 : Les avancées d'AMMA sur les interactions océan-atmosphère. *La Météorologie*, Numéro Special AMMA, 8<sup>e</sup> Série, Octobre 2012, 17-24.

Nabat P. : Modélisation des aérosols sur la région méditerranéenne, *La Météorologie*, 8<sup>e</sup> série, n° 76, pages 26-31, février 2012.

---

## Contributions to books or reports

Déqué M., 2012: Deterministic forecasts of continuous variables. In: Forecast Verification, 2nd edition. Eds. Jolliffe I.T. and D.B. Stephenson, Wiley-Blackwell, Pages 77-95.

Déqué M. and L. Batté, 2012: Flux correction and seasonal predictability. Research activities in atmospheric and oceanic modelling, 42, 6.5-6.6.

Genovese E., V. Przylyski, F. Vinit et M. Déqué, 2012 : Xynthia : le déroulement de la tempête et ses conséquences en France. Chapitre 1 de l'ouvrage Gestion des risques naturels : Leçons de la tempête Xynthia. Coordination V. Przylyski et S. Hallegatte. Editions Quae, 17-44.

Lestringant R., 2012 : Méthodes de correction du vent pour la campagne FENNEC (2011). Note de travail du groupe de météorologie expérimentale, n° 30.

Li L., A. Casado, L. Congedi, A. Dell'Aquila, C. Dubois, A. Elizalde, B. L' Hévéder, P. Lionello, F. Sevault, S. Somot, P. Ruti, M. Zampieri, 2012: Modelling of the Mediterranean climate system, In: The climate of the Mediterranean region. Ed. P. Lionello, Elsevier, 419-448.

Peings Y., M. Jamous, S. Planton et H. Le Treut, M. Déqué, H. Gallée, L. Li, 2012 : Scénarios régionalisés. Le climat de la France au XXI<sup>e</sup> siècle, Volume 2, rapport de la mission Jean Jouzel, février 2012, Ministère de l'Ecologie, du Développement Durable, des Transports et du Logement, 303 pp.

Planton S., P. Lionello, V. Artale, R. Aznar, A. Carrillo, J. Colin, L. Congedi, C. Dubois, A. Elizalde, S. Gualdi, E. Hertig, J. Jacobeit, G. Jordà, L. Li, A. Mariotti, C. Piani, P. Ruti, E. Sanchez-Gomez, G. Sannino, F. Sevault, S. Somot, M. Tsimplis, 2012: The Climate of the Mediterranean Region in Future Climate Projections, In: The climate of the Mediterranean region. Ed. P. Lionello, Elsevier, 449-502.

Planton S., A. Cazenave, P. Delecluse, N. Dorfliger, P. Gaufrès, D. Idier, M. Jamous, G. Le Cozannet, H. Le Treut, Y. Peings, 2012 : Evolution du niveau de la mer, Volume 3, rapport de la mission Jean Jouzel, février 2012, Ministère de l'Ecologie, du Développement Durable, des Transports et du Logement, 49 pp.

Schroeder K., J. Garcia-Lafuente, S. A. Josey, V. Artale, B. B. Nardelli, A. Carrillo, M. Gacic, G. P. Gasparini, M. Hermann, P. Lionello, W. Ludwig, C. Millot, E. Ozsoy, G. Pisacane, J.C. Sanchez-Garrido, G. Sannino, R. Santoleri, S. Somot, M. Struglia, E. Stanev, I. Taupier-Letage, M.N. Tsimplis, M. Vargas-Yanez, V. Zervakis, G. Zodiatis, 2012: Circulation of the Mediterranean Sea and its variability, In: The climate of the Mediterranean region. Ed. P. Lionello, Elsevier, 187-256.

Habets F., J. Boé, M. Déqué, A. Duchame, S. Gascoin, A. Hachour, E. Martin, C. Pagé, E. Sauquet, L. Terray, D. Thiéry, L. Oudin, P. Viennot and S. Thery, 2011 : Impact du changement climatique sur les ressources en eau du bassin de la Seine, Collections du programme du PIREN-Seine, Agence de l'eau Seine-Normandie, 47 pages.

Rabier F., S. Cohn, Ph. Cocquerez, A. Hertzog, L. Avallone, T. Deshler, J. Haase, T. Hock, A. Doerenbecher, J. Wang, V. Guidard, J.-N. Thépaut, R. Langland, A. Tangborn, G. Balsamo, E. Brun, D. Parsons, J. Bordereau, C. Cardinali, F. Danis, J.-P. Escarnot, N. Fourrié, R. Gelaro, Ch. Genthon, K. Ide, L. Kalnajs, C. Martin, L.-F. Meunier, J.-M. Nicot, T. Perttula, T., Potts, P. Ragazzo, D. Richardson, S. Sosa-Sesma, A. Vargas: The Concordiasi field experiment over Antarctica: first results from innovative atmospheric measurements. WMO CAS/JSC WGNE Blue Book, Edited by J. Côté., 2012.

Guedj S.: Improved assimilation of SEVIRI radiances over land in meso-scale models using Land Surface Temperature retrievals. WMO CAS/JSC WGNE Blue Book, Edited by J. Côté., 2012.

Saint-Ramond N., A. Doerenbecher, F. Rabier, V. Guidard, N. Fourrié: Forecast sensitivity to observations at Météo-France. Application to GPS radio-occultation data. WMO CAS/JSC WGNE Blue Book, Edited by J. Côté., 2012.

---

## PHD defended in 2012

Barre J., 2012 : « Etudes par assimilation de données satellites au limbe et au nadir dans un modèle de chimie-transport » le 19 novembre 2012.

Brousseau P., 2012 : « Propagation de l'information observée dans le système d'assimilation et le modèle atmosphérique Arome » le 9 juillet 2012.

Charles E., 2012 : « Impact du changement climatique sur le climat de vagues en zone côtière, par régionalisation dynamique : application à la côte Aquitaine » le 6 février 2012.

Chevalier M., 2012 : « Prévisibilité saisonnière de la glace de mer de l'océan Arctique » le 7 décembre 2012.

Dossmann Y., 2012 : « Ondes internes générées sur une dorsale océanique : du laboratoire à l'océan » le 27 septembre 2012.

Faijan F., 2012 : « Vers une meilleure utilisation des observations du sondeur IASI pour la restitution des profils atmosphériques en conditions nuageuses » le 21 novembre 2012.

Honnert R., 2012 : « Quelle turbulence dans les modèles atmosphériques à l'échelle kilométrique ? » le 22 octobre 2012.

Lacressonnière G., 2012 : « Etude par modélisation numérique de la qualité de l'air en Europe dans les climats actuel et futur » le 19 décembre 2012.

Law Chune S., 2012 : « Apport de l'océanographie opérationnelle à l'amélioration de la prévision de la dérive océanique dans le cadre d'opérations de recherche et de sauvetage en mer et de lutte contre les pollutions marines » le 15 février 2012.

Michel C., 2012 : « Rôle du déferlement des ondes de Rossby dans la variabilité climatique aux latitudes tempérées » le 26 octobre 2012.

Mokhtari M., 2012 : « Amélioration de la prise en compte des aérosols terrigènes dans les modèles atmosphériques à moyenne échelle » le 20 décembre 2012.

Oueslati B., 2012 : « Interaction entre convection nuageuse et circulation de grande échelle dans les tropiques » le 10 décembre 2012.

Ouzeau G., 2012 : « Influence de la stratosphère sur la variabilité et la prévisibilité climatique » le 28 novembre 2012.

Pantillon F., 2012 : « Transition extratropicale d'ouragans en Atlantique Nord et impact sur la prévisibilité d'événements extrêmes en Méditerranée » le 24 septembre 2012.

Singla S., 2012 : « La prévisibilité des ressources en eau à l'échelle saisonnière en France » le 13 novembre 2012.

Zczypta C., 2012 : « Hydrologie spatiale pour le suivi des sécheresses du bassin méditerranéen » le 24 septembre 2012.

Vergnes J.P., 2012 : « Développement d'une modélisation hydrologique incluant la représentation des aquifères : évaluation sur la France et à l'échelle globale » le 14 décembre 2012.

Vié Benoît, 2012 : « Méthodes de prévision d'ensemble pour l'étude de la prévisibilité à l'échelle convective des épisodes de pluies intenses en Méditerranée » le 29 novembre 2012.

Vionnet V., 2012 : « Etudes du transport de la neige en conditions alpines : observations et simulations à l'aide d'un modèle couplé atmosphère/manteau neigeux » le 30 novembre 2012.

---

## « Habilitations à diriger des recherches » defended in 2012

Montmerle T., 2012 : « Assimilation des données à moyenne échelle pour l'étude des systèmes précipitants » le 27 janvier 2012.

Rivière G., 2012 : « Dynamique des dépressions des latitudes tempérées et leur rôle dans la circulation générale de l'atmosphère » le 25 janvier 2012.

Tabary P., 2012 : « Contributions au transfert de la recherche à l'opérationnel en météorologie radar » le 11 juin 2012.

# Glossary

## Organisms and Laboratories

### Organisms

<b>ADEME</b>	Agence de l'Environnement et de la Maîtrise de l'Energie
<b>AIEA</b>	Agence Internationale de l'Energie Atomique
<b>ANR</b>	Agence Nationale de la Recherche
<b>BEC</b>	Bureau d'Etudes et de Consultance
<b>CDM</b>	Centre Départemental de la Météorologie
<b>CDMA</b>	Cellule de développement Météo-Air
<b>CEH</b>	Centre for Ecology and Hydrology
<b>CEMAGREF</b>	CEntre national du Machinisme Agricole, du Génie Rural, des Eaux et Forêts (Institut national de Recherche en Sciences et Technologies pour l'Environnement et l'Agriculture)
<b>CEN</b>	Centre d'Etudes de la Neige
<b>CEPMET</b>	Centre Européen pour les Prévisions Météorologiques à Moyen Terme
<b>CERFACS</b>	Centre Européen de Recherche et de Formation Avancée en Calcul Scientifique
<b>CMM</b>	Centre de Météorologie Marine
<b>CMRS</b>	Centre Météorologique Régional Spécialisé
<b>CMS</b>	Centre de Météorologie Spatiale
<b>CNES</b>	Centre National d'Etudes Spatiales
<b>CNP</b>	Centre National de Prévision
<b>DGA</b>	Délégation générale pour l'armement
<b>DGPR</b>	Direction Générale de la Prévention des Risques
<b>EEA</b>	Agence Environnementale Européenne
<b>ESA</b>	European Space Agency
<b>ETNA</b>	Division Ecoulements Torrentiels, Neige et Avalanches du CEMAGREF
<b>EUFAR</b>	EUropean Facility for Airborne Research
<b>EUMETNET</b>	EUropean METeorological NETwork
<b>EUMETSAT</b>	Organisation européenne pour l'exploitation de satellites météorologiques
<b>ICARE</b>	International Conference on Airborne Research for the Environment
<b>IFREMER</b>	Institut Français de Recherche pour l'Exploitation de la MER
<b>INERIS</b>	Institut National de l'Environnement et des RISques
<b>INRIA</b>	Institut National de Recherche en Informatique et en Automatique
<b>INSU</b>	Institut National des Sciences de l'Univers
<b>IPEV</b>	Institut Paul Emile Victor
<b>IRD</b>	Institut de Recherche pour le Développement
<b>IRSTEA</b>	Institut national de Recherche en Sciences et Technologies pour l'Environnement et l'Agriculture (anciennement CEMAGREF)
<b>JMA</b>	Japan Meteorological Agency
<b>MEDDTL</b>	Ministère de l'Ecologie, du Développement Durable, des Transports et du Logement
<b>MERCATOR-OCEAN</b>	Société Civile Française d'océanographie opérationnelle
<b>MetOffice</b>	United Kingdom Meteorological Office
<b>MPI</b>	Max Planck Institut
<b>NASA</b>	National Aeronautics and Space Administration
<b>NCAR</b>	National Center for Atmospheric Research
<b>NEC</b>	Nippon Electric Company
<b>NOAA</b>	National Ocean and Atmosphere Administration
<b>OACI</b>	Organisation de l'Aviation Civile Internationale
<b>OMM</b>	Organisation Météorologique Mondiale
<b>RTRA-STAE</b>	Réseau Thématique de Recherche Avancée - Sciences et Technologies pour l'Aéronautique et l'Espace
<b>SHOM</b>	Service Hydrographique et Océanographique de la Marine
<b>UKMO</b>	United Kingdom Meteorological Office
<b>VAAC</b>	Volcanic Ash Advisory Centre

### Laboratories or R&D units

<b>3SR</b>	Laboratoire Sols – Solides – Structures – Rhéologie, UJF Grenoble/CNRS/Grenoble INP
<b>CESBIO</b>	Centre d'Etudes Spatiales de la Biosphère
<b>CNRM</b>	Centre National de Recherches Météorologiques
<b>CNRM-GAME</b>	Groupe d'études de l'Atmosphère Météorologique
<b>CNRS</b>	Centre National de Recherches Scientifiques
<b>DSO</b>	Direction des Systèmes d'Observation (Météo-France)
<b>GAME</b>	Groupe d'Etude de l'Atmosphère Météorologique
<b>IFSTTAR</b>	Institut Français des Sciences et Technologies des Transports, de l'Aménagement et des Réseaux
<b>IGN</b>	Institut Géographique National
<b>IPSL</b>	Institut Pierre Simon Laplace
<b>LAMP</b>	Laboratoire de Météorologie Physique

<b>LATMOS</b>	Laboratoire ATmosphères, Milieux, Observations Spatiales
<b>LCP</b>	Laboratoire Chimie et Procédés
<b>LEGI</b>	Laboratoire des écoulements physiques et industriels
<b>LGGE</b>	Laboratoire de Glaciologie et de Géophysique de l'Environnement
<b>LMD</b>	Laboratoire de Météorologie Dynamique
<b>LOCEAN</b>	Laboratoire d'Océanographie et du Climat : Expérimentations et Approches Numériques
<b>LSCE</b>	Laboratoire des Sciences du Climat et de l'Environnement
<b>SAFIRE</b>	Service des Avions Français Instrumentés pour la Recherche en Environnement

### National or international programs or projects

<b>BAMED</b>	Balloons in the MEDiterranean
<b>CHFP</b>	Climate Historical Forecasting Project
<b>CIDEX</b>	Calibration and Icing Detection EXperiment
<b>CMIP</b>	Coupled Model Intercomparaison Project
<b>CYPRIM</b>	projet Cyclogénèse et précipitations intenses dans la zone méditerranéenne
<b>ESURFMAR</b>	Eumetnet SURFace MARine programme
<b>GHRST</b>	International Group for High Resolution SST
<b>GLOSCAL</b>	Global Ocean Surface salinity CALibration and validation
<b>HyMeX</b>	Hydrological cYcle in the Mediterranean EXperiment
<b>LEFE</b>	programme national « Les Enveloppes Fluides et l'Environnement »
<b>MEPRA</b>	Modèle Expert de Prévision du Risque d'Avalanche (modélisation)
<b>METOP</b>	METeorological Operational Polar satellites
<b>PNRA</b>	Programma Nazionale di Recerche in Antartide
<b>QUANTIFY</b>	Programme QUANTIFYing the climate impact of global and European transport systems
<b>RHYTMME</b>	Risques HYdro-météorologiques en Territoires de Montagnes et Méditerranéens
<b>SCAMPEI</b>	Scénarios Climatiques Adaptés aux Montagnes : Phénomènes extrêmes, Enneigement et Incertitudes – projet de l'ANR coordonné par le CNRM
<b>SMOS</b>	Soil Moisture and Ocean Salinity
<b>THORPEX</b>	The Observing system Research and Predictability EXperiment
<b>USAP</b>	United States Antarctic Program
<b>WCRP</b>	World Climate Research Programme

### Campaigns

<b>AMMA</b>	Analyse Multidisciplinaire de la Mousson Africaine
<b>CORDEX</b>	COordinated Regional climate Downscaling EXperiment
<b>MEGAPOLI</b>	Megacities : Emissions, urban, regional and Global Atmospheric POLLution and climate effects, and Integrated tools for assessment and mitigation
<b>SMOSREX</b>	Surface MONitoring of the Soil Reservoir EXperiment

### Other acronyms

<b>AIRS</b>	Sondeur Infrarouge avancé
<b>ALADIN</b>	Aire Limitée Adaptation Dynamique et développement InterNational
<b>AMSR</b>	Advanced Microwave Scanning Radiometer
<b>AMSU</b>	Advanced Microwave Sounding Unit
<b>AMSU-A</b>	Advanced Microwave Sounding Unit-A
<b>AMSU-B</b>	Advanced Microwave Sounding Unit-B
<b>ANASYG</b>	ANALyse Synoptique Graphique
<b>ANTILOPE</b>	ANALyse par spaTialisation hOraire des PrEcipitations
<b>ARAMIS</b>	Application Radar A la Météorologie Infra-Synoptique
<b>ARGO</b>	Array for Real time Geostrophic Oceanography
<b>AROME</b>	Application de la Recherche à l'Opérationnel à Mésos-Échelle
<b>AROME-COMB</b>	AROME - COMBinaison
<b>AROME-PERTOBS</b>	AROME (OBServations PERTurbées aléatoirement)
<b>ARPEGE</b>	Action de Recherche Petite Échelle Grande Échelle
<b>AS</b>	Adaptations Statistiques
<b>ASAR</b>	Advanced Synthetic Aperture Radar
<b>ASCAT</b>	Advanced SCATterometer
<b>ASTEX</b>	Atlantic Stratocumulus Transition EXperiment
<b>AVHRR</b>	Advanced Very High Resolution Radiometer
<b>BAS</b>	British Antarctic Survey



<b>BPCL</b>	Ballon Pressurisé de Couche Limite	<b>MODIS</b>	MODerate-resolution Imaging Spectro-radiometer (instrument)
<b>CALIPSO</b>	Cloud-Aerosol Lidar and Infrared Pathfinder Satellite Observations	<b>MoMa</b>	Méthodes Mathématiques pour le couplage modèles et données dans les systèmes non-linéaires stochastiques à grand nombre de degrés de liberté
<b>CAPE</b>	Convective Available Potential Energy	<b>MOTHY</b>	French oil spill drift model
<b>CAROLS</b>	Combined Airborne Radio-instruments for Ocean and Land Studies	<b>MRR</b>	Micro Rain Radars
<b>CFMIP</b>	Cloud Feedback Intercomparison Project	<b>NAO</b>	North Atlantic Oscillation
<b>CFO SAT</b>	Chinese-French SATellite	<b>NEMO</b>	Nucleus for European Modelling of Ocean
<b>ChArMEx</b>	Chemistry-Aerosol Mediterranean Experiment	<b>NSF</b>	Norges StandardiseringsForbund
<b>CISM F</b>	Centre Inter-armées de Soutien Météorologique aux Forces	<b>OPIC</b>	Objets pour la Prévision Immédiate de la Convection
<b>CLAS</b>	Couches Limites Atmosphériques Stables	<b>ORCHIDEE</b>	ORganizing Carbon and Hydrology in Dynamic Ecosystems
<b>CMC</b>	Cellule Météorologique de Crise	<b>OSTIA</b>	Operational Sea surface Temperature sea Ice Analysis
<b>CNRM-CM5</b>	Version 5 du Modèle de Climat du CNRM	<b>OTICE</b>	Organisation du Traité d'Interdiction Complète des Essais nucléaires
<b>COP</b>	Contrat d'Objectifs et de Performances	<b>PALM</b>	Projet d'Assimilation par Logiciel Multi-méthodes
<b>COPAL</b>	Community heavy-Payload Long endurance instrumented aircraft for tropospheric research in environmental and geo-sciences	<b>PEARP</b>	Prévision d'Ensemble ARPège
<b>CROCUS</b>	Modèle de simulation numérique du manteau neigeux développé par Météo-France.	<b>PI</b>	Prévision Immédiate
<b>DMT</b>	Droplet Measurement Technologies	<b>PN</b>	Prévision Numérique
<b>DP</b>	Direction de la Production	<b>PNT</b>	Prévision Numérique du Temps
<b>DPrévi</b>	Direction de la Prévision	<b>POD</b>	PrObabilité de Détection
<b>DSI</b>	Direction des Systèmes d'Information (Météo-France)	<b>POI</b>	Période d'Observation Intensive
<b>DSNA</b>	Direction des Services de la Navigation Aérienne	<b>PRESYG</b>	PREvision Synoptique Graphique
<b>ECMWF</b>	European Centre for Medium-range Weather Forecasts	<b>Prev'Air</b>	Plateforme nationale de la qualité de l'air
<b>ECOCLIMAP</b>	Base de données de paramètres de surface	<b>PREVIBOSS</b>	PREvisibilité à courte échéance de la variabilité de la Visibilité dans le cycle de vie du Brouillard, à partir de données d'Observation Sol et Satellite.
<b>EGEE</b>	Etude du golfe de Guinée		Projet sur les prévisions probabilistes
<b>ENVISAT</b>	ENVironmental SATellite	<b>PSI</b>	Pollutant Standard Index
<b>ERA</b>	Re-Analysis	<b>PVM</b>	Particulate Volume Monitor
<b>EUCLIPSE</b>	European Union Cloud Intercomparison, Process Study & Evaluation (Project LES : Large - Eddy Simulation)	<b>RADOME</b>	Réseau d'Acquisition de Données d'Observations Météorologiques Etendu
<b>FAB</b>	Fonctionnel Aerospace Block	<b>RCP8.5</b>	8.5 W/m <sup>2</sup> Representative Concentration Pathway corresponding to a 8.5 W/m <sup>2</sup> radiative forcing at the end of the 21st century compared to preindustrial climate
<b>FABEC</b>	Functional Airspace Block Europe Central	<b>RHI</b>	Range Height Indicator (coupe verticale)
<b>FAR</b>	Fausse Alerte	<b>ROC</b>	Relative Operating Characteristic curve
<b>FSO</b>	Forecast Sensitivity to Observations	<b>SAFNWP</b>	Satellite Application Facility for Numerical Weather Prediction
<b>GELATO</b>	Global Experimental Leads and ice for ATmosphere and Ocean	<b>SAFRAN</b>	Système d'Analyse Fournissant des Renseignements Atmosphériques à la Neige
<b>GIEC</b>	Groupe Intergouvernemental d'experts sur l'Evolution du Climat	<b>SATOB</b>	Satellite Observation
<b>GMAP</b>	Groupe de Modélisation et d'Assimilation pour la Prévision	<b>SCM</b>	Single-Column Model
<b>GMEI</b>	Groupe de Météorologie Expérimentale et Instrumentale	<b>SESAR</b>	Single European Sky ATM Research
<b>GMES</b>	Global Monitoring for Environment and Security	<b>SEVIRI</b>	Spinning Enhanced Visible and Infra-Red Imager
<b>GPP</b>	Gross Primary Production	<b>SFRI</b>	Système Français de Recherche et d'Innovation
<b>GPS</b>	Global Positioning System	<b>SIM</b>	SAFRAN ISBA MODCOU
<b>HIRLAM</b>	High Resolution Limited Area Model	<b>SIRTA</b>	Site Instrumental de Recherche par Télédétection Atmosphérique
<b>HISCRIM</b>	High Spectral resolution Cloudy-sky Radiative Transfer Model	<b>SMOSMANIA</b>	Soil Moisture Observing System – Meteorological Automatic Network Integrated Application
<b>HSS</b>	Measurement of improvement of the forecast	<b>SMT</b>	Système Mondial de Télécommunications
<b>IAGOS</b>	In-service Aircraft for Global Observing System	<b>SOERE/GLACIOCLIM</b>	Système d'Observation et d'Expérimentation sur le long terme pour la Recherche en Environnement : « Les GLACIers, un Observatoire du CLIMat ».
<b>IASI</b>	Interféromètre Atmosphérique de Sondage Infrarouge	<b>SOP</b>	Special Observing Period
<b>IFS</b>	Integrated Forecasting System	<b>SSM/I/S</b>	Special Sounder Microwave Imager/Sounder
<b>ISBA - ES</b>	Interaction between Soil, Biosphere and Atmosphere-Modèle numérique du CNRM représentant l'évolution du sol en surface (végétation incluse) et en profondeur, mettant particulièrement l'accent sur l'évolution de la couverture de neige	<b>SURFEX</b>	SURFace EXternalisée
<b>ISFC</b>	Indice de Segmentation de la Composante de Fourier	<b>SVP</b>	Surface Velocity Program
<b>ISIS</b>	Algorithme de suivi automatique des systèmes identifiés à partir de l'imagerie infra-rouge de Météosat	<b>SWI</b>	Soil Wetness Index
<b>LAI</b>	Leaf Area Index	<b>SWIM</b>	Surface Wave Investigation and Monitoring
<b>Land-SAF</b>	LAND Satellite Application Facilities	<b>SYMPOSIUM</b>	SYstème Météorologique de Prévision Orienté Services, Intéressant des Usagers Multiples – découpage du territoire métropolitain en 615 zones « climatiquement » homogènes, dont la taille varie de 10 à 30 km
<b>LCCS</b>	Land Cover Classification System	<b>TEB</b>	Town Energy Budget
<b>LES</b>	Large Eddy Simulation model	<b>TRIP</b>	Total Runoff Integrating Pathways
<b>LISA</b>	Lidar SATellite	<b>TSM</b>	Températures de Surface de la Mer
<b>MEDUP</b>	MEDiterranean intense events : Uncertainties and Propagation on environment	<b>UHF</b>	Ultra-Haute Fréquence
<b>Megha-Tropiques</b>	Satellite franco-indien dédié à l'étude du cycle de l'eau et des échanges d'énergie dans la zone tropicale	<b>UNIBAS</b>	Modèle de précipitations
<b>MERSEA</b>	Marine EnviRONment and Security for the European Area	<b>VARPACK</b>	Current tool for diagnostic analysis in Meteo-France
<b>MESO-NH</b>	Modèle à MESO-échelle Non Hydrostatique	<b>VHF</b>	Very High Frequency
<b>MFWAM</b>	Météo-France Wave Model	<b>WWLLN</b>	World Wide Lightning Location Network
<b>MHS</b>	Microwave Humidity Sounder		
<b>MNPCA</b>	Microphysique des Nuages et de Physico-Chimie de l'Atmosphère		
<b>MOCAGE</b>	MOdélisation de la Chimie Atmosphérique de Grande Echelle (modélisation)		
<b>MODCOU</b>	MODèle hydrologique COUplé surface-souterrain.		

# CNRM: Management structure

31.12.2012

Head: **Philippe Bougeault**

Deputy Head - Toulouse: **Joël Poitevin**

Scientific deputy Head - Toulouse: **Marc Pontaud**

Deputy Head - Saint-Mandé: **Pascale Delecluse**

SAFIRE: French group of Aircraft Equipped for Environmental Research

METEOROLOGICAL AVIATION CENTRE

CAM - Toulouse

Centre Head: **Lior Perez**

SNOW RESEARCH CENTRE

CEN - Grenoble

Centre Head: **Pierre Etchevers**

MARINE METEOROLOGY CENTRE

CMM - Brest

Centre Head: **Jean Rolland**

MODELLING FOR ASSIMILATION AND FORECASTING GROUP

GMAP - Toulouse

Group Head: **Alain Joly**

EXPERIMENTAL AND INSTRUMENTAL METEOROLOGY GROUP

GMEI - Toulouse

Group Head: **Alain Dabas**

CLIMATE AND LARGE SCALE MODELLING GROUP

GMGEC - Toulouse

Group Head: **Serge Planton**

MESO-SCALE MODELLING GROUP

GMME - Toulouse

Group Head: **Véronique Ducrocq**

INTERNAL KNOWLEDGE TRANSFERS GROUP

RETIC - Toulouse

Group Head: **Dominique Giard**

GENERAL SERVICES

SC/Toulouse

Head: **Joël Poitevin**

## Nota:

The GAME is the Associated Research Unit between Météo-France and CNRS. Groups on deep blue are fully included in GAME, groups on light blue are partially included in GAME.

SAFIRE is a joint unit between Météo-France, CNRS and CNES.



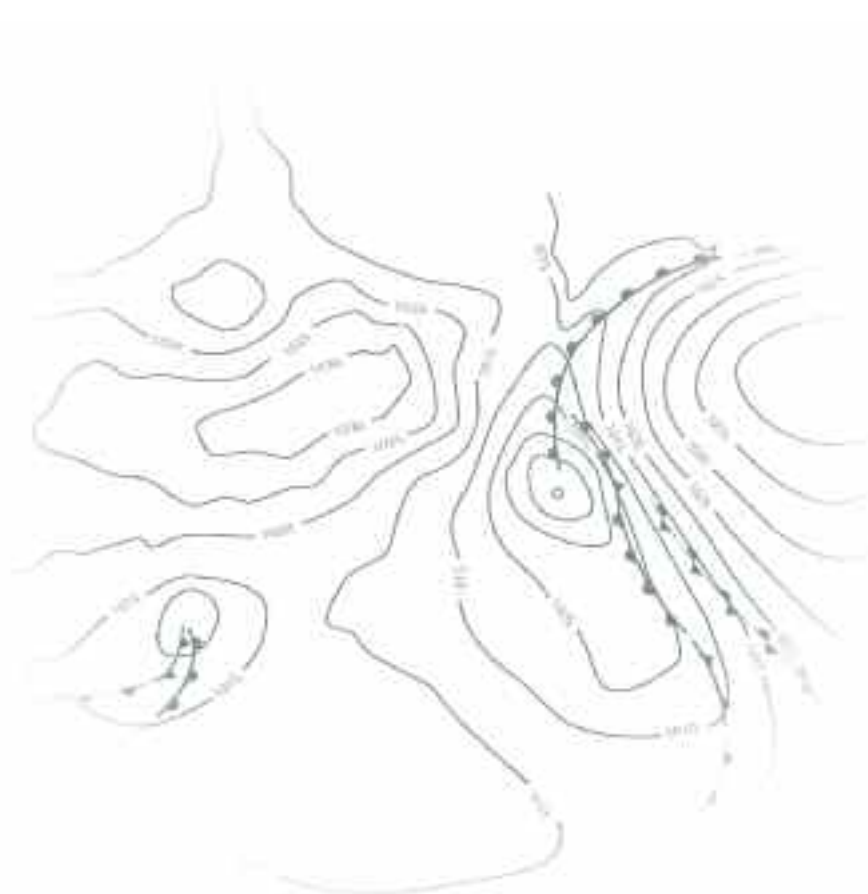


## **Météo-France**

73, avenue de Paris  
94165 Saint-Mandé Cedex  
Tél. : +33 1 77 94 77 94  
Fax : + 33 1 77 94 70 05  
[www.meteofrance.com](http://www.meteofrance.com)

## **Centre National de Recherches Météorologiques Groupe d'études de l'Atmosphère Météorologique**

42, avenue Gaspard Coriolis  
31057 Toulouse Cedex 1 France  
Tél. : +33 5 61 07 93 70  
Fax : + 33 5 60 07 96 00  
<http://www.cnrm-game.fr>  
Mail : [contact@cnrm.meteo.fr](mailto:contact@cnrm.meteo.fr)



Creation D2C/IMP Trappes

Météo-France is certified ISO 9001  
by Bureau Veritas Certification  
© Météo-France 2013  
Dépôt légal mai 2013  
ISSN : 2116-438X